UNIVERSITAT POLITÈCNICA DE VALÈNCIA

School of Industrial Engineering

Modelling the potential of Green roof installation for the decarbonization of urban areas. Case study of Valencia, Spain.

Master's Thesis

Master's Degree in Energy Technologies for Sustainable Development

AUTHOR: Pino Gallardo, Tomas

Tutor: Bastida Molina, Paula

Cotutor: Gómez Navarro, Tomás

ACADEMIC YEAR: 2023/2024

ACKNOWLEDGMENTS

At this crucial moment of the culmination of my research work, I wish to express my deep gratitude to all the people and institutions that have contributed significantly to the completion of this dissertation. Their support, advice and generosity have been fundamental in this process and have left an indelible mark on my academic journey.

I would like to express my gratitude to LINDOR and HELGA, my parents. For their constant love, concern and work supporting my development, as a person and as a professional. For always being there and never ceasing to motivate me in my career as an engineer, despite the passing of the years. To my brothers, DANIEL and NICOLE, for their love and tolerance in my professional and personal development, and for always being there for me in good times and bad.

To CATALINA, my partner and companion in this change of country and life. For not hesitating, for supporting me in the development of the Master when things got difficult, for always encouraging and advising me, and for putting up with my lack of taste for the beach in a city like VALENCIA. At the beginning I planned this journey individually, but nowadays I could not think of a change like this without her.

To all my classmates, especially to ANA, LUISE, MONTSE and EDU, key in this year and a half in VALENCIA. For always being there to work and bear to work with me in the development of the Master, as well as to share a beer, a pizza in the “Glotonería” or a simple board game. Despite the infrequency of our meetings in recent months for various reasons, I will always keep you in mind as that family that one finds along the way that motivates you to give the best of yourself and to support those who need it. To AGUSTIN, GIACOMO, GONZALO and MARIO, for adopting me into your group and making life in a country that is not yours anything but boring, and for making me feel twenty again.

To my tutor teachers. To TOMÁS, not only for the support during this work, but also for the excellent classes that motivated me to follow the path I am now investigating in this study. For taking an interest and giving me the opportunity to carry out my TFM with him. To PAULA, for her constant tutoring and interest in the development of my work. Always being present and willing to help me when I needed it most, believing in me and motivating me to achieve excellence in research.

To SANTI, EVITA and family. For generating an interest in this wonderful city, which ultimately defined my choice of university for my master's degree. They are literally the beginning of all the work presented in this TFM.

To SEBASTIAN and his family, my thesis tutor, who was the first person to welcome and support me when I arrived in a place so far away from CHILE and continued to do so throughout this experience.

Finally, I would like to thank LAURA and IÑIGO, my distant family from the Euskal Herria, who supported me in coming to the peninsula from the beginning. Even though they don't live in the same community, coming to a city as far away as VALENCIA and knowing that they are only a couple of hours away was always a support.

ABSTRACT

Nature-based solutions (NBS), in particular green roofs (GRs), play a vital role in mitigating the urban heat island and improving energy efficiency in urban environments. They offer significant environmental and social benefits by improving energy efficiency, water management, acoustic comfort and social well-being in urban areas. Despite the increasing exploration of their potential in large cities through technologies such as 3D modelling (LiDAR), high-resolution imagery and spatial data analysis, the lack of highly automated methodologies has limited their large-scale implementation.

This study presents an innovative methodology that simplifies and delimits the estimation of the potential area for GR installation in cities using artificial vision. It provides users with the ability to adapt artificial vision to specific city characteristics and apply manual modifications to improve accuracy. Updated orthophotographs are processed using MATLAB code and QGIS software support to create georeferenced masks, defining areas suitable for 50 m² GRs and preserving metadata. In addition, a second code based on LiDAR file processing provides masks associated to roofs with unsuitable slopes. Finally, using QGIS software, the masks are joined together and provide the user with a georeferenced representation of the roofs suitable for intervention in the city.

In terms of environmental and energy impact, cadastral information and the city's energy certificates are analysed to calculate the energy savings and CO_2 emission reductions in the buildings. The CO_2 capture potential of the roofs is also estimated according to the vegetation used. The results show the decrease in energy consumption for thermal comfort and the total amount of CO_2 mitigated in a specific period. In addition, they provide data that help users make strategic decisions, such as focusing efforts on key areas of the city. The method concludes by generating a geo-referenced map of the city with metadata using computer vision.

Applied in the mediterranean city of Valencia, the methodology revealed an estimated potential of approximately 625 hectares of modifiable green roofs, equivalent to 22,559 buildings intervened with green roofs. This would lead to an annual reduction of 162 GWh of final energy and a mitigation of 52,219 tonnes of CO_2.

Key words: Green roof (GR); Urban Heat Island (UHI); Leaf Area Density (LAD); Fanger's Predicted Mean Vote (PMV Fanger); Life cycle assessment (LCA); Geographic potential model (GPM); Extensive Green Roof (EGR); Differenced Vegetation Index (DVI); Light Detection and Ranging (LiDAR); Pendientes Sobre Limite Admitido (PSLA); Plan Nacional de Ortofotografía Aérea (PNOA); Tagged Image File Format (TIF); LAS compressed format (LAZ); Laser file format (LAS); Artificial Vision (AV).

RESUMEN

Las soluciones basadas en la naturaleza (SBN), en particular las cubiertas verdes (CV), desempeñan un papel crucial en la mitigación de la isla de calor urbana y la mejora de la eficiencia energética en entornos urbanos. Estas ofrecen notables ventajas ambientales y sociales al mejorar la eficiencia energética, la gestión del agua, el confort acústico y el bienestar social en zonas urbanos. A pesar de la creciente exploración de su potencial en grandes ciudades mediante tecnologías como modelos 3D (LiDAR), imágenes de alta resolución y análisis de datos espaciales, la falta de metodologías altamente automatizadas ha limitado su implementación a gran escala.

Este estudio presenta una metodología innovadora que simplifica y delimita la estimación del área potencial de instalación de cubiertas verdes en ciudades mediante el uso de visión artificial. Esta proporciona a los usuarios la capacidad de adaptar la visión artificial a características específicas de la ciudad y aplicar modificaciones manuales para mejorar la precisión. Mediante ortofotografías actualizadas, estas se procesan utilizando el código de MATLAB y soporte del software QGIS para crear máscaras georreferenciadas, definiendo áreas aptas para tejados verdes de 50 m² y preservando los metadatos. Además, un segundo código basado en el tratamiento en archivos LiDAR, proporciona mascaras asociadas a los tejados con pendientes no aptas. Finalmente, mediante el software QGIS, las máscaras se unen y entregan al usuario una representación georreferenciada de los tejados aptos a intervenir en la ciudad.

En términos de impacto ambiental y energético, se analiza la información catastral y los certificados energéticos de la ciudad para calcular el ahorro de energía y la reducción de emisiones de CO_2 en los edificios. También se estima el potencial de captura de CO_2 en los techos en función de la vegetación utilizada. Los resultados muestran la disminución de consumo energético para el confort térmico y la cantidad total de CO_2 mitigado en un período dado. Además, proporcionan datos que ayudan a los usuarios a tomar decisiones estratégicas, como centrar esfuerzos en áreas clave de la ciudad. El método concluye generando un mapa georreferenciado de la ciudad con metadatos utilizando visión artificial.

Aplicada en la ciudad mediterránea de Valencia, la metodología revelo un potencial estimado de aproximadamente 625 hectáreas de tejados verdes modificables, equivalente a 22,559 inmuebles intervenidos con cubiertas verdes. Lo cual, conllevaría anualmente una disminución de 162 GWh de energía final y una mitigación de 52,219 toneladas de CO_2.

Palabras Claves: Cubierta verde (GR); Isla de calor urbano (UHI); Densidad de área foliar (LAD); Voto medio predicho de Fanger (PMV Fanger); Evaluación del ciclo de vida (LCA); Modelo de potencial geográfico (GPM); Cubierta verde extensiva (EGR); Índice de vegetación diferenciado (DVI); Light Detection and Ranging (LiDAR); Pendientes Sobre Límite Admitido (PSLA); Plan Nacional de Ortofotografía Aérea (PNOA); Formato de Archivo de Imagen Etiquetada (TIF); Formato comprimido LAS (LAZ); Formato de archivo láser (LAS); Visión Artificial (AV).

RESUM

Les solucions basades en la naturalesa (SBN), en particular les cobertes verdes (CV), exercixen un paper crucial en la mitigació de l'illa de calor urbana i la millora de l'eficiència energètica en entorns urbans. Estes oferixen notables avantatges ambientals i socials en millorar l'eficiència energètica, la gestió de l'aigua, el confort acústic i el benestar social en zones urbans. Malgrat la creixent exploració del seu potencial en grans ciutats mitjançant tecnologies com a models 3D (LiDAR), imatges d'alta resolució i anàlisi de dades espacials, la falta de metodologies altament automatitzades ha limitat la seua implementació a gran escala.

Este estudi presenta una metodologia innovadora que simplifica i delimita l'estimació de l'àrea potencial d'instal·lació de cobertes verdes en ciutats mitjançant l'ús de visió artificial. Esta proporciona als usuaris la capacitat d'adaptar la visió artificial a característiques específiques de la ciutat i aplicar modificacions manuals per a millorar la precisió. Mitjançant ortofotografies actualitzades, estes es processen utilitzant el codi de MATLAB i suport del programari QGIS per a crear màscares georeferenciades, definint àrees aptes per a teulades verdes de 50 m² i preservant les metadades. A més, un segon codi basat en el tractament en arxius LiDAR, proporciona mastegares associades a les teulades amb pendents no aptes. Finalment, mitjançant el programari QGIS, les mastegares s'unixen i entreguen a l'usuari una representació georeferenciada de les teulades aptes a intervindre a la ciutat.

En termes d'impacte ambiental i energètic, s'analitza la informació cadastral i els certificats energètics de la ciutat per a calcular l'estalvi d'energia i la reducció d'emissions de CO_2 en els edificis. També s'estima el potencial de captura de CO_2 en els sostres en funció de la vegetació utilitzada. Els resultats mostren la disminució de consum energètic per al confort tèrmic i la quantitat total de CO_2 mitigat en un període donat. A més, proporcionen dades que ajuden els usuaris a prendre decisions estratègiques, com centrar esforços en àrees clau de la ciutat. El mètode conclou generant un mapa georeferenciat de la ciutat amb metadades utilitzant visió artificial.

Aplicada a la ciutat mediterrània de València, la metodologia revele un potencial estimat d'aproximadament 625 hectàrees de teulades verdes modificables, equivalent a 22,559 immobles intervinguts amb cobertes verdes. La qual cosa, comportaria anualment una disminució de 162 GWh d'energia final i una mitigació de 52,219 tones de CO_2.

Paraules clau: Coberta verda (GR); Illa de calor urbà (UHI); Densitat d'àrea foliar (LAD); Predicció Mitjana del Vot de Fanger (PMV Fanger); Avaluació del cicle de vida (LCA); Model de potencial geogràfic (GPM); Coberta verda extensiva (EGR); Índex de vegetació diferenciat (DVI); Light Detection and Ranging (LiDAR); Pendent Sobre Límit Admés (PSLA); Pla Nacional d'Ortofotografia Aèria (PNOA); Format d'Arxiu d'Imatge Etiquetada (TIF); Format comprimit LAS (LAZ); Format d'arxiu làser (LAS); Visió Artificial (AV).

INDEX

Figures Index

Table Index

CHAPTER 1. INTRODUCTION

In the following chapter, the fundamental foundations of this work will be laid, providing a brief analysis of the current global situation in relation to climate change and mitigation strategies. Emphasis will be placed on Nature Based Solutions (NBS), with a special focus on the green roof solution (GR), providing a detailed theoretical exploration of its characteristics and benefits, as well as a review of its implementation under various conditions. In addition, a comprehensive research on different studies related to the analysis of the potential of cities for the installation of GR will be conducted, thus contributing to a global understanding of its application and effectiveness in the context of climate change.

1.1 CONTEXT

Climate change and its effects on the environment are global challenges that require immediate and effective actions. In this context, the city of Valencia is facing several environmental problems that affect its quality of life and sustainability (Ajuntament de València, 2019). Among these problems are high carbon dioxide (CO_2) emissions and the need to implement innovative and sustainable solutions, such as NBS and GRs solutions.

The increase in CO_2 emissions due to human activities, such as the burning of fossil fuels, contributes to global warming and climate change. These phenomena have direct repercussions on the quality of life of the inhabitants of Valencia, such as increased temperatures, intensification of extreme weather events and degradation of the natural environment.

In addition, the city of Valencia faces environmental problems related to the lack of green spaces, loss of biodiversity and scarcity of water resources. These situations affect the health and well-being of the population, as well as the city's resilience to environmental challenges.

In this context, NBS and GRs are presented as innovative and sustainable strategies to address these problems in the city of Valencia. NBS, such as the creation of urban green areas, restoration of natural ecosystems, and sustainable water management, offer significant benefits, such as reducing local temperature, improving air quality, and conserving biodiversity. GRs solutions in particular, which involve the installation of vegetation on building roofs, besides helping mitigate the urban heat island effect and promote biodiversity in urban environments, can improve the energy efficiency of buildings.

1.2 OBJECTIVES

This master thesis will focus on assessing the potential of the city of Valencia for the implementation of GRs and the associated benefits, with the aim of providing viable solutions to the city's environmental challenges in terms of climate change, CO_2 emissions and quality of life. To this end, the following specific objectives are established:

- Review of the state of the art of GRs in the built environment. Complete understanding of their technical, economic and environmental features.

- Development of a Code with Semi-Assisted Artificial Vision: this code will seek to identify and quantify the potential area of the city of Valencia for the implementation of GRs using orthophotographs, facilitating the accurate estimation of roof surfaces susceptible to intervention.
- Analysis of Roof Slopes in Buildings: Through the development of a specialised code, a point cloud generated by a LiDAR (Light Detection and Ranging) file will be analysed to identify the slope levels on the roofs of buildings. This analysis will allow to discard those buildings that are not suitable for the installation of GRs.
- Estimation of GRs to be Installed in Valencia: A detailed calculation of the number of GRs that could be installed in the city will be carried out, considering the relevant urban and architectural variables.
- Calculation of Energy Savings and their associated CO_2 Emission Reduction: The potential energy savings and consequent reduction in CO_2 emissions that could be achieved through the implementation of GRs in Valencia will be estimated.
- Evaluation of CO_2 Sequestered by GRs: The amount of CO_2 that could be sequestered by the installed GRs will be calculated, thus contributing to a comprehensive quantification of the environmental benefits of this initiative.

1.3 STATE OF ART

In the following section, there will be a deeper exploration of the NBS, exploring in detail the characteristics and benefits of GRs. In addition, an analysis of case studies that have investigated objectives similar to those of this paper will be included, providing valuable insights and contextual understanding.

1.3.1 NATURE BASED SOLUTION

NBS are defined as solutions with approaches and strategies that use natural processes and elements to address environmental, social, and economic challenges. These solutions are inspired by nature and seek to emulate or work in harmony with natural ecosystems to achieve sustainable outcomes (CONAMA, 2020). This is based on the recognition that natural ecosystems provide a wide range of services and benefits for human well-being, such as the provision of clean water, climate change mitigation, protection against natural disasters, biodiversity conservation, and improved quality of life. By incorporating these services into the design and planning of solutions, NBS seeks to harness nature's benefits effectively.

NBS can take many forms and address a variety of challenges. Common examples include restoration of natural habitats, creation of urban green areas, implementation of green infrastructure, sustainable water management, sustainable agriculture and forestry, protection, and conservation of key ecosystems, among others. The application of NBS in different contexts, such as mediterranean cities, aims to address specific problems facing these areas, such as water scarcity, land degradation, rising temperatures and biodiversity loss.

Some examples of the most common applications of NBS in mediterranean cities are:

1. Green infrastructure: The creation of urban green areas, parks and biological corridors can help to increase biodiversity, reduce the urban heat island effect, and improve air and water quality.
2. Sustainable drainage systems: The implementation of sustainable urban drainage techniques, such as GRs, rain gardens and artificial wetlands, can help mitigate flooding problems and improve water management in cities.
3. Restoration of natural habitats: Rehabilitation and conservation of coastal ecosystems, forests and natural protected areas can help preserve biodiversity, protect the coastline, and provide key ecosystem services such as flood protection and water filtration.
4. Urban agriculture and community gardens: Promoting urban agriculture and community gardens in mediterranean cities can foster local food security, reduce carbon emissions associated with food transport and promote social cohesion.

1.3.2 GREEN ROOFS

GRs are an ancient practice used around the world for centuries to achieve thermal comfort in buildings. From the iconic Hanging Gardens of Babylon to their revival in the 20th century, especially in Germany, they have experienced technological advances and have become an efficient and valuable technique. Germany led the GR market with an estimated value of 254 million euros in 2015. Within the NBS, GRs stand out as an innovative solution in the green infrastructure category. These systems, which integrate vegetation on the roofs of buildings, represent an effective way of utilizing urban spaces for environmental and social benefits. Their implementation is a clear example of how NBS can be adapted to address specific challenges in urban areas, offering multiple benefits for both the environment and local communities. Therefore, the following topics in this section will be devoted to exploring in detail these types of solutions, elaborating on their definition, types, and benefits.

1.3.2.1 Definition

GRs represent a structure that involves covering the surface of a roof with vegetation, substrate, and drainage systems suitable for promoting plant growth. These roofs can vary in design and complexity, ranging from thin layers of low-maintenance vegetation to raised gardens with a wide variety of plants, including grasses, shrubs, and even trees. In addition, they incorporate advanced technologies and materials such as waterproof membranes and specialised anti-root layers, along with drainage systems and substrates specifically designed to optimize plant growth and water management, as detailed in (Cascone, 2019).

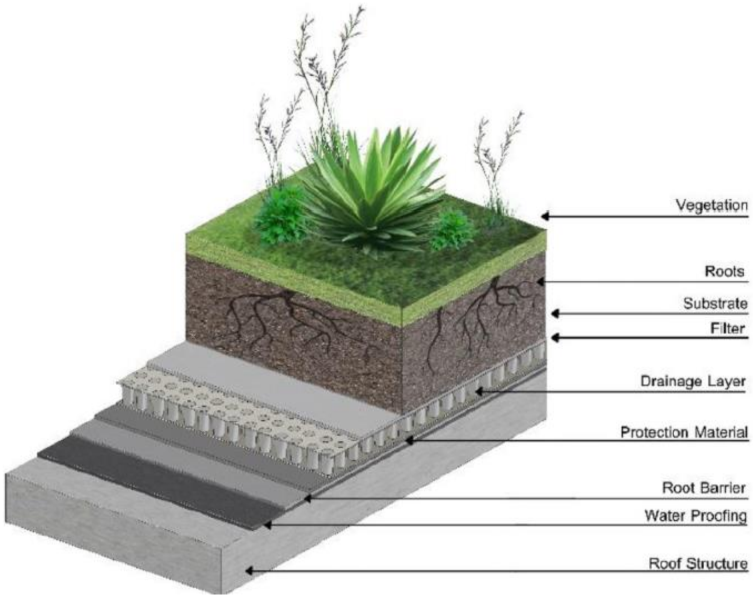

Figure 1*: Typical structure of a GR (Mihalakakou, et al., 2023).*

GRs not only have aesthetic value but also offer several environmental and social benefits. These include improving air quality by filtering pollutants, reducing the Urban Heat Island (UHI) effect by reflecting more heat and absorbing less, increasing biodiversity by providing habitats for insects and birds, and sustainable water management by retaining and filtering rainwater. In addition, GRs improve the energy efficiency of buildings by acting as thermal insulation, thereby reducing the need for heating and cooling. They also provide additional green space in densely populated urban areas, contributing to the well-being and mental health of residents by providing places for recreation and relaxation.

According to the literature, GRs are defined as vegetated structures with multiple layers including vegetation, soil, a filter layer, a drainage layer, a waterproofing layer, and a structural cover (Figure 1), as outlined in (Tabatabaee, Mahdiyar, Durdyev, Reza Mohandes, & Ismail, 2019). The choice of plants adapted to the local climate and roof conditions is crucial for the long-term success of GRs, underlining their role in sustainable urban design and in improving the quality of life in urban environments. These structures have a rich history and evolution, as reflected in (Oliver, 1997), showing their integration into different cultures and habitats. In Scandinavian architecture, GRs are an example of the harmony between building and nature. (Abass, Ismail, Abd Wahab, & Elgadi, 2020) highlights the complexity and diversity of GRs, from simple vegetal layers to ecological systems integrated into modern urban architecture.

About what is mentioned (Cascone, 2019), the structure of a GR consists of several layers, from the base upwards: an impermeable membrane, an anti-root barrier, a protection layer, a water storage and drainage layer, a filter layer, a substrate and vegetation. Each layer has a specific function to ensure the success of the GR. For example, the waterproof membrane prevents infiltration and resists environmental conditions, using bituminous membranes. The anti-root barrier protects against damage caused by vegetative roots and is integrated with the waterproof membrane.

The protection layer protects the lower layers during construction and use, while the water storage and drainage layer prevents waterlogging and excessive structural loading. The filter layer separates the substrate from the drainage layer, preventing blockages. The substrate is essential in GRs as it serves several long-term functions, such as improving water quality, reducing peak flow, and providing thermal and acoustic insulation. Its thickness and weight depend on factors such as vegetation, roof geometry, and climatic conditions, and it must have appropriate physical and chemical parameters.

The choice of plants is critical to the success of a GR, as they influence water and air quality as well as thermal performance. Sedum-type plants are common in GRs due to their ability to withstand drought and store water. Other suitable species vary according to climate. GRs offer numerous benefits, such as the absorption of solar radiation, which prevents the waterproofing membrane from heating up during the day and cooling down at night, which could crack it and reduce its durability. They can also reduce daily temperature variation, maintain lower internal temperatures, and improve sound insulation.

However, it is important to note that GRs can have a higher initial cost compared to traditional roofs, so their choice depends on environmental concerns and the location of the project. In regions with mediterranean climates, GR design faces particular challenges due to mild winters and hot summers with summer droughts. In these conditions, the choice of plants, substrates, and adaptive design techniques is critical to the success of GRs in the mediterranean region.

1.3.2.2 Types

There are several types of GRs, each with unique characteristics that make them suitable for different contexts and objectives. From low-maintenance GRs and hardy vegetation to impressive, raised gardens. Below are the three main types (Figure 2):

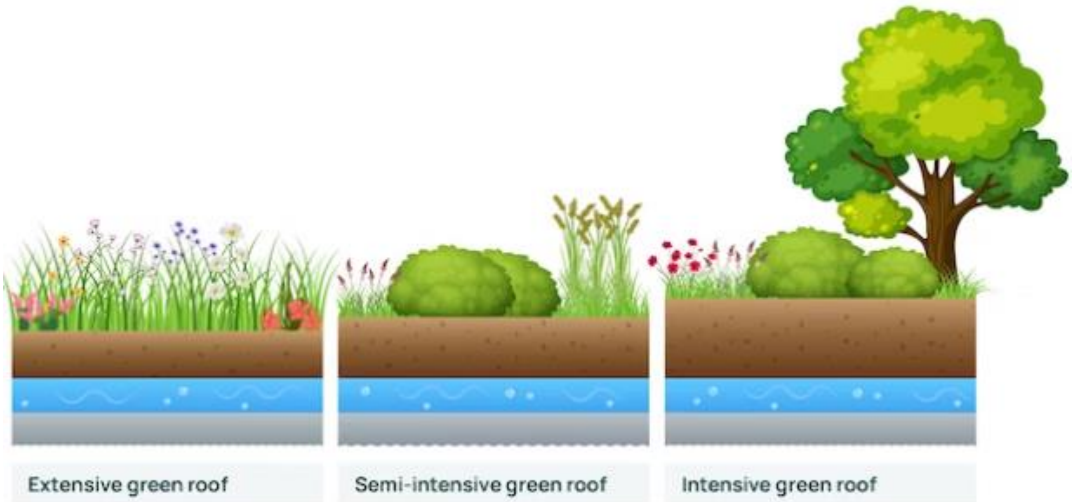

Figure 2*: Types of green roofs. Source: ANS Group Global, https://www.ansgroupglobal.com/blog/what-are-the-best-plants-for-green-roof-systems.*

Extensive Green Roof

Extensive Green Roof (EGR) is a type of GR characterised by a thin substrate layer (usually 2.5 to 15 centimetres thick) and a lighter design compared to intensive green roofs (IGR). In this type of GR, mainly low-growing plants such as Sedum, succulents and other species resistant to the extreme conditions of the urban environment are used.

Due to their lighter design and choice of low-maintenance plants, EGRs require less attention and care than IGR, making them a popular choice for green infrastructure projects in urban areas. In addition to the aforementioned features, these roofs are ideal for improving energy efficiency and rainwater management in buildings, as detailed in (Berardi, GhaffarianHoseini, & GhaffarianHoseini, 2013).

Regarding the size of this type of roof, values are not standardised, ranging from 10 to 100 m^2. Studies such as, (Koroxenidis & Theodosiou, 2021) consider 100 m^2 or others such as (Saadatian, et al., 2013) and (Bevilacqua, Bruno, & Arcuri, 2020) consider 50 m^2. In the case of this study, which focuses on EGR, a standard size of 50 m^2 will be used to cover a larger potential area, taking into account sizes that will be studied in later stages.

Intensive Green Roof

IGR is a type of GR that is characterised by a thicker substrate layer (usually 15 to 60 centimetres thick) and a more complex and varied design compared to EGR. Regarding the size of the IGRs, this depends entirely on the size of the surface on which they are mounted.

In IGRs, a wide variety of vegetation can be planted, including trees, shrubs, flowers, and other larger and faster-growing plants. This allows for the creation of more elaborate and diversified gardens and green spaces, often with recreational areas, paths, and recreational areas for the residents or users of the building.

Due to their more complex design and the presence of a greater variety of vegetation, IGRs require more attention and maintenance compared to EGRs. Greater care is needed for watering, pruning and fertilisation to maintain the health and proper growth of the plants. However, these roofs can act as important recreational areas and enhance local biodiversity, as discussed in (Gagliano, Detommaso, Nocera, & Evola, 2015) and are especially valuable in densely populated urban areas.

IGRs are often used in architectural projects that seek to create more elaborate and multifunctional green spaces in urban environments, contributing to the enhancement of biodiversity and the improvement of the urban landscape. However, due to their greater weight and complexity, they require proper planning and may require a stronger supporting structure to ensure the safety and stability of the building.

Semi-Intensive Green Roof

Semi-Intensive Green Roof (SIGR) is a type of GR that combines characteristics of extensive and intensive GRs. It is midway between the two types in terms of substrate thickness and vegetation selection. As with IGRs, the size of a SIGR is limited by the available roof surface area. They can range from small areas to large roof spaces on commercial or residential buildings.

In a SIGR, the substrate layer is usually thicker than in an extensive one, generally between 10 to 30 centimetres thick. This allows for a greater diversity of plants than those found in an EGR, but still focuses on low-maintenance, low-growing species. The vegetation used includes a mix of low-growing plants, such as Sedum and other hardy species, along with some larger species, such as grasses and shrubs.

The advantage of this type of cover is that they can provide some of the benefits of IGRs, such as increased biodiversity and aesthetic appeal, without requiring the same level of care and maintenance. In other words, they offer a balance between ecological benefits and ease of maintenance. They can be particularly useful in urban regeneration projects where green spaces are sought. However, as with other types of IGRs, proper planning and an appropriate support structure are required to ensure their success and durability.

1.3.2.3 Benefits

Key benefits of GRs in the fight against climate change include reducing energy consumption, improving air quality through indirect CO_2 sequestration and abatement, and increasing urban water quality (Mihalakakou, et al., 2023). Each of these main benefits is specifically detailed below:

Energetic benefits

As indicated in the article (Mihalakakou, et al., 2023), an average of 20% of urban surfaces are roofs, adding to this that numerous studies indicate that the installation of GRs provides a reduction in energy demand for air conditioning. The energy benefit of installing this type of NBS leads to a decrease in energy consumption and an improvement in thermal comfort in both summer and winter.

The performance of GR depends directly on the type, the vegetation used, local climatic conditions and the geometry of the building. In parallel, the reduction of the outdoor temperature depends on the GR surface and its vertical distance from the pedestrian level. On the other hand, indoor temperature regulation is affected by the reduction of the roof temperature and is limited to the area where GR is installed. Although GRs do not contribute significantly to winter heating needs, they can reduce point source pollution through combined systems designed to purify flue gas emissions from HVAC systems.

The main benefits obtained in different models studied by (Mihalakakou, et al., 2023) are presented below in a general way, considering different locations and forms of GRs:

a) Overall decrease in energy use for cooling (about 70%) and thus an increase in annual energy savings ranging from 10% to 60%.
b) Decrease in indoor temperature in summer, which in some extreme cases can reach 15°C.
c) The effects of GRs can be greatly enhanced by using green walls or trees.
d) The effects may not be as efficient in reducing heating needs in winter, but still offer benefits in terms of energy efficiency and sustainability in a variety of climates.

It should be noted that the points mentioned above correspond to a summary of the extensive work carried out by the mentioned reference. However, for this study it is key to delve into the results obtained in other works in mediterranean cities in order to understand the benefits of GRs in the city of Valencia.

The first case corresponds to the city of Athens in Greece (Foustalieraki, Assimakopoulos, Santamou, & Pangalou, 2017), where an experimental test of heating and cooling effects showed that GRs act as an effective insulating layer. Since, surface temperatures decreased significantly compared to a conventional roof, obtaining energy savings in heating (peak of 11.4%) and cooling (peak of 18.7%) of approximately 15%.

Among the studies reviewed, (Berardi, GhaffarianHoseini, & GhaffarianHoseini, 2013) analyses GRs as ecological systems integrated in urban environments with a high effectiveness in reducing energy consumption, reducing it by up to 90% in summer and 30% in winter thanks to their thermal insulation capacity. This reflects how GRs contribute significantly to the mitigation of the UHI effect, reducing the surface temperature by up to 7.3 °C and the ambient air temperature by approximately 0.5 °C.

Another outstanding case corresponds to the experimental test accompanied by a simulation of the heating and cooling effects in the city of Lisbon in Portugal. In the trial (Matos Silva, Gomes, & Silva, Green roofs energy performance in Mediterranean climate, 2016) the energy efficiency of different types of GRs (extensive, semi-intensive and intensive) is analysed in comparison with traditional roofs. It is highlighted that SIGR and IGR are more efficient in terms of cooling energy needs, reducing these needs by 36% and 17% respectively, compared to EGR. In addition, it is mentioned that these types of GRs are more efficient on an annual basis than traditional roofs, and that the level of thermal insulation influences the energy savings achieved.

The experimental test accompanied by a simulation carried out in Rome, Italy, (Evangelisti, Guattari, Grazieschi, Roncone, & Asdrubali, 2020)on the cooling effect produced by GRs showed that, during a typical winter week, the PMV index remained within a range between -1 and 1 (PMV is a measure of the overall thermal sensation corresponding to a given thermal environment). This range indicates a generally acceptable level of thermal comfort, with 0 representing thermal neutrality. Most people would feel neither hot nor cold, suggesting that conditions remained within an acceptable thermal comfort range during the winter.

Finally, the potential area estimation model study by (Zayas Orihuela, 2023) presents an assessment of the energy savings and carbon emission reductions associated with the implementation of GRs. Based on several studies conducted by the Polytechnic University of Valencia, Zayas et al. indicate that, in the climatic context of Valencia, single family dwelling can anticipate a 17% decrease in their energy consumption following the installation of GRs. These results are consistent with similar findings from research in the Valencia metropolitan area. For high-rise buildings, energy savings vary by floor, with a 17% reduction on the highest floor and progressively smaller reductions of 6%, 1.5% and 0.5% on the lower floors. The total energy savings are calculated by considering the energy consumption per living area of each building and this information is used to estimate the reduction in energy-related carbon emissions, considering the local energy composition.

Air Quality

The impact of GRs on air quality is closely related to the plants that make them up. In general terms, the characteristics of these plants that provide benefits are as follows:

a) Ability to remove pollutants (O_3, NO_2, SO_2) and capture particulate matter.

b) Evapotranspiration and shading for the reduction of surface temperatures, contributing to reduce photochemical reactions and the generation of atmospheric pollutants, while promoting energy savings in cooling, resulting in a reduction of CO_2 emissions.

c) Photosynthesis process making a key contribution to CO_2 sequestration.

Various literary sources have dealt in depth with the subject of GRs and their relationship to climatic conditions and their constituent components. In this context, the study by (Tan, Kong, Yin, & Coo, 2023) stands out for its detailed analysis of CO_2 sequestration by GRs. This work focuses on the direct and indirect CO_2 reduction processes in these systems, considering factors such as vegetation, substrate and building environment. In addition, it addresses different methods to quantify CO_2 reduction and discusses the environmental benefits of GRs, highlighting the importance of interdisciplinary research for a better understanding and evaluation of the potential of GRs in CO_2 reduction in urban areas.

On the other hand, (Mihalakakou, et al., 2023) indicates that the capture and storage capacity of GRs, according to several studies analysed, is effective in cleaning a total of 1,675 kg of polluted air in an area of 19.8 hectares. This study presents the results obtained from experiments carried out in the city of Manchester, England, using endemic vegetation. The records provided indicate a significant decrease in annual air pollution, with a cumulative reduction of 0.21 tonnes of PM_{10} particulate matter and a decrease in $PM_{2.5}$ particulate matter levels ranging from 7% to 33% across the urban area. In a similar context, (Kong, Shi, & Chu, 2014) analyse carbon storage capacities in Hong Kong, observing significant differences between grass and soil biomass. While grass biomass stores between 0.05 to 0.21 kg C/m², soil can store between 1.26 to 4.89 kg C/m² to a depth of 15 cm. The study also examines the carbon emissions associated with the maintenance of these turfgrasses and their offset by stored carbon, which could occur over a period of 5 to 24 years, further highlighting the seasonal variation in the relationship between turfgrass respiration and soil carbon storage capacity, especially during the wet season.

Additionally, (Shafique, Xue, & Luo, An overview of carbon sequestration of green roofs in urban areas, 2020) investigates CO_2 sequestration through the performance of GRs in urban areas, focusing on the direct and indirect reduction of carbon emissions. The direct impact involves vegetation and soil media in capturing and storing air pollutants at the building level, while the indirect impact includes long-term effects, such as decreasing the energy consumption of buildings. The paper highlights the importance of vegetation and soil properties in the performance of GRs, providing quantitative data on CO_2 sequestration according to the plant used in GRs in Spain.

Finally, (Ondoño, Martínez-Sánchez, & Moreno, 2018) explores the CO_2 sequestration potential of GR prototypes in a mediterranean climate. This study focuses on how the composition and depth of the substrate, together with the selected plant species, influence the carbon and nitrogen sequestration capacity. It reveals that deeper substrates and the selection of perennial plants can significantly improve CO_2 sequestration, providing quantitative data such as the achievement of sequestering up to 1,702.19 g C and 183.21 g N_2 per m² in two years with a specific substrate and plant combination.

Life cycle assessment

As discussed in this section, GRs provide greater environmental benefits than a conventional roof. This is due not only to their performance, but also to their entire product life cycle.

The analysis provided by (Mihalakakou, et al., 2023) covers a wide range of comparisons between study types (comparative or case studies), the types of GRs investigated (EGR, IGR, SIGR or conventional roofs), or the layers of GRs (root barrier or substrate), the selected duration, functional unit, and system boundary, along with environmental impact categories, methodologies and corresponding key results. At each stage of the life cycle, these comparisons demonstrate significant advantages over a conventional roof.

Finally, this study concludes that during the manufacturing stage, the process represents the greatest environmental impact over the entire life cycle of a typical roof. Roofing materials such as polyurethane, polyethylene, mineral wool, among others, require a substantial amount of energy to produce, resulting in substantial emissions of pollutants.

Other Benefits

GRs offer a variety of additional benefits beyond their direct impact on climate change and air quality. According to (Mihalakakou, et al., 2023), they have the capacity to retain 40-60% of rainwater, which varies depending on roof type, substrate depth, humidity, plant species, plant size, as well as rainfall duration and intensity. This water retention capacity improves water quality in cities, reducing the risk of flooding and overloading urban drainage systems. In addition, GRs contribute significantly to noise reduction, both inside and outside buildings, thanks to the higher acoustic absorption provided by vegetation compared to conventional roofs. This feature is particularly valuable in densely populated urban environments, where noise can have a negative impact on quality of life (Shafique, Kim, & Rafiq, Green roof benefits, opportunities and challenges – A review, 2018).

In terms of biodiversity and ecosystem, GRs act as important renaturation points in cities. They create habitats for diverse species and increase urban biodiversity, improving the health of the local ecosystem. From a socio-aesthetic and psychological point of view, they provide tranquil and aesthetically pleasing green spaces that can improve the mental and physical health of urban residents, as well as foster social cohesion and a sense of community.

In terms of economic benefits, GRs can contribute to green building certification and offer long-term savings in terms of energy and water management. However, it is important to consider the initial installation and maintenance costs, as well as the additional structural requirements that may be necessary.

Among the works that study these benefits. (Berardi, GhaffarianHoseini, & GhaffarianHoseini, 2013), analyses GRs as ecological systems integrated in urban settings, presenting numerous environmental benefits. Indicating that these systems function as natural filters that improve air quality and manage rainwater efficiently, which reduces urban runoff and alleviates the load on drainage systems. Furthermore, GRs offer additional benefits such as sound insulation, reducing noise pollution in densely populated areas, and promote biodiversity by providing new habitats for various species.

Finally, the study by (Møller Francis & Bergen Jensen, 2017) evaluates the effectiveness of GRs in three areas: reduction of the UHI, reduction of urban air pollution and reduction of energy consumption of buildings. Focusing on the benefits discussed in this topic, the study found that GRs can reduce street temperatures by up to 3°C, with a highly variable range of effectiveness. In terms of air purification, GRs can remove up to 9.1 g/m² per year of PM_{10} particles.

1.3.3 LITERATURE REVIEW: GREEN ROOF MODEL ANALYSIS

Considering the definition of GR and its advantages, it is essential to review the existing literature to assess how other authors have approached the analysis of the potential of roofs in different cities to be transformed from a conventional roof into a GR. This review will also focus on the use of image recognition technologies and artificial vision (AV).

Different studies consider a wide range of indicators to classify potential areas within a city that can be converted to GRs. As indicated in the study by (Santos, Tenedório, & Gonçalves, 2016), which presents a methodology to assess urban potential considering ground level and rooftop areas in cities with mediterranean climate.

In this study, mainly the topic associated to rooftops, a 3D model based on LiDAR and VHR (Very High Resolution) images was used to perform a detailed estimation of the available roof surfaces considering physical aspects, such as slope, orientation and shadows cast by surrounding buildings and topography.

This surface estimation of vegetation in Lisbon was carried out using planimetric and altimetric data. A VHR image and a map from the municipal cartography were used, together with 3D data obtained from a 2006 LiDAR flight. Additionally, a WorldView-2 (WV-2) image captured on 29 June 2010 was used, with a spatial resolution of 2 m in multispectral mode (8 bands), a pixel size of 0.5 m in panchromatic mode, and a radiometric resolution of 11 bits.

Once the roof surface model was obtained, the roofs were classified by their material, since roofs made of tiles are not viable for the assembly of GRs due to their high need for investment in the replacement of structure and materiality. For this, the classifier considered features such as spectral/colour response, size, shape, texture, pattern, shadow and spatial association to find features that are similar to those defined in the training set. Finally, the result was a map with the rooftops of the city without red tiles, which represent 19% of the total surface of Lisbon. It is important to mention that roofs with at least 85% of their area without tiles were considered as roofs without tiles, in order to reduce the delimitation errors of the software used.

On the other hand, characteristics such as the inclination of the roofs, together with the area and the level of light they receive, were modelled using the DSM (Digital Surface Model) altimetry, the location from the footprints of the buildings and the solar radiation analysis tools of ArcGIS (ESRI).

Finally, in order to select the roofs with the greatest potential, roofs with areas greater than 10 m^2 and inclinations of less than 45° were considered as selection criteria, since values greater than the angular limit implied greater investment in complex models and maintenance. In addition to the above, the criteria based on the incident sunlight on the roofs should be added for the selection of plants requiring or not requiring irradiation, which was divided into sunny roofs (3 to 4 hours of sun per day), shady roofs (less than 3 hours of sun per day) and sunny to cloudy (generic roofs). With the defined criteria, the results obtained were divided into two scenarios: "Flat Green Roof Scenario" (roofs with a slope equal to or less than 11° and low investment in infrastructure) and "Pitched Green Roof Scenario" (roofs with a slope equal to or less than 20° and high investment in infrastructure to avoid plant slides, protection against erosion and impermeability).

For first case, a sunny to cloudy roof condition was considered, resulting in a total of 4,545 buildings suitable for retrofitting. On the other hand, for second case where the same type of solar condition was again selected, 4,592 buildings were identified with the possibility of green retrofitting. Each scenario represents in total an increase of 14.4% of Lisbon's total green areas, with new green surfaces of 2,184,291 m^2 and 1,534,337 m^2, respectively. It should be noted that the methodology used by (Santos, Tenedório, & Gonçalves, 2016) does not consider obstacles on rooftops, such as chimneys, overhangs, antennas, among others, as it involved a DMS with a sub-metric resolution, obtained from a point cloud with higher density (more than four points/m^2) and a derived DMS with higher resolution.

Another study to highlight is the one carried out by (Matos Silva, Flores-Colen, & Antunes, Step-by-step approach to ranking green roof retrofit potential in urban areas: A case study of Lisbon, Portugal, 2017) in the city of Lisbon. This study presents a methodology for classifying the level of potential of buildings for the installation of GRs, by identifying real possibilities for rehabilitation and using an urban index that indicates the need to increase green areas in each neighbourhood.

The first step of this methodology consisted of determining the indices necessary for the selection of neighbourhoods. Nineteen indices were identified and divided into two groups: Indices typifying building characteristics (Year of construction (YC), Floor area ratio (FAR), Number of floors (NF), Green quality (GQ), Roof type (RT), GR type (GRT), Roof slope (RS), Building load capacity (BLC), Roof load capacity (RLC), Solar orientation (SO), Building use (BU), Rooftop available area (RAA)) and indices representing the urban environment (Built density (BD), Green urban areas (GUA), Census data (CD), Population density (PD), Site coverage (SC), Green surface area (GSA), Urban trees (UT)). Of these indices, the most used are roof type, GR type, number of floors, solar orientation, building use, land cover type, building density and urban green areas. However, for this study, the indices of building use and GR type were omitted.

Following the methodology presented by Matos Silva et al. the next step is to define the number of zones to divide the city. Then, the mentioned indices are ranked by a scale from 1 to 5 in order to have an equal weighting between them. Finally, 5 different levels are created for the buildings, where level 1 represents buildings with no possibility of retrofitting with GRs or urban areas with large green areas with no need for retrofitting and level 5 represents buildings with adequate structural capacity and slopes as well as urban areas with a crucial need for greening. In other words, areas are classified according to the YC and RS criteria.

An example of this classification presented in the study are buildings constructed before 1930, which are typically categorised between level 1 and 3. In contrast to buildings constructed after 1930, which are typically categorised between levels 4 and 5. Continuing with the classification, in order to deepen the characterisation for selection, selection criteria are added based on the existing green areas in the city. These criteria correspond to SC, GSA and UT.

Finally, a comparison is made between the first 3 indices given by means of three tests (A, B and C) that attribute a proportionality to each value scaled from 1 to 5. According to the fact that the YC criterion (for the author) is more important than RS, Matos Silva et al. considers that only 9 districts of Lisbon are suitable for vegetal rehabilitation, corresponding to 79.2 to 75.2 % of the total area of the city.

In the same line of studies, but corresponding to a non-mediterranean climate, is the work carried out by (Slootweg, et al., 2023). This study developed a spatial analysis model capable of simultaneously identifying the geographical potential of rooftops for EGR and photovoltaics (PV) panels. This model examines building characteristics such as slope, orientation, load-bearing capacity and roof shading.

The work by Slootweg et al. was carried out in the municipality of Amsterdam (Netherlands), which has approximately 900,000 inhabitants and a total of 400,000 houses of different years of construction and used a model consisting of 5 working methodologies.

The first step of the model focused on analysing the spatial data of the municipality of Amsterdam, focusing specifically on the elevation and building of the area. Once this data was obtained, the model was asked to evaluate and classify the roofs in terms of adequate and moderate, taking into account their orientation and slope as the main criteria.

For the classification of roofs, Slootweg et al. consider the criterion that roof slopes less than 10° are considered adequate, while those greater than 10° but less than 45° are considered moderate. Roof orientation, on the other hand, was only taken into account to assess the potential for mounting PV panels, so it does not have a major impact on the analysis of roof potential for retrofitting. It should be noted that this model does not consider the load-bearing capacity of the roofs, as the buildings are of such varied age that a one-by-one analysis must be carried out.

With the data and the classified buildings, the geographic potential of EGRs, PVs and the EGR-PV combination was modelled. ArcGIS was used to calculate the slope and orientation of the roofs, based on AHN3 data ('Actueel Hoogtebestand Nederland', corresponding to topographic dataset of the Netherlands) with a resolution of 0.5 × 0.5 m. Suitable and moderate roofs were clustered, considering areas of at least 10 m^2 for accuracy. The clusters were then aggregated to each neighbourhood and normalised to the total area of roofs in each neighbourhood.

Once the three roof systems (EGRs, PVs and EGR-PVs) are classified as suitable and moderately applicable, they are then plotted on maps corresponding to the municipality for spatial analysis. Finally, and as a complement to the generated maps, a classification of the buildings according to their use (industrial, commercial, service, residential and others) and their years of construction is introduced to understand how the year of construction can give an indication of the bearing structure of the buildings.

Finally, the results obtained by the model indicate that the potential of the municipality is approximately 1,197 hectares in EGR alone. However, if an EGR-PVs system is considered, the potential is lower and corresponds to approximately 1,057 hectares. In the case of EGR alone, the potential amounts to 47% of the total available area in Amsterdam. In parallel, this potential translates into an increase of 5.5% of the existing green areas in the municipality. On the other hand, the ERG-PVs synergy, in addition to a potentially smaller area, requires ideally flat roofs or roof slopes of less than 10°, and the initial investment of this joint system represents a large cost due to the requirement of extra materials according to the literature review indicated by Slootweg et al.

Regarding building types, the model indicates that industrial buildings have a higher potential for an ERG-PVs system, as they have the highest number of flat roofs. On the other hand, residential buildings have the highest potential for retrofit areas by means of ERGs. At the same time, buildings constructed after 1977 were considered to be suitable for the installation of the mentioned systems, as they comply with the regulations introduced in the EUROCODE.

As the last study to be analysed, the work carried out by (Brenner, Schmidt, & Albert, 2023) stands out for its distinctive approach in the evaluation of the potential of urban roofs. The fundamental purpose of this research was to develop and apply a socio-ecological approach to explore and prioritise current and future opportunity spaces for the implementation of GRs. This approach was based on the analysis of remote sensing data and had as its main objective the mitigation of the effects of the UHI.

This study was carried out in the city of Krefeld, which is located in the urban area of Mönchengladbach and has an area of 137 km^2 with a total of 234,000 inhabitants. A modular approach was applied in three consecutive steps to identify priority areas for the creation of GRs in the years 2019 and 2030 (for the present study, only the results obtained in the year 2019 will be mentioned).

The first step, carried out by Brenner et al., was the analysis of the heat vulnerability of urban areas, assessing the heat exposure of urban structures and the heat sensitivity of urban inhabitants and facilities. Secondly, an inventory of GRs was carried out and their potential to be converted into green space was assessed using spectral data from aerial imagery using the Differentiated Vegetation Index (DVI), which was done by detecting vegetation in these areas. Subsequently, by calculating DVI for each of the high-definition images used in the study, areas were classified to distinguish between non-vegetated, extensive roof greening and intensive roof greening. The potentials for roof greening were derived under the following assumptions: unvegetated roof areas were assigned a high potential; extensive roof greening and pixels classified as uncertain were classified with a medium potential; and intensive roof greening was assigned a low potential. On the other hand, the definition of thresholds for this classification varied according to the reflectance (a measure of the ability of a surface or material to reflect light falling on it) of the features, which could differ between images due to various factors such as time of day, phenology, incident radiation, cloud cover, shooting angle and vegetation spectral information.

As a third step, the results obtained from the vulnerability analysis and the inventory of GRs were cross-checked in order to identify the areas of opportunity that present a high priority for roof rehabilitation. ArcGIS Desktop 10.6.1. was used for this purpose, considering roof areas highly affected by heat and with a high or medium potential for vegetation as the highest priority, as they are the most suitable for reducing the UHI effect. Roofs with low vegetation potential were assessed as medium priority in the prioritisation process.

Finally, the results indicate that 7% of the city area is classified as an area of high heat vulnerability. Within this vulnerable area, 49% (59 hectares) of the total area covered is considered to have a high potential for rehabilitation. In parallel, it is indicated that utilisation of this potential could decrease the air temperature by 0.2°C at two metres above the ground. The roofs considered for retrofitting were flat or with a slope of less than 45°, however, the properties of these roofs, such as the maximum load bearing capacity, as well as other roof types such as offset gable roofs, mixed roof types or also steeper areas such as pitched roofs, were not considered.

In response to the previous studies reviewed, it is evident that there is a remarkable diversity in the methodologies used to analyse the potential of cities or localities based on images or similar data. However, until now, none of these studies has provided a standardised approach that can be applied in a generalised manner to different locations. Furthermore, in this comprehensive review of the existing literature, a marked paucity of research related to GR intervention in cities along the Spanish mediterranean coast, in particular in the Valencia region, has been noted.

This highlights the urgent need, on the one hand, to develop a standardised methodology for estimating the total potential roof area in various cities around the world that could benefit from such interventions, including an estimate of the savings in energy consumption and CO_2 emissions mitigation. Furthermore, taking advantage of Valencia's status as a green capital, this study could not only contribute to consolidate this quality and maintain its prominent position, but could also provide valuable solutions to effectively address the challenges posed by the urban environment of cities with predominantly flat roofs.

CHAPTER 2. METHODOLOGY

In the following chapter, the methodology to be used in this study will be explained in a general way for its massive application. This methodology will follow the steps indicated in the Figure 3.

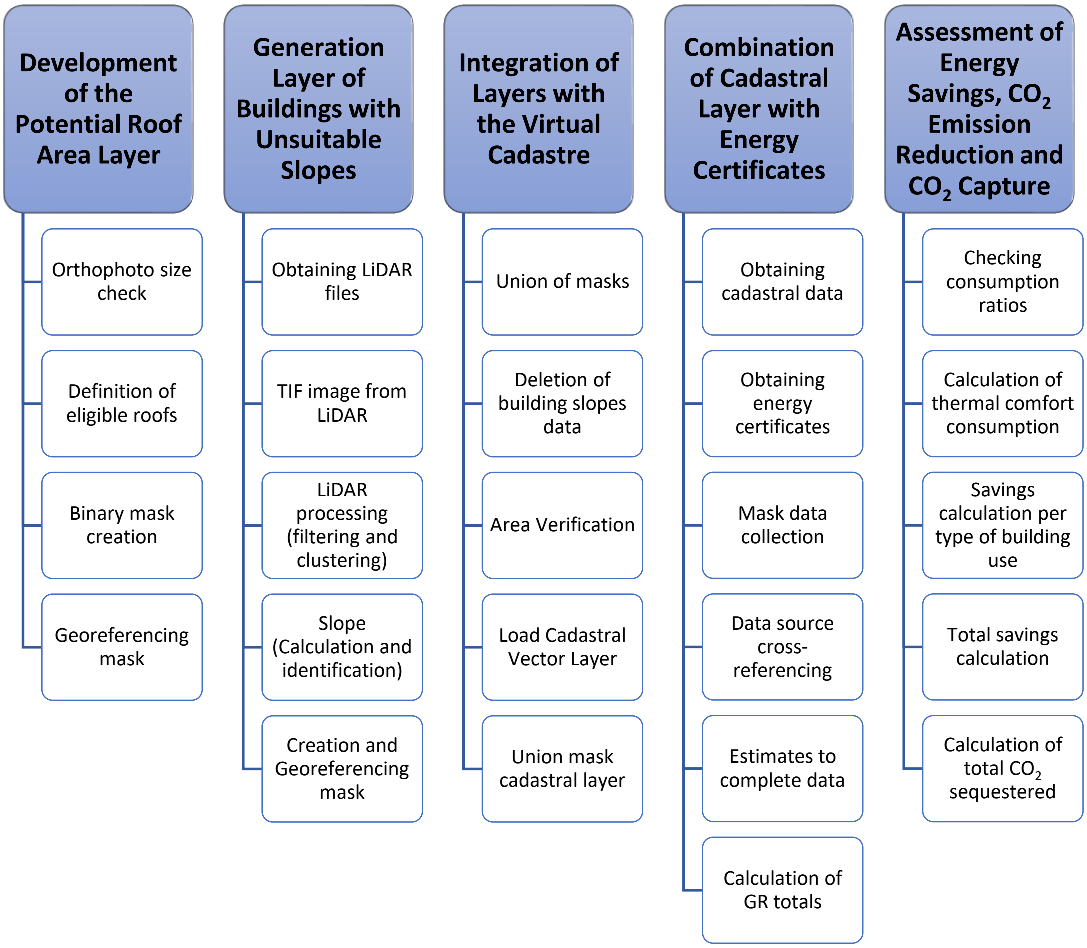

***Figure 3**: Diagram representing the general step-by-step to be followed in the methodology presented in this section.*

2.1 DEVELOPMENT OF THE POTENTIAL ROOF AREA LAYER

This section presents the first step of the methodology corresponding to the elaboration of the potential roof area layer. The main objective of this step of the methodology is to generate, using georeferenced images in *TIF* format (a graphic file format that stands out for its flexibility and wide compatibility, ideal for storing high quality images), a visual representation of the roofs that present surfaces potentially suitable for the installation of GRs. To achieve this, two *MATLAB* codes were developed:

- *ROOFTYPESET.m:* Code that provides a graphical interface for loading and selecting rooftop images. It allows users to define and add new roof types or colour regions to an existing database, thus facilitating the accurate and automated identification of different types of roofs, crucial in geospatial analysis and urban planning studies (see CHAPTER. ANNEX:ROOFTYPESET.m).

- *ROOFTYPEDETECTION.m*: A code that represents a comprehensive tool for the identification and assessment of roofs suitable for GR installation. This code integrates advanced techniques for georeferencing and comprehensive analysis of roof characteristics. It allows users to upload georeferenced images and generate binary masks, which are arrays of pixels assigned a value of 0 or 1 to each, used to represent and manage specific areas of interest in the image. It is notable for offering interactive editing, enabling users to modify these masks manually using drawing tools. In addition, it incorporates advanced visualisation functionalities, superimposing the masks on the original images for clearer visual interpretation (see CHAPTER. ANNEX:ROOFTYPEDETECTION.m).

Before continuing with the processing of the images in *MATLAB* codes, it is crucial to verify the size of the orthophotographs and to evaluate the technical specifications of the computer to be used, including aspects such as RAM, graphics card and processor. This check is important because, depending on these characteristics, it may be necessary to split the images into several parts to ensure efficient handling and processing.

For those cases where image splitting is necessary without compromising the metadata (key data such as date, time, coordinates, altitude and resolution, crucial for the geospatial analysis of the image), the use of *QGIS* software, preferably version 3.34.1 or later, is recommended. The procedure involves the creation of a grid of a suitable size that allows the images to be divided in an optimal way using the extraction tool called *"Cut raster by mask layer"* in *QGIS*. This method facilitates the extraction of each segment of the original image through the squares defined by the grid, resulting in a specific set of images ready to be processed.

In the initial stage of creating the binary mask, process starts with the definition of the **"roofType"** array, a structure that stores different types of roofs, including their names, associated colour regions and relevant statistics, using the ***ROOFTYPESET.m*** (hereafter *RTS*) code. In this step, the user interacts with an interface to manually select representative pixels. Subsequently, the *RTS* code processes these selections to identify new roof types or add colour regions to existing roof types. Detailed statistics are calculated for each colour region in the RGB and HSV colour spaces, models that are based on the mixture of red, green and blue light, and hue, saturation and value, respectively. It is crucial to define representative colours of the rooftops of the city under study, in order to achieve an automatic and efficient capture of as many of these rooftops as possible in the later stages of the code. It is important to note that the selection of characteristic colours in the analysis allows for the exclusion of roofs that are physically unsuitable for GRs, such as those consisting of tiles. However, in general, the *RTS* code, as well as the ***ROOFTYPEDETECTION.m*** (hereafter *RTD*) code, do not directly assess the capacity of roofs to support additional loads. This implies that, although potential areas for the implementation of GRs may be identified based on visual characteristics, the specific structural assessment required to determine load-related feasibility is not comprehensively included in this initial process, but is presented separately, depending on the colour criteria of the roofs selected as typical for the city.

After pixel selection, the *RTS* code executes a number of key operations. Initially, these pixels are organised into a region of interest called **"colorRegion"** (subsection within the **"roofType"** structure), which collects information about the selected pixel values in the RGB and HSV colour spaces, along with statistics such as minimum, maximum, mean and standard deviation.

Then, using the *RTD* code, the previously defined regions are used to create specific binary masks. These masks have the function of identifying the pixels of the original image that correspond to the region of interest. Two types of binary masks are generated: one based on the minimum and maximum thresholds of the RGB and HSV values, and another focusing on the mean and standard deviation of these same values. The fusion of these masks forms a total binary mask that accurately reflects the designated region of interest.

The *RTD* code also integrates advanced functions to refine the binary masks used in image processing by applying morphological processing techniques such as erosion and dilation. These techniques focus on modifying the size of objects in the image, either by reducing them (erosion) or enlarging them (dilation). Additionally, it provides the ability to implement additional filters based on the size of the objects present in the image, which improves the accuracy and effectiveness in identifying and selecting relevant areas.

In the final phase of the *RTD* code, georeferencing of the binary roof masks is carried out based on the original *TIF* image, areas are calculated, and the specific data structure is updated. This process starts with the loading of georeferenced information from the image, followed by the loading and georeferencing of the binary roof mask. The code then visualises the mask and proceeds to calculate the areas, transforming the pixel measurements to square metres. Thresholds are set and the corresponding binary masks are created. The calculated areas are added to the **"roofType"** structure, and the results are printed and copied in a tabular format. Finally, the updated structure with all processed information is saved.

2.2 GENERATION LAYER OF BUILDINGS WITH UNSUITABLE SLOPES

In the second phase of the methodology (Figure 3), and taking into consideration section 1.3.3, it is essential to identify buildings whose slopes are optimal for the installation of GRs. However, to carry out this process more efficiently, it has been decided to initially identify the areas of roofs that are not suitable for such structural renovations and eliminate them from the pre-screening results. In this context, a specific code was developed in *MATLAB* to fulfil this purpose:

- *SLOPE.m*: Designed code that processes *LiDAR* point cloud data in *LAZ* (LAS compressed data) format with the aim of analysing the slope of building roofs. Its main functionalities include the ability to load and extract georeferenced and point classification information from *LAZ* files, identify points related to buildings, generate binary masks representing the roof areas, calculate the area of these masks and visualise the results in 3D (see CHAPTER. ANNEX:SLOPE.m)

It is important to note that *LiDAR* is a remote technology that uses laser pulses to measure distances and create detailed 3D maps of the environment. In the geospatial context, *LiDAR* systems are commonly used to generate Digital Elevation Models (DEM), obtain information on land topography, characterise forest cover, conduct urban studies and manage natural resources.

In the specific case of *LiDAR* files in *LAZ* format, this format is based on the *LAS* (LiDAR Aerial Survey) standard, which is a common file format for storing *LiDAR* data. The *LAZ* compression allows to reduce the size of the *LiDAR* files, facilitating their storage and distribution without significant loss of information. These data, captured from the air or from the ground, generate dense clouds of three-dimensional points representing the Earth's surface.

These points are geo-referenced, meaning that each point has associated spatial coordinates (latitude, longitude and altitude), allowing precise geographic location. This is key to the operation of the *MATLAB* **SLOPE.m** (hereafter Slope) code, as through the spatial coordinates and point classification, roofs with slopes greater than the recommended angle of 15 degrees can be identified (see section 1.3.3).

Prior to the use of the *SLOPE* code, it is essential to transform and save the *LAZ* format files into *TIF* format using the *"blast2dem"* tool of the *QGIS* LAStools add-on (without deleting the original *LAZ* format files). The *blast2dem* is an extension designed to generate DEM Models from *LiDAR* data, with the ability to handle significantly larger datasets compared to *"las2dem"*. While *las2dem* operates in memory and has a limit of around 20 million points, *blast2dem* uses a unique technology called streaming TIN (Triangulation Irrestricted Delaunay) to efficiently process datasets of up to 2 billion points. Streaming TIN technology enables Delaunay triangulation of large numbers of *LiDAR* points with efficient use of main memory. That is, instead of loading all the data into memory, *blast2dem* processes the points sequentially, using advanced techniques to handle large volumes of data efficiently.

The first step performed by the *SLOPE* code is the loading of the *LAZ* file and the creation of a *TIF* image from it (not to be confused with the previous step, the TIF image created has no metadata), for subsequent geo-reference transfer. After loading the file, the code filters the points associated with class 6 or 7, which generally corresponds to the points associated with the constructions. It is essential to check that the classification of the points provided by the *LAZ* file has the standard format, which is as follows:

- 1-0: Unclassified points
- 2: Terrain points
- 3-5: Low, medium and high points
- 6-7: Buildings
- 8-10: Other
- 11: Water surface
- 12: Ground surface

In the process of analysing the *LAZ* file data, the first step is to filter the points to identify the minimum height value (the lowest Z value). This approach aims to facilitate data processing by allowing a height threshold to be set based on the minimum point and a default height, which is set to 3 metres by default. Once this step is done, a new point cloud is created that contains less information and is therefore easier to process.

Then, in order to cluster the points and model the geometries of the buildings, the *'k-means'* algorithm is implemented. This technique is fundamental to classify the three-dimensional points of the *LiDAR* cloud into different clusters, facilitating the identification of similar structures. The algorithm starts with a defined number of centroids (k) and iteratively adjusts them to minimise the variance within each cluster. *MATLAB's k-means* function is a key tool in this process, as it allows the centroids to be assigned and updated efficiently. The choice of the number of centroids (k) is based on the analysis of the histogram of heights of the point cloud, which allows to automatically determine the limit for clustering buildings and improve the accuracy of the model. It is crucial to mention the importance of defining a seed in the *k-means* algorithm, which serves to control the random initialisation of the centroids. This seed guarantees the reproducibility of the results when running the algorithm repeatedly, which is essential in research and in applications where consistency is critical. In addition, a fixed seed allows for more consistent comparisons between different runs of the algorithm and helps to avoid anomalous results caused by unfortunate centroid initialisations. As a complement to the seed definition, it is necessary to iterate an arbitrary minimum of 10 times per image to obtain consistent results, thus ensuring the stability and reliability of the clusters identified in the data analysis.

The resulting visualisation of this process shows the point cloud, coloured according to the identified clusters, providing a clear and structured representation of the building. This method provides an intuitive visual interpretation and simplifies the analysis of the spatial distribution of the structures captured by the *LiDAR*.

Subsequently, with the points already grouped, a linear adjustment is performed in the XY plane to obtain the slope coefficients. This analysis is visualised in a three-dimensional representation of the point cloud, where the groups are coloured according to their category. A maximum slope limit is established, and those groups that exceed it are highlighted, allowing the identification and visual analysis of roofs with significant slopes.

Once the groups with slopes above the allowed limit (PSLA, for its acronym in spanish) have been defined in the *LiDAR* point cloud, the creation of a binary mask is initiated, identifying the points belonging to these groups. Then, a closing and filling operation is performed to improve the consistency and integrity of the mask, thus ensuring a more accurate and reliable representation of the areas with critical slopes.

As a final step, the previously generated binary mask is read, creating a file name for the georeferenced version. The georeferencing information from the *TIF* image, elaborated in the stage prior to the use of the code, is used to store the mask in a geographic format that maintains the same projection. This georeferenced mask is stored in a specific folder, facilitating its integration and use in geographic information systems (GIS). This process guarantees the spatial coherence between the mask and the original image, enhancing the usefulness of the information generated from the *LiDAR* data.

2.3 INTEGRATION OF LAYERS WITH THE VIRTUAL CADASTRE

After the generation of a proportional number of binary masks in relation to the orthophotos and *LAZ* files, it is necessary to unify them for the interpretation and calculation of the potential area of the city under study.

Starting with the binary masks obtained according to the methods described in section 2.1, these are loaded into the *QGIS* software as a raster, a digital image modality that represents spatial data by means of a matrix of pixels. Through the miscellaneous *"fusion"* function available in *QGIS*, these masks are fused, resulting in a georeferenced mask encompassing the area in question, hereafter referred to as ***GEO_MASK_WS***. A similar procedure is then applied to integrate the masks from section 2.2 (filtering of properties with unsuitable slopes), hereafter referred to as ***GEO_MASK_SLOPE***.

With both binary masks ready, it is necessary to use the *"Raster Calculator"* function to extract from ***GEO_MASK_WS*** the buildings shown by ***GEO_MASK_SLOPE***, resulting in ***GEO_MASK***.

Simultaneously, it is imperative to verify the total area of ***GEO_MASK_WS*** and ***GEO_MASK***. For this purpose, the *"raster information"* function is used, which provides all the data inherent to these capabilities, including the area of each of their categories. In this case, since these masks are composed of binary values (1 and 0), only the area generated by category 1 will be considered. This verification also involves the calibration of the last section of the code implemented in section 2.1.

On the other hand, it is crucial to use the cadastral information of the city in the evaluation process. In this sense, it is necessary to load a cadastral vector layer (collection of geometric elements such as points, lines or polygons, each with its own attributes) into the *QGIS* software. A thorough review of the data in this layer must then be carried out, ensuring that the number of floors, the cadastral reference and the current use of the buildings are included. It is also necessary to add a new column in the attribute table of the cadastral vector layer to record the values of the graphic surface of each element, hereafter referred to as *Total Roof Area*.

Simultaneously, the ***GEO_MASK*** raster needs to be transformed into a vector layer using the *"Polygonise"* function in *QGIS*, which will be named ***GEO_MASK_VECTORIAL***, and adjustments made using the *"Raster Calculator"* again. Subsequently, through the geoprocessing tool *"Cut"*, and using the cadastral vector layer of the city as an input layer and the ***GEO_MASK_VECTORIAL*** as an overlay layer, a final layer is obtained that brings together all the relevant cadastral information of the city, centred on the roofs identified by means of AV techniques.

Finalising this process, the result provides a georeferenced layer called ***GEO_MASK_CADASTRAL_CITY***, which also provides data on the total surface of the selected buildings and their area potentially reformable through the use of GR.

2.4 COMBINATION OF CADASTRAL LAYER WITH ENERGY CERTIFICATES

In this section of the methodology, the information obtained from the layer generated in the previous section will be used and combined with the data available in the energy certificates to estimate the savings in energy consumption and emissions. In addition, the CO_2 sequestration attributable to the installation of GRs will be calculated.

Once the ***GEO_MASK_CADASTRAL_CITY*** vector layer has been obtained from the previous section and using the *QGIS* software, the attribute table is extracted, which from now on will be called ***DATA_CITY***, in the format "MS Office Open XML Spreadsheet [XLSX]". It is essential to verify that this table contains essential information such as the cadastral registration, the year of construction, the number of floors, the type of use, and the postal code or address of the property. Subsequently, an additional column must be added to this table using the *"Raster Calculator"* function, reflecting the values of the current graphic surface of each register, called *Total Potential Roof Area*.

In parallel, it is of utmost importance to obtain from official sources a register of energy certificates including data on energy consumption and CO_2 generated to cover this consumption, as well as detailed information related to the cadastre or the address of the considered properties. Additionally, to complement the information collected in ***DATA_CITY***, it is recommended to download an updated official Cadastre. It is relevant to note that the cadastre used from *QGIS* may not be as up to date as those provided by the relevant authorities. Therefore, updating this data is crucial to ensure the accuracy and relevance of the results.

Once the information in the ***DATA_CITY*** file is updated, it is crucial to cross-check the data with the available energy certificates. To perform this task, the cadastral value or address of each property will be used as a reference to link the energy consumption (in kWh) and CO_2 emission (in kg CO_2) data from both sources.

In cases where properties are found without specific data on their energy consumption and emissions, it is necessary to generate an average estimate based on factors such as geopolitical location, use, year of construction and surface area of these properties. If data are still missing after this estimation, a second average calculation is performed, omitting the total floor area of the building. If the necessary information is still missing, a third average estimate is made. This time, the variables of the second estimate are maintained, but the geopolitical location considered is extended, e.g. from a neighbourhood to an entire district. For exceptional situations, a fourth approach will be considered which, unlike the previous ones, will not be based on an average, but a direct comparison will be made based on similarities between the factors mentioned, such as the year of construction, the current use of the property and the built-up area. This approach ensures a more comprehensive and accurate approximation of the energy consumption and CO_2 emissions associated with each property.

With all the necessary information already updated and the energy consumption data associated with the property, the next step is to create a new file containing only the most relevant information. To do this, a filter focused on *Total Potential Roof Area* will be applied, with a focus on working with a smaller and more manageable dataset to streamline the process. This filter will be designed to include only those properties whose potential areas exceed 50 m^2, following the recommendation of section 1.3.2.2 in chapter 1, which indicates that this value corresponds to the optimal size for a GR. This selection criterion will allow the generation of a new, more specific and manageable database, which will be named ***DATA_CITY_50m2***.

Finally, with the new database under consideration, it will be possible to obtain the total count of properties susceptible to renovation. This figure will coincide in an equivalent way with the total number of GRs to be installed. It should be noted that these roofs will have the minimum surface area indicated in the previous paragraph but will be of a variable size depending on the availability of each roof selected.

2.5 ASSESSMENT OF ENERGY SAVINGS, CO_2 EMISSION REDUCTION AND CO_2 CAPTURE

Before proceeding with the calculation of energy savings and emission reductions, it is essential to verify that the units of measurement used are correct. In case the consumption and emissions are expressed in terms of annual consumption per square metre, an additional step is necessary: multiplying these values by the total building area of the building (not to be confused with Total Potential Roof Area). This procedure is key to accurately determine the total annual energy consumption and total annual emissions of the building, and is therefore carried out using the following equations:

$$\boldsymbol{Energy\ Consumption = EC' \cdot Area_{Constructed}} \left[\frac{\boldsymbol{kWh}}{\boldsymbol{year}}\right]$$

$$\boldsymbol{CO_2\ Emissions = ECO_2{}' \cdot Area_{Constructed}} \left[\frac{\boldsymbol{kg\ CO_2}}{\boldsymbol{year}}\right] \quad (1)$$

EC': Annual energy consumption per total floor area of a building $[\mathrm{kWh/m^2 \cdot year}]$

$\mathrm{ECO_2'}$: Annual $\mathrm{CO_2}$ emissions per total floor area of the building $[\mathrm{kg\ CO_2/m^2 \cdot year}]$

$\mathrm{Area_{Constructed}}$: Total floor area of the building $[\mathrm{m^2}]$

2.5.1 ENERGY SAVINGS AND CO_2 EMISSION REDUCTION

Once the annual data on total energy consumption and the corresponding CO_2 emissions have been obtained, the percentage of these that is specifically attributed to energy consumption for the air conditioning of the building, specifically heating, air conditioning and domestic hot water, will be determined. This is due to what is indicated in the 1.3.2.3 section, where it is shown that the main effects of the roof are mainly associated with thermal comfort. This percentage will vary depending on the type of climate in the city under study, reflecting how local climatic conditions directly influence the need for air conditioning, either heating or cooling, within the building. Therefore, the following equations will be used to obtain the energy consumption and CO2 emissions associated with the air conditioning of the building:

$$\boldsymbol{EC_{conditioning} = Energy\ Consumption \cdot factor_{conditioning}} \left[\frac{\boldsymbol{kWh}}{\boldsymbol{year}}\right]$$

$$\boldsymbol{ECO_{2\,conditioning} = CO_2\ Emissions \cdot factor_{conditioning}} \left[\frac{\boldsymbol{kg\ CO_2}}{\boldsymbol{year}}\right] \quad (2)$$

$\mathrm{factor_{conditioning}}$: Location − dependent climate factor [%]

Subsequently, it is crucial to consider two additional factors in the energy savings analysis. The first one refers to the literature review conducted in section 1.3.2.2 on energy savings resulting from the installation of GRs in mediterranean cities, directly related to the current use of the property. In this context, a reduction in energy consumption of 17% is anticipated for single family dwellings. For residential buildings, the savings are distributed as follows: 17% on the top floor, 6% on the penultimate floor, 1.5% on the penultimate floor and 0.5% on the next floor. The remaining floors will not show a significant percentage of savings. Buildings that do not fit into these two categories, such as cultural, commercial and health buildings, among others, will experience 15% energy savings (Zayas Orihuela, 2023).

The second factor corresponds to the total use of the roof with GRs, this factor determines what percentage of the roof will have a GR. For this, the *Total Potential Roof Area* is considered and divided by the *Total Roof Area*, obtaining a utilisation factor. The factor will be calculated using the following equation:

$$\boldsymbol{factor_{use}} = \frac{\textbf{Total Potential Roof Area}}{\textbf{Total Roof Area}} [-] \tag{3}$$

Total Potential Roof Area: Area considered for GR assembly $[m^2]$

Total Roof Area: Total area of the roof considered for intervention $[m^2]$

In this way, the values of savings in energy consumption and CO_2 emissions are obtained, determined from the following expressions:

$$\begin{aligned} &\boldsymbol{Energy\ Savings_{building}} = \boldsymbol{EC_{conditioning}} \cdot \boldsymbol{factor_{use}} \cdot \boldsymbol{factor_{floor}} \left[\frac{\boldsymbol{kWh}}{\boldsymbol{year}}\right] \\ &\boldsymbol{CO_2\ Emissions\ Reduction_{building}} \\ &\quad = \boldsymbol{ECO2_{conditioning}} \times \boldsymbol{factor_{use}} \times \boldsymbol{factor_{floor}} \left[\frac{\boldsymbol{kg\ CO_2}}{\boldsymbol{year}}\right] \end{aligned} \tag{4}$$

$factor_{floor}$: Representing the decrease per building use and floor $[-]$

It is important to highlight that a proportional reduction in CO_2 emissions is estimated, as it is assumed that the energy savings correspond to final energy, which is the secondary energy delivered to the end user and available for use in devices and systems. In other words, the percentage decrease in energy consumption leads to a proportional reduction in CO_2 emissions generated by the production of that energy, and since it is final energy, this decrease is considered directly, with a 1:1 ratio.

Finally, the calculated values represent the savings per building considered, so they should be added together to determine the expected energy savings and the expected reduction in CO_2 emissions. In relation to the expected total, this will be obtained by means of the following equations:

$$\begin{aligned} &\boldsymbol{Energy\ Savings_{city}} = \sum \boldsymbol{Energy\ Savings_{building}} \left[\frac{\boldsymbol{kWh}}{\boldsymbol{year}}\right] \\ &\boldsymbol{CO_2\ Emissions\ Reduction_{city}} \\ &\quad = \sum \boldsymbol{CO_2\ Emissions\ Reduction_{building}} \left[\frac{\boldsymbol{kg\ CO_2}}{\boldsymbol{year}}\right] \end{aligned} \tag{5}$$

2.5.1 CO_2 CAPTURE

In relation to the calculation of the total CO_2 sequestered by the GRs to be installed, the <u>*Total Potential Roof Area*</u> shall be multiplied by a specific sequestration factor. This factor will vary depending on the type of vegetation selected for installation on the GR, the substrate used, the number of layers of the roof, and other relevant factors that may influence the CO_2 sequestration capacity. This shall be done using the following expression:

$$\boldsymbol{CO_2\ sequestration_{building}} = \boldsymbol{Total\ Potential\ Roof\ Area \cdot factor_{sequestration}} \left[\frac{\boldsymbol{kg\ CO_2}}{\boldsymbol{year}}\right] \tag{6}$$

$$factor_{sequestration}: CO_2\ sequestration\ rate\ of\ GR\ \left[\frac{kg\ CO_2}{m^2 \cdot year}\right]$$

Finally, as in the previous section, the calculated results represent the emissions sequestered per building. Due to the above, the sum of all these should be added together to obtain total CO_2 sequestration for the city under study, which will be done using the following equation:

$$\boldsymbol{CO_2\ sequestration_{city}} = \sum \boldsymbol{CO_2\ sequestration_{building}} \left[\frac{\boldsymbol{kg\ CO_2}}{\boldsymbol{year}}\right] \tag{7}$$

CHAPTER 3. CASE STUDY: VALENCIA CITY

In this chapter, the case study of this work will be shown. In particular, the city of Valencia has been selected as a case study. Located on the east coast of Spain, Valencia (Figure 4) is a city made up of 19 districts and 88 neighbourhoods that is distinguished by its mediterranean climate, characterised by warm summers and mild winters, and is the third largest city in the country. It is noted for its rich cultural heritage and economic dynamism, but also for its strong commitment to sustainability. This commitment is reflected in aspects such as the access of approximately 97% of its inhabitants to urban green spaces within 300 metres of their homes, the presence of the largest urban park in Europe and an extensive network of more than 160 kilometres of cycle paths. Such characteristics contributed to its selection as European Green Capital 2024 (Batlle Cardona, 2023), a recognition that emphasises its work in promoting a sustainable city, the enrichment of green spaces and effective environmental management.

In the geographical analysis to be carried out, the Coordinate Reference System "EPSG:25830 - ETRS89 / UTM zone 30N" will be used. This standard guarantees an accurate manipulation of spatial data, an essential element for the correct evaluation of sustainable urban interventions, as well as the environmental impact generated by the implementation of GRs in the city of Valencia. In order to focus the study on the main urban area of Valencia, the districts called "POBLATS DEL NORD" and "POBLATS DEL SUD" will be excluded. This exclusion results in a reduction of the number of neighbourhoods considered in the study, so that 72 of the 88 existing neighbourhoods will be analysed (Table 21).

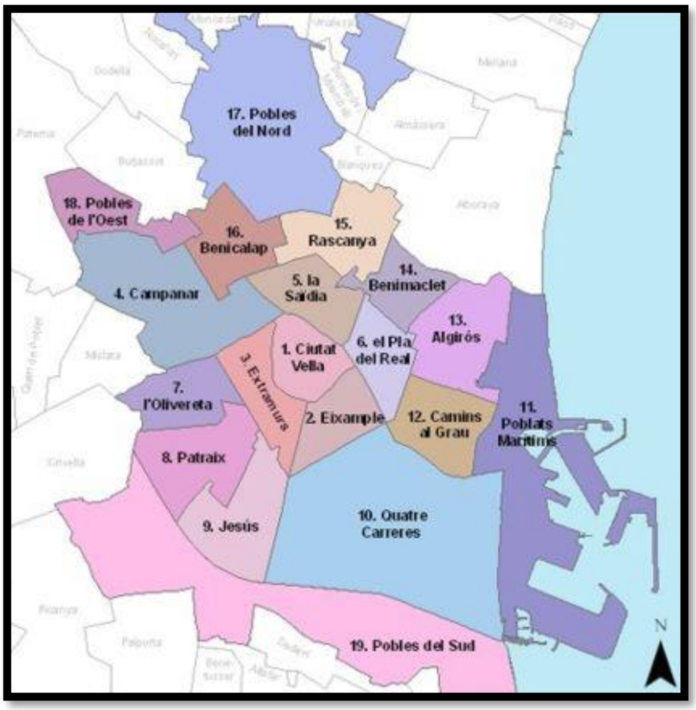

Figure 4: District representation of the City of Valencia, obtained from (Ajuntament de Vàlencia, 2024).

3.1 POTENTIAL ROOFTOPS

The following section will proceed according to the guidelines specified in section 2.1 of the methodology chapter. The process in question can be summarised by the diagram illustrated in Figure 5:

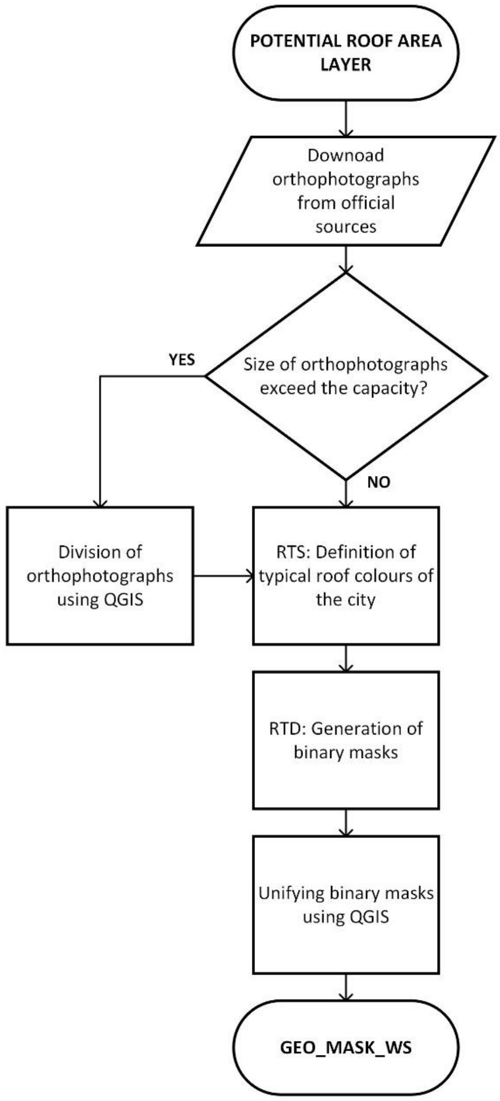

Figure 5: *Step-by-step summary of methodology 2.1 DEVELOPMENT OF THE POTENTIAL ROOF AREA LAYER.*

Orthophotographs obtained from PNOA (National Aerial Orthophotography Plan) in *TIF* format are retrieved from the website "Centro de Descargas" owned by the Spanish National Centre for Geographic Information (CING, 2020). The orthophotographs are divided into quadrants, so to obtain those corresponding to the city of Valencia, quadrants 0696-3, 0696-4, 0722-1 and 0722-2 were considered (see Figure 6).

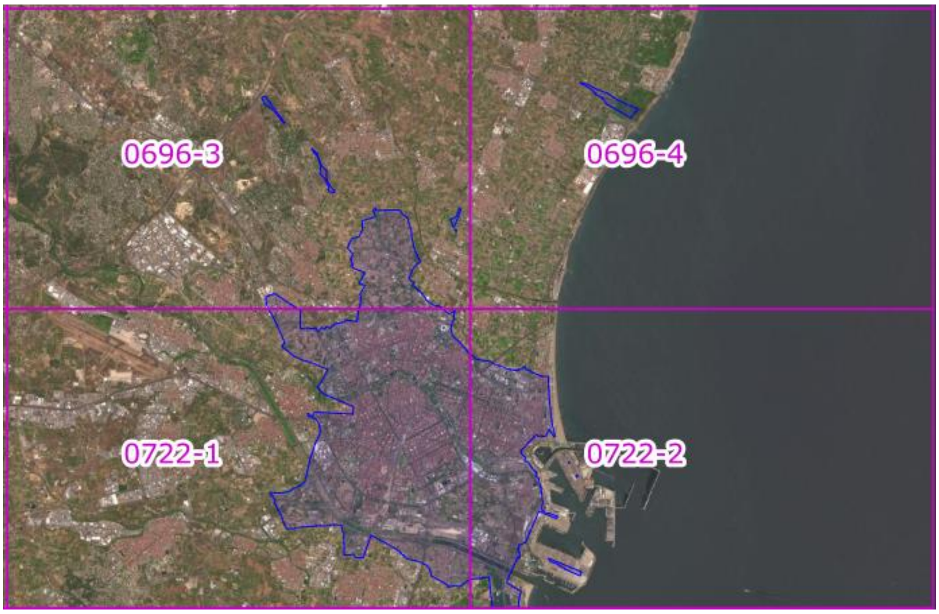

***Figure 6**: Quadrants corresponding to the city of Valencia.*

As mentioned in section 2.1, to facilitate the work according to the technical capabilities of the computer used, two processes of division of the images were carried out using the *QGIS* software. For the present case study, version 3.34.1 of the software was considered.

In the first phase of the process, the areas of interest in each quadrant were extracted using the *QGIS* tool *"Cut raster by mask layer"*. For this procedure, the vector layer **"districtes-distritos.geojson"**, available in the "Open Government" section of the Valencia City Council website (Ajuntament de València, 2024), was used. Prior to its application, this mask was modified using the selection tool and the *"Cut raster by extension layer"* function of *QGIS*, in order to exclusively represent the city of Valencia. In this way, a raster was obtained from the orthophotographs that accurately reflects the city, excluding the areas that form part of the municipality of Valencia, but not the city itself (Figure 7).

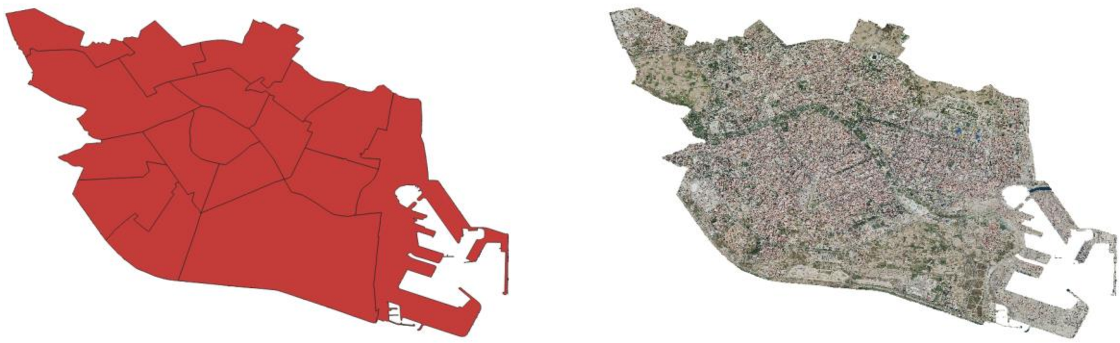

(a) (b)

***Figure 7**: Vector layer Valencia Urbana. a) Treated vector layer of the districts belonging to the city of Valencia (does not consider the districts POBLATS DEL NORD and POBLATS DEL SUD). b) Final image of the cut of the quadrants using the modified vector layer of the districts as a base.*

Subsequently, using the same function and for each of the subdivisions of the quadrants generated in the previous step, grids divided into "n" equal parts were created, where "n" represents an arbitrary number that will depend directly on the technical capabilities of the computer used. This means that, if the computer has limited capabilities, it is advisable to select a high value of "n", which will result in lighter images with equal proportions between them (Figure 8). The purpose of this process is to facilitate the extraction of each square belonging to a grid as an individual image, thus optimising the handling and analysis of the data according to the technological infrastructure available.

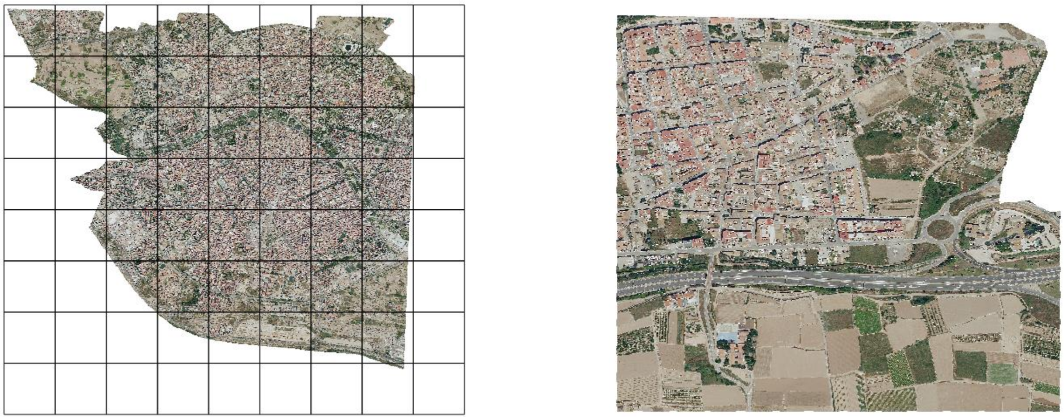

(a) *(b)*

***Figure 8**: Example of image division process by grid. a) Quadrant 0722-1 with a grid for the division process. b) Part of quadrant 0722-1 extracted using the drawn grid as a base.*

Finally, for this project, 1 image was obtained for quadrant 0696-4, 15 images for quadrant 0696-3, 48 images for quadrant 0722-1 and 87 images for quadrant 0722-2. All the resulting images are in *TIF* format and therefore retain all the metadata of the original images.

When starting with the implementation of the RTS code for the identification of rooftops in Valencia, it was necessary to create a **roofType** array that reflects the peculiarities of the city. This step included selecting the most iconic rooftops from the orthophotographs analysed. Thus, a **roofType** array was formed with distinctive colours of Valencia, ranging from light brown and beige to deep red, with average RGB values between (197, 178, 155) and (207, 194, 178). This approach allows the system to automatically identify and classify the variety of rooftops when compiling, capturing the visual essence of the city (see Figure 9).

With the **roofType** array already created and the *RTD* code initialised, the program prompts the user to upload an image in *TIF* format. Subsequently, the corresponding binary masks are generated for each predefined colour in the array. These masks are merged, and the final result is presented to the user (Figure 10). Then, through the polygon drawing tool, the user has the ability to remove or add regions to the binary mask, allowing to obtain a final result adjusted to the specific requirements (Figure 11).

***Figure 9**: Example of typical roofs of Valencia used for the creation of the rooftype arrangement.*

(a) *(b)*

***Figure 10**: (a) First processing of image 34 of quadrant 0722-1. (b) First processing of the mask generated from image 34 of quadrant 0722-1.*

Finally, the final binary mask is presented (Figure 11), which is georeferenced using the original orthophoto data. In addition, the potential area of the selected rooftops is calculated. It is important to remember to calibrate the X and Y resolution of the masks for the accurate calculation of the total area.

(a) (b)

***Figure 11**: Final stage of the process carried out by RTD. a) Final processing of image 34 of quadrant 0722-1. b) Final processing of the mask generated from image 34 of quadrant 0722-1.*

From the initial divisions of the quadrangles and the generated binary masks, the miscellaneous tool *"Combine"* in *QGIS* was used to merge them, thus obtaining 4 combined binary masks. This procedure was applied again to the 4 resulting masks, using the corresponding function in *QGIS*. As a result, a final binary mask for the city of Valencia is generated in raster layer format, named ***GEO_MASK_WS*** (Figure 12).

This mask contains all the roofs identified with potential to be refurbished in Valencia regardless of their slope, selected by means of AV and user intervention through the *RTD* code. Thanks to its georeferencing, the mask becomes an essential tool for urban visualisation, analysis and planning, improving the implementation of development and refurbishment projects using accurate data and its geographic integration.

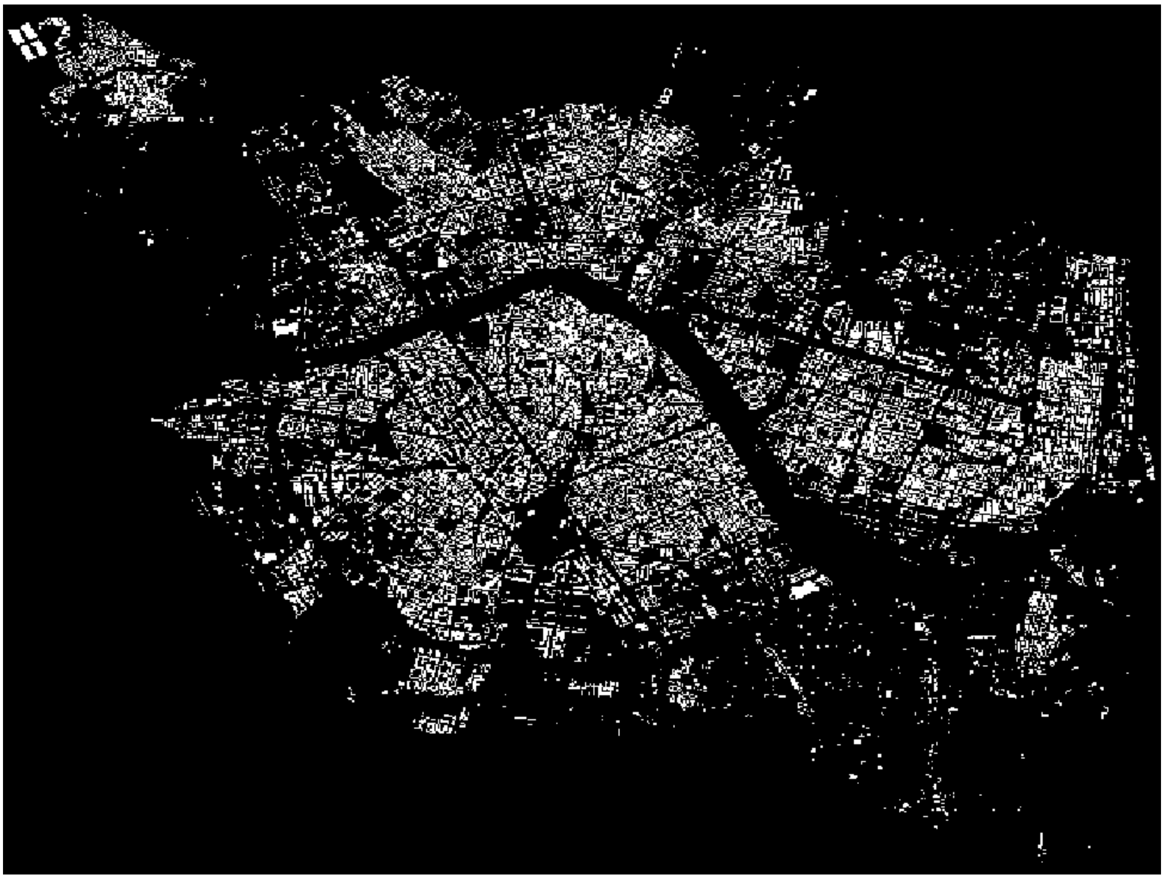

Figure 12: *Final mask or GEO_MASK_WS delivered by the ROOFTYPEDETECTION.m MATLAB code. This mask does not consider the slope of the buildings.*

3.2 SLOPE ANALYSIS

The subsequent section outlined in chapter 2 involves generating a vector layer binary mask that delineates the buildings with unsuitable slopes for intervention, as described in Section 2.2. Step-by-step process is summarised in Figure 13.

LiDAR files in *LAZ* format are downloaded from the "Download Centre" portal, property of the Autonomous Organism National Centre for Geographic Information of Spain (CING, 2020). These files are digital files containing 3D point clouds captured by *LiDAR* technology in files distributed in 2x2 km, covering a national scope and coloured with true colour (RGB) or infrared (IRC) information. The point clouds were captured by flights equipped with *LiDAR* sensors, reaching a density of 0.5 points per square metre or higher. For this project, only files in RGB format were collected, totalling 26 files (example in Figure 14).

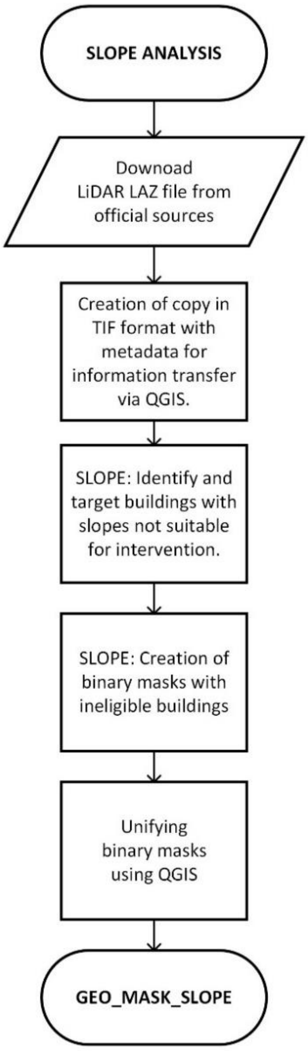

***Figure 13**: Step-by-step summary of methodology 2.2 GENERATION LAYER OF BUILDINGS WITH UNSUITABLE SLOPES.*

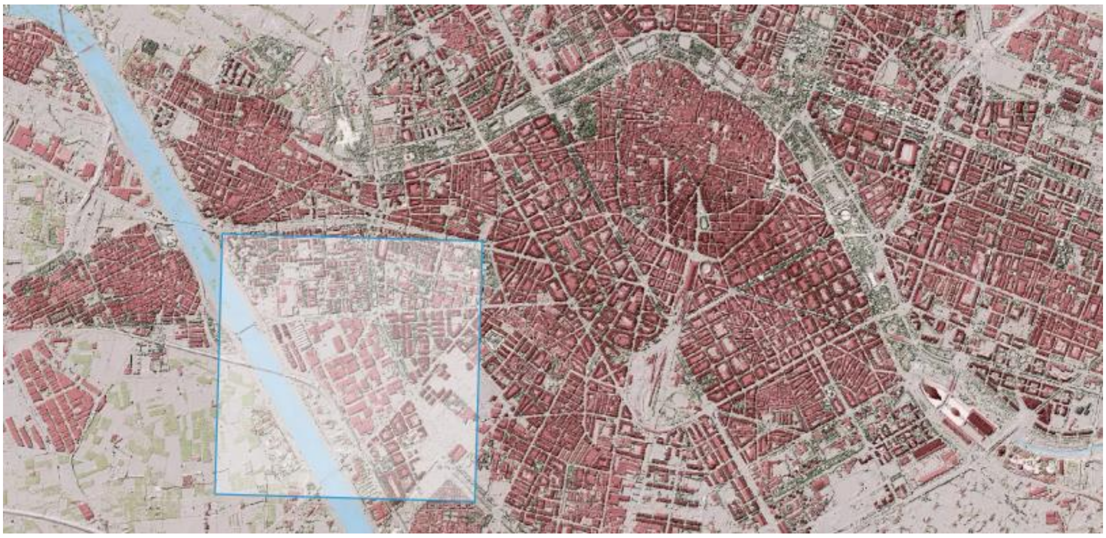

***Figure 14**: Highlighted box representing the file concerned corresponding to PNOA-2015-VAL-722-4372-ORT-CLA-RGB.LAZ.*

Once the files were obtained, the initial procedure consisted of generating orthophotographs in *TIF* format, using the *"blast2dem"* function of the LAStools add-on in *QGIS*. This step was performed to transfer the metadata contained in the *LAZ* files to the final binary mask, which would be derived from the subsequent stages of the process.

The first step in the application of the *MATLAB SLOPE* code was to directly select a file from the folder of the files and automatically load the previously generated *TIF* image, using the same name of the selected file. In the same way, the selected *LAZ* file was converted into a *LAS* file to have access to all the information, since the latter is an uncompressed and larger file.

Once the *LAS* file is loaded, *SLOPE* code proceeds to filter out from the point cloud those classified as category 6. As mentioned in section 2.2, it is crucial to verify the classification of the points loaded in each file using any available software, such as *QGIS* or *ArcGIS*, to ensure the accuracy of the classification of the points.

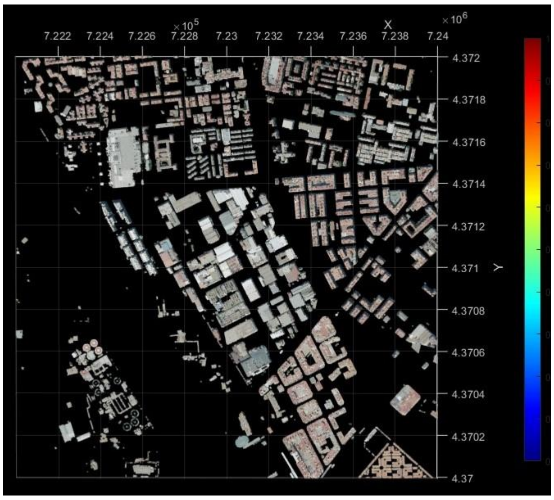

(a)

(b)

***Figure 15**: Point cloud representation. a) Point cloud of the selected file corresponding only to the classification of buildings. b) Zoom to building representation of the file using the point cloud.*

To further simplify the process, a function was used to identify the minimum height points in the *LAS* files. In this way, knowing the lower limit on the Z-axis, base is removed from the classification in order to speed up the subsequent calculation of the slope. Taking as an example the processing of the *PNOA-2015-VAL-722-4372-ORT-CLA-RGB.LAZ* file, the classification filter reduced the number of points from 4,639,440 to 891,510, and with the height filter 890,549 points were reached.

As shown in Figure 15, the buildings represented by the point cloud are still individual points and are near each other. Therefore, it is crucial to associate them with each other to form clusters representing the structures in the analysed area. For this purpose, a histogram of the grouping heights of the points is generated, where the X-axis represents the heights of the points in the filtered point cloud. The Y-axis, on the other hand, reflects the frequency of occurrence of the heights in the intervals defined by the edges of the bins. *"k-means"* function mentioned in section 2.2 is applied in order to cluster the closest points based on centroids, which generates the geometry of the buildings (Figure 16).

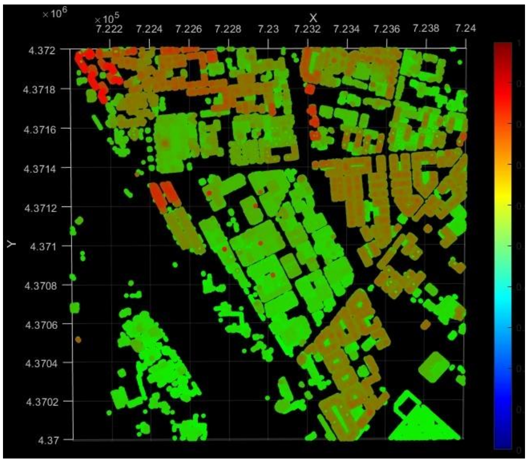

(a)

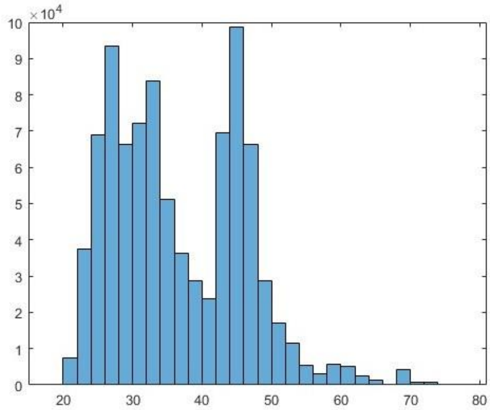

(b)

***Figure 16**: Representation group of buildings. a) Representation of the geometry of the buildings from the PNOA-2015-VAL-722-4372-ORT-CLA-RGB file generated using the "k-means" function. b) Histogram showing the distribution of heights in the filtered point cloud, where the height of the bins on the Y-axis indicates how many points have heights within those specific intervals on the X-axis.*

In the final section of the calculation performed by the *SLOPE* code and based on the literature reviewed in section 1.3.2, a maximum angle of 15° was established as a selection criterion. This step allowed identifying, within the set of analysed points, those slopes that exceeded the predefined angle. As a result, the height values exceeding this limit were determined, generating a diagram illustrating their locations by means of a differentiated colouring.

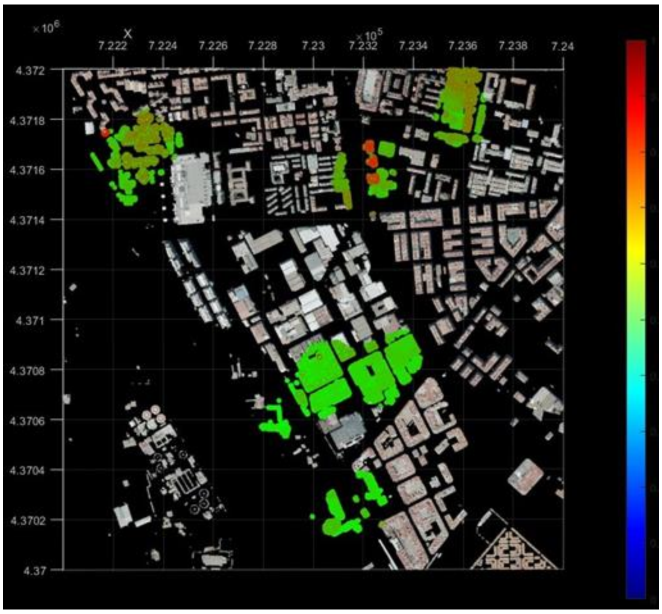

***Figure 17**: Buildings of the PNOA-2015-VAL-722-4372-ORT-CLA-RGB file differentiated by colour to highlight those with a slope greater than the limit indicated in the SLOPE.m code.*

Finally, from the graph illuminating the points with the steepest slopes (example Figure 17), a binary mask representing the groups of points that exceeded the established limits was produced (example **Figure 18**). Then, using the TIF image created in the previous step by applying the slope calculation code, the metadata was transferred to the binary mask corresponding to each file.

Figure 18*: Binary mask corresponding to file PNOA-2015-VAL-722-4372-ORT-CLA-RGB.*

Thus, by combining all the generated binary masks, a global georeferenced binary mask is created in raster layer format that identifies buildings with slopes greater than 15°, called ***GEO_MASK_SLOPE*** (Figure 19).

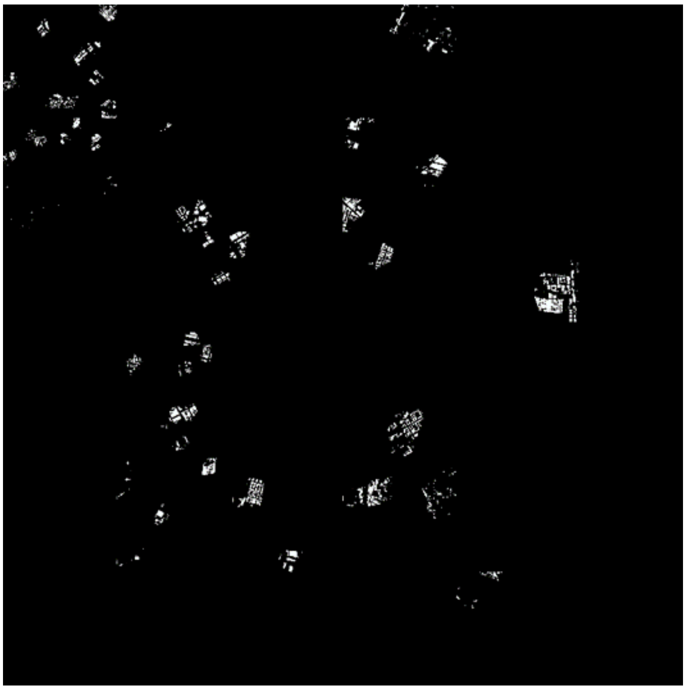

Figure 19*: Building mask with slope greater than 15° or GEO_MASK_SLOPE, delivered by the MATLAB code SLOPE.m.*

3.3 TOTAL AVAILABLE AREA FOR GRs

In the following section, the process for the calculation of the *Total Potential Roof Area* in the city of Valencia for the installation of GRs will be detailed. This explanation will be divided into two sections corresponding to the treatment of the cadastre of the city and the layers obtained in the previous points. However, this process still retains the process detailed in section 2.3 (see summary in Figure 20).

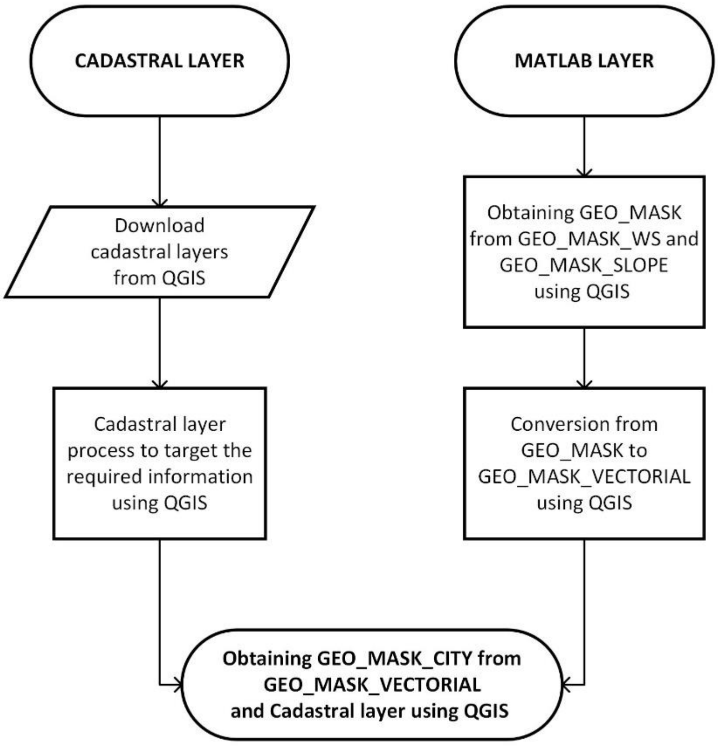

***Figure 20**: Step-by-step summary of methodology 2.3 INTEGRATION OF LAYERS WITH THE VIRTUAL CADASTRE.*

3.3.1 CADASTRAL LAYER PROCESSING

To calculate the potential area of roofs to be refurbished within the city of Valencia, the first phase involved the use of the city's cadastre obtained through the *"Spanish Inspire Cadastral Downloader"* add-on of the *QGIS* software (Soriano, 2023). Using this tool, the cadastre was downloaded, selecting the corresponding province and municipality (46900) and including information on cadastral parcels, addresses and buildings.

This process was carried out to identify the location of potential buildings for roof refurbishment, i.e. to identify those properties with a suitable area larger than 50 m^2 to be refurbished with GRs. As a result of these actions, the following files were generated:

- *A.ES.SDGC.AD.46900*
- *A.ES.SDGC.BU.46900.building*
- *A.ES.SDGC.BU.46900.buildingpart*
- *A.ES.SDGC.BU.46900.otherconstruction*
- *A.ES.SDGC.CP.46900.cadastralparcel*
- *A.ES.SDGC.CP.46900.cadastralzoning*

From the six files obtained, those corresponding to *A.ES.SDGC.BU.46900.building* (*"building"*) and *A.ES.SDGC.BU.46900.buildingpart* (*"buildingpart"*) were loaded into the *QGIS* software. Subsequently, a new vector layer called *A.ES.SDGC.BU.46900.Constru_Part* in GeoJSON format (*"Constru_Part"*) was created from the latter.

(a) (b)

Figure 21: Vector layer municipality of Valencia. a) Vector layer "Constru_Part" corresponding to the municipality of Valencia. b) Enlarged focus of the vector layer "Constru_Part" in the centre of the city of Valencia.

Consequently, the vector layer *Constru_Part* (Figure 21) was integrated with the vector layer building, using the 14 cadastral digits included in the former. This process culminated in the generation of a consolidated vector layer, named *A.ES.SDGC.BU.46900.Constru_PartInfo* (*"Constru_Partinfo"*).

This last vector layer is mainly constituted by the following types of information of interest in its attribute table:

- Cadastral Registry (14 digits): Land registry number associated with the property.
- localId: Registry number divided by parts according to the properties within the property.
- Date of Construction: Date of construction of the property.
- InformationSystem: URL link to the cadastral record of the property.
- Current_Use: Use of the property such as residential, industrial, public service, among others (1_residential, 2_agriculture, 3_industrial, 4_1_office, 4_2_retail, 4_3_publicServices, 5_Parking/Storage, 6_Others and No Construction land)
- NumberOfFloorsAboveGround: Number of floors above ground level.
- NumberOfFloorsBelowGround: Number of floors below ground level.
- NumberOfBuildingUnits: Number of cadastral units within the property.
- NumberOfDwellingsUnits: Number of dwellings registered within the property.
- ConstructedArea: Total area of the cadastral constructed area of the private part of the property plus the corresponding part of the area of common elements.
- GraphicArea: Graphic area of the cadastral parcel.

In addition, an extra column was added to the attribute table of the vector layer *Constru_Partinfo* by means of the "*field calculator*" function, representing the graphic area of the roof of the property of the displayed figures. This new column will be named "Total Roof Area" (see Figure 22).

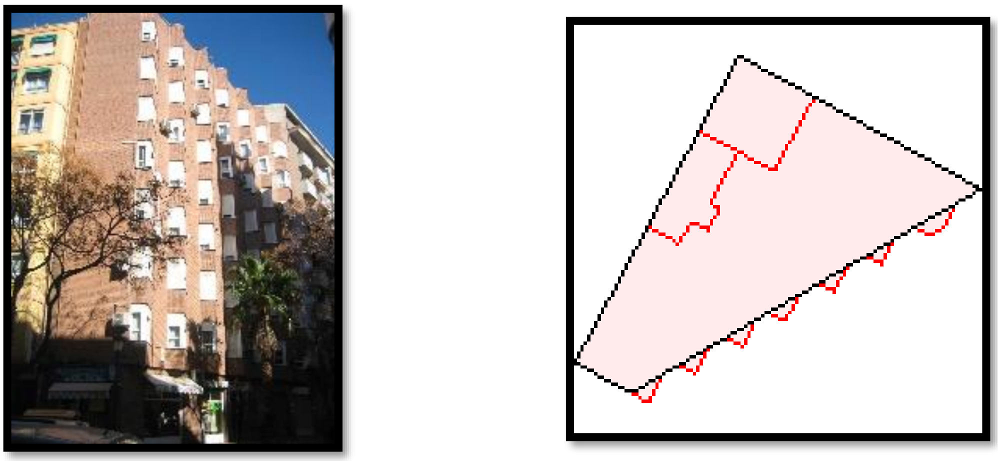

(a) *(b)*

***Figure 22**: Example cadastral house 6915211YJ2761F. a) Property seen in all its dimensions, where the sum of all the square metres built corresponds to "ConstructedArea". b) Property seen from a higher plane, where the visualised supervision corresponds to Total Roof Area.*

It is crucial to highlight that, in order to advance in the use of the data provided by the vector layer *Constru_Partinfo*, the tool *"Correct geometry"* must be used, with the purpose of adjusting the geometric configuration of the mentioned vector layer. This need arises after the use of the *"check validity"* function belonging to the same tool, where anomalies were detected that could compromise the correct integration with other layers during the analysis of the structural elements.

Finally, using the adjusted vector layer and the vector layer **"districtes-distritos.geojson"** (Figure 7), the geoprocessing tool *"Cut"* was applied. This procedure allowed limiting the scope of the *Constru_Partinfo* layer, focusing exclusively on the data belonging to the city of Valencia. In this way, data not relevant to the specific area of interest within the municipality were excluded. As a consequence of this operation, the vector layer named *A.ES.SDGC.BU.46900.ValenciaUrbano_PartInfo* was generated, which from now on will be identified as *"ValenciaUrbano_PartInfo"* (Figure 23).

Figure 23: *"ValenciaUrbano_PartInfo". Representative layer of the buildings of the city of Valencia with their corresponding cadastral information.*

3.3.2 MATLAB LAYER PROCESSING

Regarding the raster layers obtained in points 3.1 and 3.2, these are merged using the *"Raster Calculator"* tool. The process was performed using the expression:

$$"\boldsymbol{GEO\_MASK\_WS@1}" - "\boldsymbol{GEO\_MASK\_SLOPE@1}" \tag{8}$$

In this way, the final binary mask is obtained in raster layer format corresponding to the potential of the roofs of Valencia without considering the buildings with a slope greater than 15° degrees, called ***GEO_MASK*** (see Figure 24).

Figure 24*: "GEO_MASK". Binary mask representing the buildings considered with potential for GR assembly by the AV developed within the MATLAB code.*

3.3.3 FINAL LAYER PROCESSING

In the last phase of the area calculation, the raster layer ***GEO_MASK*** was converted into a vector layer using the conversion function *"Polygonise"*, thus generating the vector layer called ***GEO_MASK_VECTORIAL.***

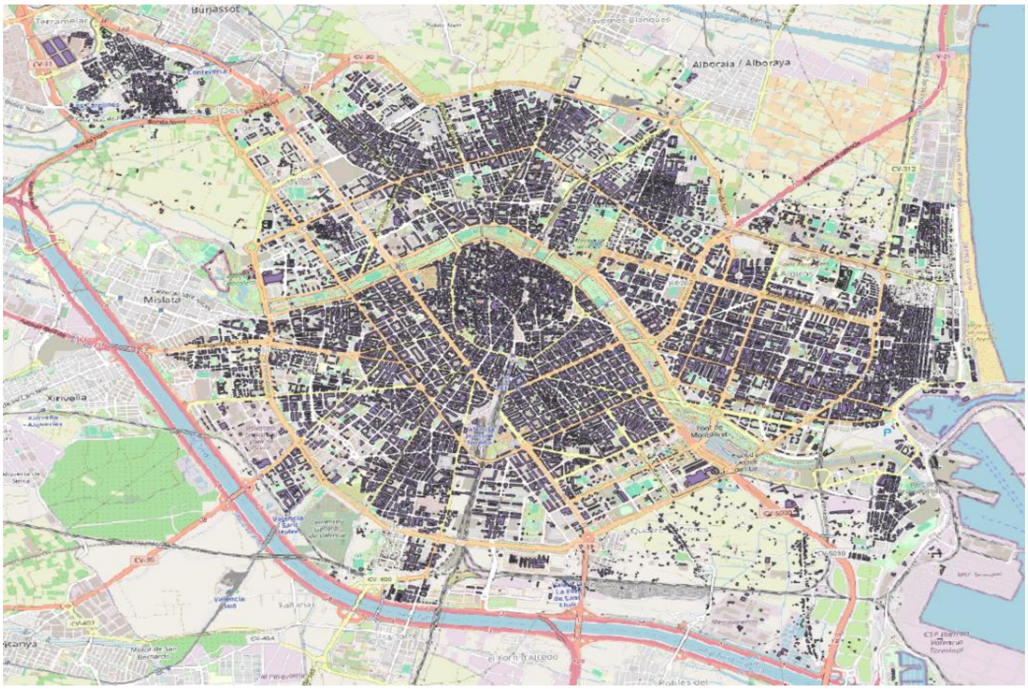

***Figure 25**: "GEO_MASK_VECTORIAL". Layer corresponding to the raster transformation obtained "GEO_MASK" in Section 3.3.2.*

Then, through the geoprocessing function *"Cut"* applied to the vector layer *ValenciaUrbano_PartInfo* (Figure 23), in superposition with the vector layer *GEO_MASK_VECTORIAL* (Figure 25), the final vector layer representing the potential area of roofs to be refurbished in the city of Valencia, named ***GEO_MASK_CADASTRAL_VALENCIA***, was generated. This layer contains geolocation metadata and detailed information on the available surfaces and the composition of the buildings.

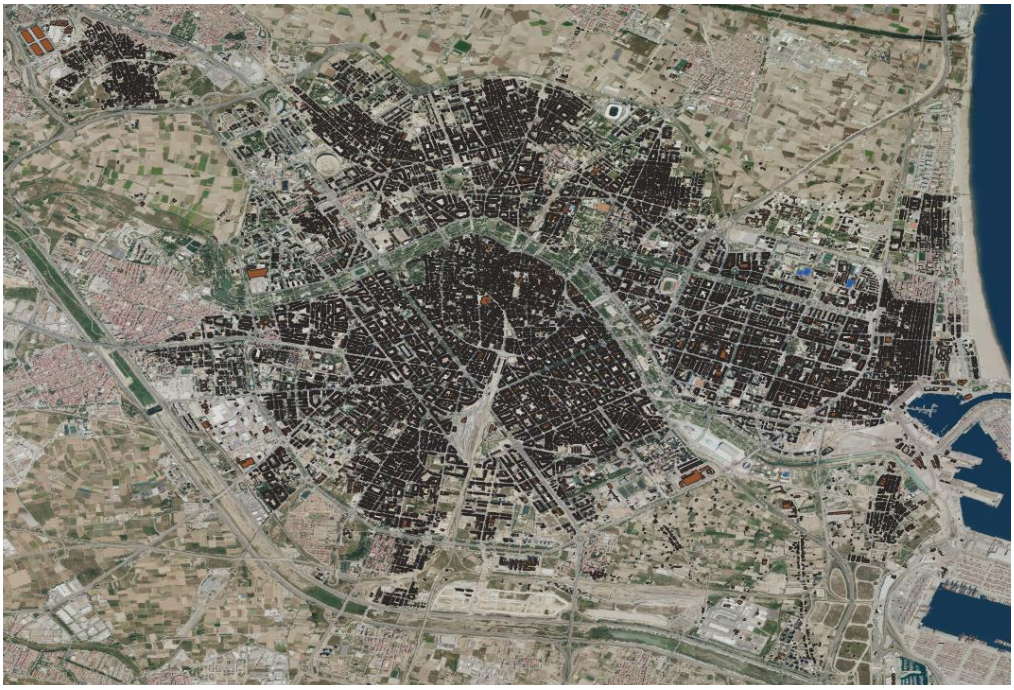

Figure 26: *"GEO_MASK_CADASTRAL_VALENCIA". Vector layer corresponding to the superposition of the layer "GEO_MASK_VECTORIAL" on the layer "ValenciaUrbano_PartInfo" obtained in section 3.3.2.*

3.4 ENERGY SAVINGS AND EMISSIONS REDUCTION

To assess the energy savings and CO_2 emission reductions from the implementation of GRs, as detailed in Section 2.4 and 2.5.1 (see summary in Figure 27). Attribute table was extracted from the vector layer ***GEO_MASK_CADASTRAL_VALENCIA***, in MS Office Open XML [XLSX] spreadsheet format, named *"DATA_VALENCIA"*. Prior to this operation, a consistency check of the table data with the information mentioned in section 3.3.1 was carried out. This included the addition of a new column using the *"field calculator"* function to determine the "*Total Potential Roof Area*" suitable for the placement of GRs.

Subsequently, using the digital cadastre of the city of Valencia, obtained from the "Sede Electrónica del Catastro" (Gobierno de España, 2024), which operates under the supervision of the Ministry of Finance, the data in *DATA_VALENCIA* was updated and supplemented. These include the full address of the properties (street name and number), the postal code, as well as the areas corresponding to the constructed area (*"ConstructedArea"*) and the total area of the cadastral parcel (*"GraphicArea"*). It should be noted that the digital cadastre provides additional relevant information, such as the year of construction, the cadastral identification of specific buildings and units, their detailed location, the classification of the area (urban or rural), and the percentage that each 20-digit record represents within the total of the property.

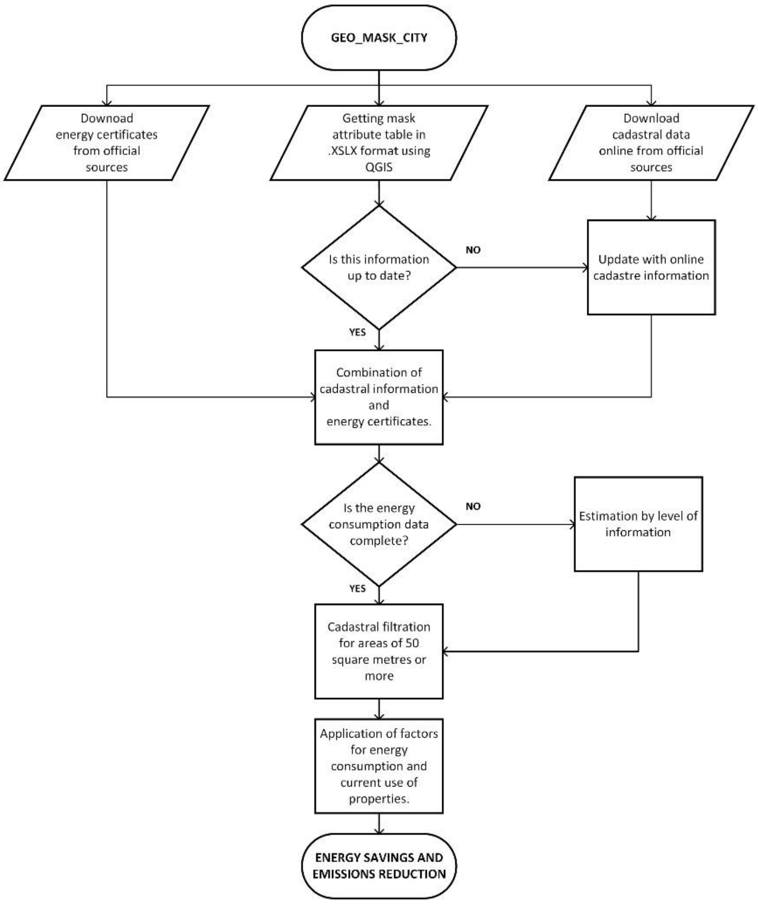

Figure 27*: Step-by-step summary of methodology 2.4 and 2.5.1.*

In parallel, and using the *QGIS* geoprocessing tool *"Cut"*, the vector layer ***GEO_MASK_CADASTRAL_VALENCIA*** was segmented into the different districts that make up the city of Valencia, using the modified vector layer **"districtes-distritos.geojson"** mentioned in section 3.1 as a reference (Figure 7). This procedure resulted in the generation of a new vector layer, composed of the 18 districts, thus facilitating the correlation between the cadastre and the districts to complete the information present in *DATA_VALENCIA.*

Subsequently, through the IVACE website (Institut Valencià de Competitivitat Empresarial, 2024), the energy certificates corresponding to the province of Valencia were downloaded, covering a period from 2013 to 2023, given their ten-year validity. This database includes the cadastral registration (with a variability of 14 to 20 digits), the year of construction, the address of the property (in non-standardised format), the energy classification letter, the annual energy consumption per square metre, and the annual CO_2 emissions per square metre.

In order to integrate this valuable information, the link between the energy certificates and *DATA_VALENCIA* was made using the 14-digit cadastral register, assigning each property an average annual energy consumption (kWh/m^2) and CO_2 emissions (kg C/m^2).

With the information from *DATA_VALENCIA* properly updated and linked with the data relevant to energy consumption and CO_2 emissions, a specific selection criterion was implemented on the column "Total Potential Roof Area". This criterion consisted of the exclusive inclusion of those properties whose surfaces available for the installation of GRs were equal to or greater than 50 m^2. This measure was adopted based on section 1.3.2.2 of the document, which specifies the optimal size for the implementation of GRs. The filtering process culminated in the creation of a refined database, called *"DATA_VALENCIA_50m2"*, consisting only of those properties that meet the minimum surface area requirement. Additionally, since *DATA_VALENCIA* organised each cadastral entry into separate segments, it was necessary to consolidate these fragments into a single record representing each property property in a comprehensive manner for *DATA_VALENCIA_50m2*, since each part already met the minimum size and could be considered as an individual property.

Subsequently, the missing data related to energy consumption and CO_2 emissions were completed in the *DATA_VALENCIA_50m2* file. It is important to note that, unlike in section 2.5.1 of this document, in this case study the estimation was made after applying the filter for the ideal GR size. The objective was to reduce the number of properties without information to analyse, which reduced the percentage of estimated values and optimised the calculation process.

Initially, of the 22,559 cadastral records contained in *DATA_VALENCIA_50m2*, only 16,884 (equivalent to 74.84% of the total) had data on consumption or emissions. Therefore, a first average estimate was made based on the neighbourhood of the property, its use, the year of construction and the constructed area (*"ConstructedArea"*). Thus, information was completed for 4,978 cadastral records (22.07% of the total), leaving 697 records (3.09% of the total) without information. For those records that still lacked the necessary data, a second average estimation was carried out, this time omitting the *ConstructedArea* as a criterion. This resulted in 593 additional cadastral records (2.63% of the total) with information on consumption and emissions. As for the remaining 104 records (0.46% of the total) that remained without information, 79 (0.35% of the total) were completed by a third average estimation, which, instead of considering neighbourhoods, considered the districts of Valencia. The remaining 25 records (0.11% of the total) were completed by direct comparison.

This rigorous process culminated in the complete update of the *DATA_VALENCIA_50m2* file, incorporating all cadastral records with energy consumption and CO_2 emissions data. In this way, the data collection and analysis phase for the study in question was successfully completed, in addition to obtaining the total GRs to be assembled equivalent to the number of cadastral records as indicated in section 2.5.1. It is important to underline that the values concerning energy consumption and CO_2 emissions are presented per square metre of the property. Therefore, it is necessary to apply equation (1) to derive these values in kWh or kg CO_2 per year.

Subsequently, taking into consideration the mediterranean climate characteristic of the city of Valencia, a thermal conditioning factor of 48.5% has been adopted, in accordance with the guidelines established by the IDAE in the report "Analysis of the energy consumption of the residential sector in Spain" (IDAE & Gobierno de España, 2011).This percentage is made up of 40.9% heating, 1.1% air conditioning and 6.53% domestic hot water, corresponding to 1/3 of the total allocated to this item (Figure 28).

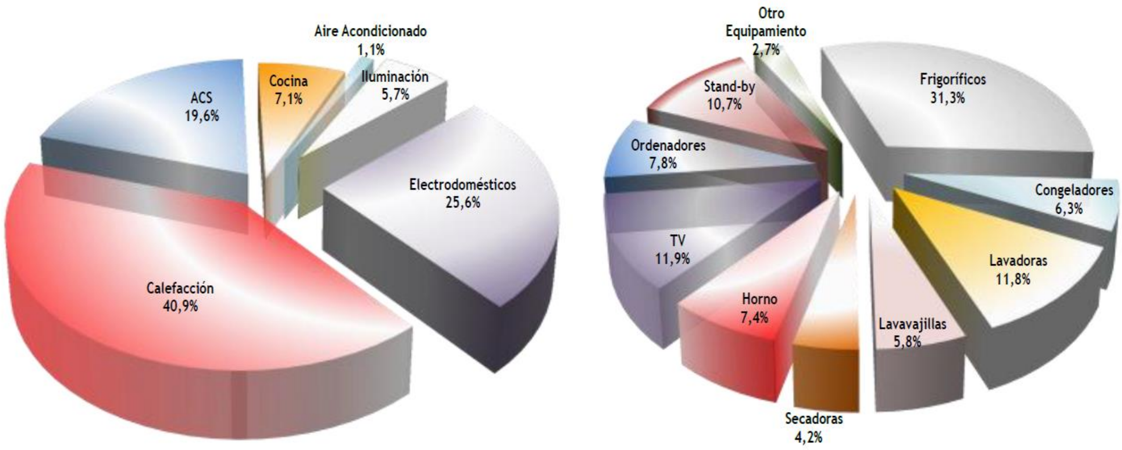

***Figure 28**: Energy Consumption Structure by Energy Uses for the mediterranean climate (IDAE & Gobierno de España, 2011).*

The ratio of residential energy consumption, supported by various studies, underlines the connection between efficiency in heating/cooling systems and domestic hot water consumption. The (IEA, 2018) states that a 1% reduction in heating and cooling translates into a 0.4% saving in domestic hot water, implying that a 10% reduction in these systems could generate a 4% saving in hot water consumption. Similarly, research by (Lawrence Berkeley National Laboratory (LBNL), 2021) shows a high correlation (0.8) in households with high hot water consumption, above 10% of their total energy consumption. (PNNL, 2017) also finds that a 10% reduction in heating and cooling results in a 3% saving in hot water. Based on these studies, the selection of consumptions for the energy calculation is justified, especially the focus on the allocation of one third for domestic hot water.

It is relevant to mention that this percentage has also been applied to non-residential buildings. By implementing equations (2), it was possible to calculate the annual energy consumption and CO_2 emissions attributable exclusively to thermal loads in each building.

$$\mathbf{factor_{conditioning}} = \mathbf{48,5}\ [\%]$$

Subsequently, two crucial aspects described in section 2.5.1 were taken into consideration, concerning the energy savings derived from the installation of GRs and the percentage of use of GRs on roofs. Concerning the first aspect and based on the stipulations of section 1.3.2.2, a 17% decrease in energy consumption is expected for single family houses, which for this study are those houses with 2 floors or less (including the ground floor). For buildings, the energy savings are distributed as follows: 17% for the top floor, 6% for the penultimate floor, 1.5% for the floor above the penultimate floor and 0.5% for the following floors. Buildings that do not fit these categorisations will experience energy savings of 15% (Zayas Orihuela, 2023). To determine the percentage use of GRs, equation (3) was used.

Finally, equation (4) is used to calculate the savings in energy consumption, as well as the reduction of CO_2 emissions due to energy generation, on an annual basis for each of the buildings. On the other hand, to estimate the total energy savings for the city of Valencia, equations (5) were applied.

3.5 CO_2 EMISSIONS CAPTURED PER GREEN ROOFS

In relation to CO_2 sequestered emissions, the CSB10-S substrate (composed of compost, soil and bricks in a volumetric ratio of 1:1:3) has been selected together with the perennial species Silene Vulgaris, as indicated in section 1.3.2.3 of this document (Ondoño, Martínez-Sánchez, & Moreno, 2018). This choice is based on the suitability of this combination for a mediterranean climate such as that of Valencia, as it provides the ability to improve the organic content of the substrate, retain water and nutrients, and encourage a deeper root system, resulting in an increase in carbon and nitrogen sequestration, as well as promoting sustainable plant growth. According to this choice and considering that one molecule of carbon dioxide (CO_2) contains one carbon atom, the sequestration factor of this combination has been considered, which corresponds to:

$$\boldsymbol{factor_{sequestration} = 0.851 \left[\frac{kg\ C}{m^2\ year}\right] \cong\ 3.16 \left[\frac{kg\ CO_2}{m^2\ year}\right]} \tag{9}$$

where $1 \left[\frac{\text{kg C}}{\text{year}}\right]$ equals approximately $3.67 \left[\frac{\text{kg CO}_2}{\text{year}}\right]$

Then, considering the ***Total Potential Roof Area*** and the sequestration factor of the substrate/plant combination, according to equation (6), the total amount of CO_2 sequestered by each building is obtained. From this, using equation (7), the total amount of CO_2 sequestered by the installation of GRs in the city of Valencia is calculated.

CHAPTER 4. RESULTS

The following chapter of this study will present the results obtained for the case study using the methodology presented in chapter 2.

4.1 POTENTIAL AREA

Taking into account the vector and raster layers obtained during section 3.3 of the previous chapter, this section will be divided by presenting the area values.

4.1.1 TOTAL AREA OBTAINED FROM MATLAB's GEOLOCATED MASK

In section 3.3.2, the raster layer ***GEO_MASK*** was visualised, which resulted from the merging of the data obtained by the *MATLAB* codes *RTD* and *SLOPE*. From this mask in raster format (Figure 24), and using the raster analysis function *"Report unique values of raster layer"*, it is determined that the total area potentially available for roof installation is:

$$\mathrm{Geo_{Mask}} - \mathrm{AREA_{Potencial\ Roof}} = 8{,}211{,}740\ [\mathrm{m}^2]$$

Following this, the vector layer called ***GEO_MASK_VECTORIAL*** was analysed. Through an exhaustive review of its attribute table using *QGIS* software, relevant data related to the specific dimensions of each recorded area were extracted. Key results, obtained from this detailed analysis, are summarised as follows:

$$\mathrm{Geo_{Mask}} - \mathrm{AREA_{A<50[m^2]}} = 26{,}439\ [\mathrm{m}^2]$$

$$\mathrm{Geo_{Mask}} - \mathrm{AREA_{A\geq 50[m^2]}} = 8{,}181{,}545\ [\mathrm{m}^2]$$

These results become relevant when considering the discussion in section 1.3.2.2 on EGR, where it is mentioned that the minimum size of a GR should be 50 m² to ensure the cost-effectiveness of its installation and maintenance, compared to the environmental and sustainability benefits they provide. In this context, of the <u>*Total Roof Area*</u> selected through MATLAB code, a significant 99.63% turns out to be suitable for the implementation of GRs.

On the other hand, from the vector layer *Constru_Partinfo*, the <u>*Total Roof Area*</u> of the city of Valencia is obtained:

$$\text{Total Roof Area} = 18{,}405{,}212\ [m^2]$$

4.1.2 TOTAL MASK AREA OBTAINED FROM FINAL LAYER

From the vector layer ***GEO_MASK_CADASTRAL_VALENCIA*** resulting from section 3.3.3, together with its attribute table ***DATA_VALENCIA***, the following results were obtained:

$$\mathrm{Data}_{\mathrm{Valencia}} - \mathrm{AREA}_{\mathrm{Potencial\ Roof}} = 7{,}535{,}126\ [\mathrm{m}^2]$$

$$\mathrm{Data}_{\mathrm{Valencia}} - \mathrm{AREA}_{\mathrm{A<50[m^2]}} = 1{,}288{,}953\ [\mathrm{m}^2]$$

$$\mathrm{Data}_{\mathrm{Valencia}} - \mathrm{AREA}_{\mathrm{A\geq 50[m^2]}} = 6{,}246{,}173\ [\mathrm{m}^2]$$

This means that 82.89% of the total surface area obtained from the vector layer is suitable for the installation of GRs. Therefore, it can be stated that 6,246,173 m^2 correspond to the total surface area with the potential for GR renovation in the city of Valencia.

$$\mathrm{Total\ Potential\ Roof\ Area} = 6{,}246{,}173\ [m^2]$$

On the other hand, according to the *DATA_VALENCIA* register, a total of 28,049 buildings have been identified. Of this number, and according to *DATA_VALENCIA_50m2*, 22,559 properties have one or more surfaces that meet the minimum size required for the installation of GRs. In other words, as mentioned in section 2.4, the total number of roofs to be intervened is equal to the total number of GRs to be installed. Therefore, the total number of GRs corresponds to:

$$\mathrm{Number\ of\ GRs} = 22{,}559\ [\mathrm{un}]$$

Of the total number of buildings suitable for refurbishment according to use, these are divided as follows:

***Table 1**: Distribution of building types according to their current use suitable for refurbishment in the city of Valencia.*

Current Use	Total buildings [-]	Representation [%]
Residential Building (over 4 floors)	15,168	67.24%
Single Family Dwelling	3,180	14.10%
Residential Building (4 floors or less)	1,895	8.40%
Industrial	828	3.67%
Cultural or Health Establishment	713	3.16%
Commerce	502	2.23%
Offices	240	1.06%
Others	33	0.15%

In parallel, the data is represented visually in the section CHAPTER. ANNEX:VALENCIA PER CURRENT, both for the city of Valencia as a whole and for each specific category of current use within the city.

On the other hand, considering the distribution of building current use according to the districts considered for this study.

***Table 2**: Distribution of building current use according to the districts considered in this study.*

Current Use / District	Residential Building (less 4 floor)	Residential Building (over 4 floors)	Cultural or Health Establishment	Single Family Dwelling	Industrial	Commerce	Offices	Others	Total Buildings
POBLATS MARITIMS	590	1,117	100	798	213	84	22	3	2,927
L'EIXAMPLE	103	1,748	36	10	17	31	30	0	1,975
QUATRE CARRERES	148	1,139	40	480	113	21	7	8	1,956
CIUTAT VELLA	146	1,433	146	5	19	69	94	3	1,915
EXTRAMURS	125	1,524	33	5	11	27	13	0	1,738
CAMINS AL GRAU	63	986	30	112	57	47	5	3	1,303
RASCANYA	42	787	27	251	56	15	4	1	1,183
LA SAIDIA	70	982	38	47	17	18	3	1	1,176
POBLATS DE L'OEST	150	286	16	599	94	20	2	0	1,167
JESUS	53	757	20	226	44	52	3	3	1,158
PATRAIX	57	809	27	81	66	21	17	1	1,079
BENICALAP	106	698	27	152	56	22	3	1	1,065
BENIMACLET	129	590	19	169	13	38	2	2	962
L'OLIVERETA	56	791	35	58	15	1	3	2	961
ALGIROS	8	626	43	40	6	11	7	3	744
CAMPANAR	39	436	37	143	23	19	8	2	707
EL PLA DEL REAL	10	459	39	4	8	6	17	0	543

Finally, about the distribution according to the neighbourhoods that make up the districts mentioned in Table 2, this is presented in Table 22 of the CHAPTER. ANNEX: RESULTS OBTAINED FOR VALENCIA'S NEIGHBORHOODS. In addition, values obtained are presented graphically in the VALENCIA PER DISTRICTS section of CHAPTER. ANNEX.

4.1.3 TOTAL DISTRIBUTION BY BUILDING CURRENT USE

The distribution of the *Total Potential Roof Area* available for intervention in the city of Valencia is presented according to the specific property uses as follows:

__Table 3__: Distribution of Total Potential Roof Area for intervention in the city of Valencia by building current use. Percentage of representation with respect to 6,246,173 m² of surface area to be intervened.

Current Use	Total Area [m²]	Representation [%]
Residential Building	4,413,783	70.66%
Cultural or Health Establishment	763,006	12.22%
Single Family Dwelling	369,165	5.91%
Industrial	304,214	4.87%
Commerce	265,763	4.25%
Offices	112,590	1.80%
Others	17,652	0.28%

Regarding the district distribution of the potential surface area within the city of Valencia, it is as follows:

__Table 4__: Distribution of Total Potential Roof Area for intervention in the city of Valencia by districts considered in the study. Percentage of representation with respect to 6,246,173 m² of surface area to be intervened.

Districts	Total Potential Area [m²]	Representation [%]
POBLATS MARITIMS	577,793	9.25%
QUATRE CARRERES	571,507	9.15%
CAMINS AL GRAU	463,773	7.42%
CIUTAT VELLA	429,182	6.87%
PATRAIX	425,165	6.81%
L'EIXAMPLE	423,106	6.77%
EXTRAMURS	392,805	6.29%
ALGIROS	361,106	5.78%
JESUS	334,769	5.36%
RASCANYA	325,729	5.21%
LA SAIDIA	311,874	4.99%
L'OLIVERETA	309,049	4.95%
BENICALAP	306,614	4.91%
CAMPANAR	280,659	4.49%
POBLATS DE L'OEST	265,242	4.25%
BENIMACLET	234,972	3.76%
EL PLA DEL REAL	232,827	3.73%

Finally, with respect to the distribution according to the neighbourhoods that constitute the districts mentioned in Table 4, this is presented in Table 23 of the CHAPTER. ANNEX:RESULTS OBTAINED FOR VALENCIA'S NEIGHBORHOODS.

4.1 ENERGY SAVINGS AND EMISSIONS REDUCTION

Regarding the results obtained from the case studies shown in section 3.4, the total energy that can be saved and the CO_2 reduction per generation resulting from the installation of 22,559 GRs in the city of Valencia corresponds to:

$$\text{Energy Saving} = 161{,}951{,}027 \left[\frac{\text{kWh}}{\text{year}}\right] \approx 161.951 \left[\frac{\text{GWh}}{\text{year}}\right]$$

$$\text{CO}_2 \text{ Emissions Reduction} = 32{,}711{,}209 \left[\frac{\text{kg CO}_2}{\text{year}}\right] \approx 32{,}711.209 \left[\frac{\text{ton CO}_2}{\text{year}}\right]$$

Of the total consumption and emissions produced by the 22,559 buildings considered suitable for renovation, corresponding to 9,228.187 GWh and 1,887,330.838 tonnes of CO_2 per year approximately, the percentage reduction resulting from the action of GRs is equivalent to:

$$\text{Total Decrease} = 1.75\ [\%]$$

Of the amounts of energy savings and CO_2 reductions presented, these can be segregated according to the current use of the building, in addition to the estimated decrease in consumption associated with their use (Decrease Current Use), the total savings generated (Decrease Total) and the representation of each use in the amounts saved (Representation). The results are presented in the following table:

***Table 5**: Distribution of energy savings, emission reductions and total percentage variations in the city of Valencia by building current use.*

Current Use	Energy Saving [kWh/year]	CO_2 Emissions Reduction [kg CO_2/year]	Decrease Current Use [%]	Decrease Total [%]	Representation [%]
Residential Building	78,760,321	16,231,112	1.09%	0.853%	48.63%
Cultural or Health Establishment	36,889,928	7,165,930	3.72%	0.400%	22.78%
Single Family Dwelling	11,384,420	2,324,264	7.04%	0.123%	7.03%
Industrial	9,663,278	1,890,391	5.00%	0.105%	5.97%
Commerce	14,297,387	2,864,288	3.42%	0.155%	8.83%
Offices	10,894,202	2,224,717	4.52%	0.118%	6.73%
Others	61,492	10,508	1.360%	0.001%	0.04%

On the other hand, the same amounts obtained are represented according to the districts that constitute the city of Valencia:

***Table 6**: Distribution of energy savings, emission reductions and total percentage variations in the city of Valencia by districts considered in the study.*

Districts	Energy Saving [kWh/year]	CO_2 Emissions Reduction [kg CO_2/year]	Decrease Districts [%]	Decrease Total [%]	Representation [%]
QUATRE CARRERES	17,849,592	3,590,842	2.20%	0.19%	11.02%
CIUTAT VELLA	17,598,623	3,658,072	2.49%	0.19%	10.87%
POBLATS MARITIMS	14,365,702	2,871,912	1.78%	0.16%	8.87%
L'EIXAMPLE	11,035,152	2,308,345	1.59%	0.12%	6.81%
CAMINS AL GRAU	10,051,680	2,019,711	1.42%	0.11%	6.21%
EXTRAMURS	9,430,006	1,942,568	1.48%	0.10%	5.82%
CAMPANAR	9,319,011	1,837,114	2.00%	0.10%	5.75%
PATRAIX	9,246,962	1,874,986	1.59%	0.10%	5.71%
EL PLA DEL REAL	8,620,713	1,632,413	1.83%	0.09%	5.32%
ALGIROS	8,359,688	1,700,184	1.46%	0.09%	5.16%
POBLATS DE L'OEST	7,306,727	1,468,896	3.16%	0.08%	4.51%
JESUS	7,254,566	1,466,957	1.56%	0.08%	4.48%
L'OLIVERETA	6,748,160	1,324,934	1.53%	0.07%	4.17%
RASCANYA	6,575,338	1,342,261	1.48%	0.07%	4.06%
BENICALAP	6,568,739	1,306,822	1.61%	0.07%	4.06%
LA SAIDIA	6,529,088	1,310,874	1.43%	0.07%	4.03%
BENIMACLET	5,091,282	1,054,318	1.59%	0.06%	3.14%

Finally, with respect to the distribution according to the neighbourhoods that make up the districts mentioned in Table 6, this is presented in Table 24 of the CHAPTER. ANNEX: RESULTS OBTAINED FOR VALENCIA'S NEIGHBORHOODS. Additionally, in Figure 56 of CHAPTER. ANNEX, the percentage distribution of energy savings and CO_2 emissions reduction in the city of Valencia can be seen.

4.2 CO_2 CAPTURED PER GREEN ROOFS

Regarding CO_2 capture by GRs composed of CSB10-S substrate together with the perennial species Silene Vulgaris, the total gas capture was obtained as follows:

$$\mathrm{CO_2\ Emissions\ Captured} = 19{,}507{,}862 \left[\frac{\mathrm{kg\ CO_2}}{\mathrm{year}}\right] \approx 19{,}507.862 \left[\frac{\mathrm{ton\ CO_2}}{\mathrm{year}}\right]$$

In relation to the distribution of this CO_2 capture according to the current use of the property, it is distributed as follows:

***Table 7**: Distribution of CO_2 sequestration in the city of Valencia through building current use.*

Current Use	CO_2 Emissions Captured [kg CO_2/year]	Representation [%]
Residential Building	13,784,996	70.66%
Cultural or Health Establishment	2,382,997	12.22%
Single Family Dwelling	1,152,966	5.91%
Industrial	950,113	4.87%
Commerce	830,022	4.25%
Offices	351,638	1.80%
Others	55,131	0.28%

In relation to the distribution of CO_2 captured based on the different districts that constitute the city of Valencia, the results are as follows:

***Table 8**: Distribution of CO_2 sequestration in the city of Valencia by districts considered in the study.*

Districts	CO_2 Emissions Reduction [kg CO_2/year]	Representation [%]
POBLATS MARITIMS	1,804,547	9.25%
QUATRE CARRERES	1,784,915	9.15%
CAMINS AL GRAU	1,448,441	7.42%
CIUTAT VELLA	1,340,410	6.87%
PATRAIX	1,327,864	6.81%
L'EIXAMPLE	1,321,432	6.77%
EXTRAMURS	1,226,796	6.29%
ALGIROS	1,127,797	5.78%
JESUS	1,045,540	5.36%
RASCANYA	1,017,308	5.21%
LA SAIDIA	974,035	4.99%
L'OLIVERETA	965,212	4.95%
BENICALAP	957,608	4.91%
CAMPANAR	876,547	4.49%
POBLATS DE L'OEST	828,396	4.25%
BENIMACLET	733,859	3.76%
EL PLA DEL REAL	727,157	3.73%

Finally, with respect to the distribution according to the neighbourhoods that make up the districts mentioned in Table 8, this is presented in Table 25 of the CHAPTER. ANNEX: RESULTS OBTAINED FOR VALENCIA'S NEIGHBORHOODS. Additionally, in Figure 57 of CHAPTER. ANNEX, the percentage distribution of the amount of CO_2 sequestered in the city of Valencia can be seen.

4.3 DISCUSSION OF RESULTS

In the following section, the results obtained from the results obtained in the previous sections of this chapter will be analysed and discussed.

4.4.1 AVAILABLE AREA FROM CODES AND DISTRIBUTION OF BUILDINGS

The analysis developed, based on the results presented in section 4.1.1, demonstrates a high reliability in the *RTS*, *RTD* and *SLOPE* codes, supported by the 8,211,740 m² of surface area identified as potentially viable for the implementation of GRs. From this area obtained, 99.63% complies with the minimum requirement of 50 m² necessary for the installation of a GR, demonstrating the adequacy of the methodology used for the identification of areas suitable for intervention.

On the other hand, when considering the 18,405,212 m² of roofs available in the city of Valencia, 44.45% of this surface area is susceptible to renovation. This underlines the considerable capacity of Valencia to integrate green infrastructure solutions, which could have a significant impact on promoting sustainability and improving urban wellbeing.

Regarding results obtained in section 4.1.2, a decrease in the potential area for the installation of GRs to 7,535,126 m² is observed with respect to the results of section 4.1.1, with 82.89% of the roofs complying with the minimum size required for intervention. This variation can be mainly attributed to two factors: the possible outdatedness of the Valencia cadastral vector layers (Soriano, 2023) obtained from the *QGIS* plug-in compared to the orthophotographs of the (CING, 2020) and the temporal discrepancy between the data. The orthophotographs, captured in 2021, and the last significant update of the cadastral vector layers, carried out in 2018, suggest that some buildings present in the more recent data might not be included in the less updated records and conversely. This implies that the difference in the potential surface areas identified through the codes and the cadastral vector information is due to the outdatedness of the latter, which presented a lower number of buildings compared to those identified through the *MATLAB*-based software. Second factor is the use of *QGIS* for the processing of vector and raster layers. While *QGIS* is a powerful and accessible tool, its open-source status may entail certain restrictions compared to licensed alternatives such as *ArcGIS*.

Now, regarding the distribution of property use (Table 1), a significant proportion of buildings suitable for refurbishment are mainly residential with more than 4 floors (67.24%), followed by single family dwellings (14.10%) and residential buildings of 4 floors or less (8.40%). This reflects a clear opportunity to improve the green infrastructure in residential buildings, implying a possible decrease in energy consumption and emissions depending on the number of floors, as well as economic savings by reducing the need for energy for air conditioning of property.

Finally, analysing the distribution of the 17 districts in Valencia (Table 2 and VALENCIA PER DISTRICTS) it is highlighted that *POBLATS MARITIMS* and *L'EIXAMPLE* stand out for having the highest number of properties susceptible to intervention. These districts are characterised by their high density of residential buildings of more than four floors, where *POBLATS MARITIMS* also stands out for its considerable number of single family dwellings, offering a unique perspective in the predominant urban context. In addition, *QUATRE CARRERES* and *L'EIXAMPLE* stand out not only for the number of residential properties, but also for a notable presence of commercial, cultural and health buildings.

Lastly, the *EXTRAMURS* district stands out for maintaining an appreciable number of residential buildings with 4 or more floors, together with a diversity of properties. These findings provide valuable information for urban planning and development in Valencia.

4.4.2 DISTRIBUTION OF AREA AND GREEN ROOFS PER BUILDING

An analysis of the distribution of the 22,559 GR units planned for installation shows that residential buildings are the main type of building current use with the greatest influence on the surface area to be intervened. These represent an area of 4,413,783 m², equivalent to 70.66% of the total, corresponding to approximately 17,063 GRs (75.64% of the total to be installed). On the other hand, even though there is a low number of GRs to be installed on cultural and health buildings, which amount to approximately 713 units (3.16%), they are positioned as the second group with the second largest potential area of intervention, contributing 763,006 m² (12.22%). This finding indicates that, although individual dwellings and industrial buildings have a larger number of units, their total area available for intervention is smaller. To better illustrate these evident points, a factor was developed that measures the square metres available for intervention for each property suitable for refurbishment in relation to its current use:

Table 9*: Urban intervention factor corresponding to square metres to be intervened per total number of eligible buildings to be refurbished according to current use.*

Current Use	Urban intervention factor per current use [m²/buildings]
Residential Building	259
Cultural or Health Establishment	1,070
Single Family Dwelling	116
Industrial	367
Commerce	529
Offices	469
Others	4,017

On the other hand, interaction between the districts reflects similar patterns. Although *POBLATS MARITIMS* has approximately 1,000 more buildings suitable for refurbishment compared to *QUATRE CARRERES* (Table 2), the percentage difference in the distribution of potential surface area between the two districts does not exceed 0.10% according to the values indicated in Table 3. This underlines the remarkable potential of *QUATRE CARRERES* as a district to be intervened, considering its lower number of buildings, but high potential for refurbishment through GRs. A similar analysis applies to *L'EIXAMPLE* and *CAMINS AL GRAU*, where the former, despite being the district with the second highest number of buildings, has a lower potential than *CAMINS AL GRAU*, which has almost 700 buildings less suitable for intervention. Particularly noteworthy is the case of *ALGIROS*, the third district with the smallest number of buildings to intervene but which, due to its great potential, exceeds more than half of the districts in terms of the amount of potential surface area to be reformed.

In order to better illustrate these points, and in the same way as was done with the properties by current use, a factor measuring the available square metres was developed:

***Table 10**: Urban intervention factor corresponding to square metres to be intervened per total number of eligible buildings to be refurbished according to district.*

Districts	Urban intervention factor per district [m^2/buildings]
ALGIROS	485.36
EL PLA DEL REAL	428.78
CAMPANAR	396.97
PATRAIX	394.04
CAMINS AL GRAU	355.93
L'OLIVERETA	321.59
QUATRE CARRERES	292.18
JESUS	289.09
BENICALAP	287.90
RASCANYA	275.34
LA SAIDIA	265.20
BENIMACLET	244.25
POBLATS DE L'OEST	227.29
EXTRAMURS	226.01
CIUTAT VELLA	224.12
L'EIXAMPLE	214.23
POBLATS MARITIMS	197.40

Data about urban intervention factor per district presented in Table 10 confirms the above statements, highlighting that *ALGIROS* has the most favourable factor and, consequently, the greatest potential for intervention among the 17 divisions of the city of Valencia under study, followed by *EL PLA DEL REAL*, *CAMPANAR* and *PATRAIX* in order of potential. Furthermore, this table reinforces this assessment by showing *POBLATS MARITIMS*, the district with the greatest quantity of potential surface area and properties to be intervened, as the district with the least potential. This analysis ratifies previous observations and underlines the relevance of considering both the number of buildings and the available surface area in the planning of GR interventions, prioritising districts with higher surface area per building ratios in order to achieve an optimal environmental and social impact.

4.4.3 ENERGY SAVINGS EXPECTED AND CO_2 DECREASE

Before present the energy analysis and emissions in relation to the city of Valencia, it is essential to note that the abatement percentages always refer to the consumption of the 22,559 buildings identified as suitable for refurbishment, according to the data provided by *DATA_VALENCIA_50m2*. Therefore, the abatement percentages will be calculated based on those buildings that have the potential for refurbishment and can directly benefit from the measures described in section 1.3.2

As outlined in section 4.2, the planned installation of 22,559 GR units would generate energy savings and CO_2 emission reductions of approximately 161,951 GWh and 32,711,209 tonnes of carbon dioxide per year, respectively. This would represent a decrease of 1.75% in relation to total annual consumption and emissions. It is important to note that this decrease in both factors is proportional, as it is based on the reduction of final energy consumption.

Regarding the distribution of the impact on energy consumption and CO_2 emissions, residential buildings show the highest expected decrease with a percentage of 48.63%. However, among the various categories of current building usage, the projected energy savings in relation to their own consumption show the lowest percentage decrease. On the contrary, single-family dwellings with two floors or less represent the third highest current use category in terms of expected savings, accounting for 7.03% of the total. Furthermore, this category experiences the most significant reduction in consumption and emissions relative to its own values, reaching 7.04%.

With respect to the districts of Valencia, *QUATRE CARRERES* and *CIUTAT VELLA* stand out for having almost identical percentages in terms of the reduction of consumption and emissions, both standing at over 10.5%. They are followed by *POBLATS MARITIMS* and *L'EIXAMPLE*, with reductions of 8.87% and 6.81%, respectively. However, when focusing on the reduction in specific consumption by district, rather than on the total consumption of the buildings analysed, POBLATS *DE L'OEST* is the district that benefits most from the installation of GRs, with a 3.16% reduction in its specific consumption. Subsequently, *QUATRE CARRERES* and *CIUTAT VELLA* also show notable reductions in their consumption, with percentages of 2.20% and 2.49%, respectively.

Additionally, when analysing emission reductions, it is crucial to consider the CO_2 sequestration potential provided by GRs. As discussed in section 4.3, the total potential CO_2 sequestration by GRs is estimated at 19,507.862 tonnes of CO_2 per year. Of this quantity, a significant 70.66% would come from residential buildings. In terms of districts, *POBLATS MARITIMS* and *QUATRE CARRERES* stand out for their impact on CO_2 sequestration, with 9.25% and 9.15% respectively. Finally, considering the emission savings together with the expected CO_2 sequestration for building current use equivalent to 52,219.071 tonnes of CO_2 mitigated per year, the following results are obtained regarding the CO_2 mitigated:

***Table 11**: Total CO_2 mitigation in the city of Valencia by building current use.*

Current Use	CO_2 Mitigation [kg CO_2/year]	Representation [%]
Residential Building	30,016,107	57.48%
Cultural or Health Establishment	9,548,927	18.29%
Single Family Dwelling	3,477,230	6.66%
Industrial	2,840,504	5.44%
Commerce	3,694,309	7.07%
Offices	2,576,355	4.93%
Others	65,639	0.13%

Now, regarding the district division:

Table 12: Total CO_2 mitigated in the city of Valencia by districts considered in the study.

Districts	CO_2 Mitigation [kg CO_2/year]	Representation [%]
QUATRE CARRERES	5,375,757	10.29%
CIUTAT VELLA	4,998,481	9.57%
POBLATS MARITIMS	4,676,459	8.96%
L'EIXAMPLE	3,629,777	6.95%
CAMINS AL GRAU	3,468,152	6.64%
PATRAIX	3,202,850	6.13%
EXTRAMURS	3,169,364	6.07%
ALGIROS	2,827,980	5.42%
CAMPANAR	2,713,661	5.20%
JESUS	2,512,497	4.81%
EL PLA DEL REAL	2,359,570	4.52%
RASCANYA	2,359,570	4.52%
POBLATS DE L'OEST	2,297,292	4.40%
L'OLIVERETA	2,290,145	4.39%
LA SAIDIA	2,284,909	4.38%
BENICALAP	2,264,430	4.34%
BENIMACLET	1,788,176	3.42%

In both distribution categories, residential buildings, as well as those dedicated to cultural and health purposes, continue to stand out for their significant contribution to both the reduction of CO_2 emissions and their capture. Similarly, in terms of geographical distribution, the districts of *QUATRE CARRERES*, *CIUTAT VELLA* and *POBLATS MARITIMS* are reaffirmed as the most influential in this respect.

4.4.4 ASSESSMENT OF URBAN INTERVENTIONS IN DISTRICTS

As a complement to the analysis of the results obtained through this study and with the aim of assessing the suitability of different urban interventions, it is essential to employ a methodical and structured approach, which will be carried out using the Hierarchical Analysis Method (AHP). AHP (Saaty, 1994) is a multi-criteria decision technique that helps to prioritise and make the best decision when criteria are numerous and complex.

In the context of our analysis, the factors considered are:

- Urban intervention factor per current use [m^2/buildings]
- Urban intervention factor per district [m^2/buildings]
- Energy Saving [kWh/year]
- CO_2 mitigation [kg CO_2/year]

It is important to note that CO_2 mitigation is taken into account since CO_2 emission savings are directly related to energy savings. This suggests that neither aspect should be more important than the other.

However, by considering sequestered CO_2 together, emissions can play a more distinctive and autonomous role.

The assignment of importance to the different factors is done through a pairwise comparison matrix, using AHP principles. These factors highlight the specific potential of each current use and district for interventions, considering both energy efficiency and CO_2 sequestration capacity. The AHP methodology involves comparing each pair of factors, assessing which has greater relevance to the main objective of this study. Therefore, higher priority is given to CO_2 mitigation, considering its contribution to the reduction of CO_2 emissions in the city and its positive impact on the quality of life of the population, both for those who implement GRs on their properties and for the rest of the community. Secondly, energy savings are valued, based on their role in the fight against climate change and the direct benefits for individuals. In third and fourth place, the urban intervention factor by district and the urban intervention factor by current use are placed respectively, due to the fact that it is more feasible and relevant to intervene in locations with similar characteristics rather than in all types of buildings associated with a specific current use.

The result is a matrix that reflects the decision-maker's perception of the relative importance of each factor (Table 13). The weights or priorities of each factor are then calculated by analysing the matrix, which provides a ranking based on its contribution to the overall objective (Table 15).

The results of the methodology are presented below:

***Table 13**: Pairwise comparison matrix.*

Decision factors	Urban intervention factor per current use	Urban intervention factor per district	Energy Saving	CO_2 Mitigation
Urban intervention factor per current use	1.00	0.33	0.17	0.11
Urban intervention factor per district	3.00	1.00	0.33	0.17
Energy Saving	6.00	3.00	1.00	0.33
CO_2 mitigation	9.00	6.00	3.00	1.00

According to the comparison matrix, the weight of each factor corresponds to:

***Table 14**: Weights of criteria.*

Decision factors	Weight
Urban intervention factor per current use	0.0466
Urban intervention factor per districts	0.1052
Energy Saving	0.2571
CO_2 mitigation	0.5912

Considering the values detailed in Table 27, included in the annex of this document, and based on the weight of the factors indicated in Table 14, the decision criteria table (CHAPTER. ANNEX: Table 27). From this table, the districts with the greatest potential for interventions are identified, based on the use of the property, which are:

Table 15: Districts with the greatest potential for intervention according to type of current use of the property.

Districts	Current Use	Weighting
L'EIXAMPLE	Residential Building	4.072
EXTRAMURS	Residential Building	3.761
CAMINS AL GRAU	Residential Building	3.705
POBLATS MARITIMS	Residential Building	3.684
QUATRE CARRERES	Residential Building	3.571
PATRAIX	Residential Building	3.299
CIUTAT VELLA	Residential Building	3.242
ALGIROS	Residential Building	2.775
CIUTAT VELLA	Cultural or Health Establishment	2.757
JESUS	Residential Building	2.709

It is important to note that among the 10 districts identified with the greatest potential for interventions, 9 prioritise implementation on residential buildings. This approach underlines the strategy of maximising the impact by implementing GRs on the largest possible area, concentrating efforts on the smallest number of buildings. Such an approach not only optimises the benefits in terms of energy savings and CO_2 emission reductions, but also highlights the effectiveness of targeting interventions where they will have the greatest effect.

To complement the analysis carried out and considering the district of *L'EIXAMPLE* as the most appropriate one, the information presented in the CHAPTER. ANNEX: DISTRICTS AND NEIGHBORHOODS and RESULTS OBTAINED FOR VALENCIA'S NEIGHBORHOODS. Following the same methodology and criteria used in this section (Table 14), it is identified which of the neighbourhoods that make up this district, in terms of residential buildings, present the greatest potential for intervention. For this, the values detailed in Table 28, included in the appendix, were used to obtain a new table of decision criteria (CHAPTER. ANNEX:Table 29). This table identifies the neighbourhoods with the greatest potential in the district of L'EIXAMPLE in terms of residential buildings, which are:

Table 16: Potential of neighbourhoods belonging to the district of L'EIXAMPLE.

Neighborhood	Current Use	Weighting
RUSSAFA	Residential Building	48.650
EL PLA DEL REMEI	Residential Building	25.734
LA GRAN VIA	Residential Building	25.616

Within the *L'EIXAMPLE* district (Figure 29) and taking into consideration the data presented in Table 16, it is evident that the *RUSSAFA* neighbourhood clearly stands out as it has the highest weighting in this category. This positions it as the leading candidate for significant interventions in the district.

However, considerations regarding the economic costs associated with the installation and maintenance of GRs were omitted from this analysis. In addition, the social costs of intervening in residential buildings, particularly those affecting ground floor dwellers, who may perceive little or no direct energy benefits, were also not taken into account.

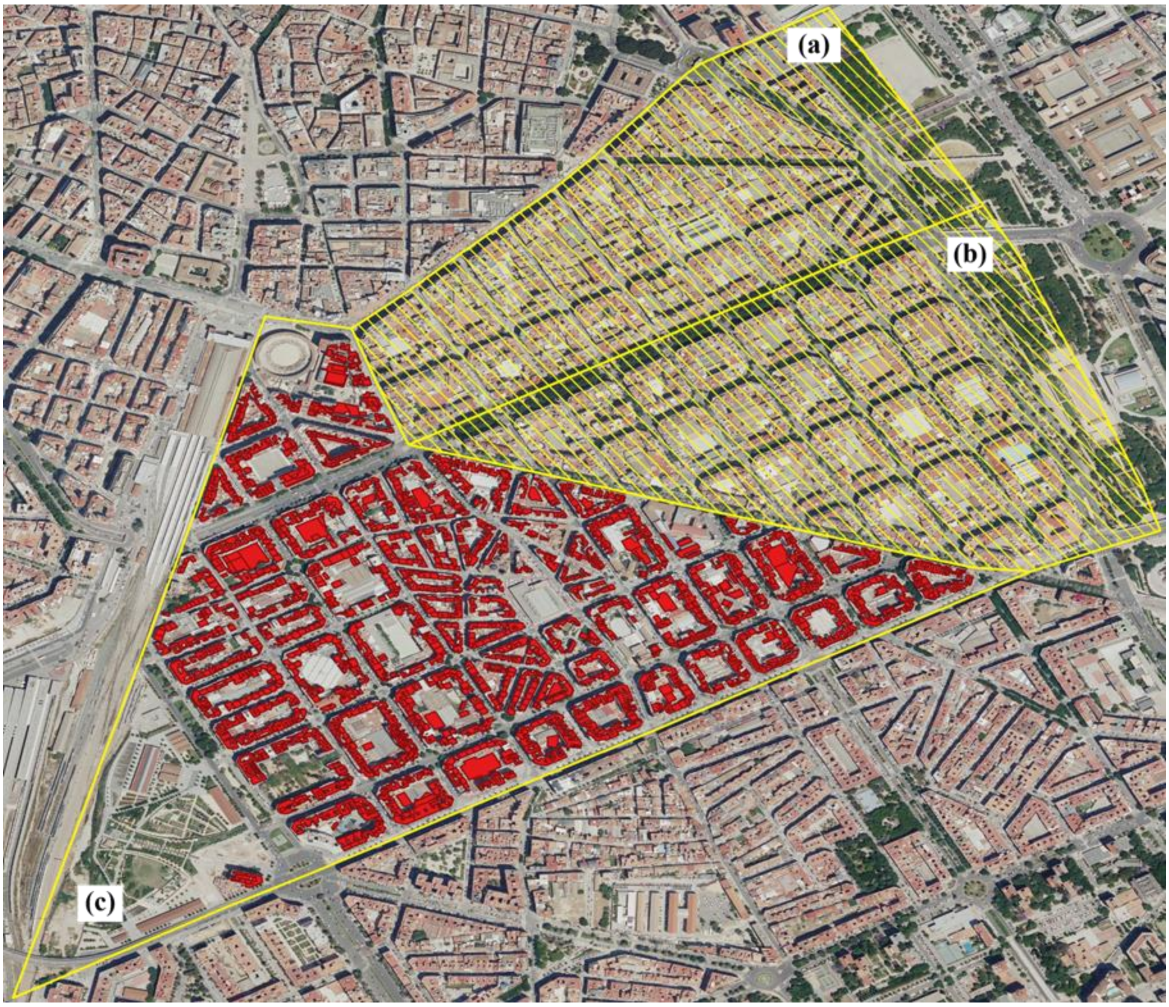

Figure 29*: District of L'EIXAMPLE. (a) EL PLA DEL REMEI neighbourhood. (b) LA GRAN VIA neighbourhood. (c) Residential buildings in RUSSAFA, the neighbourhood with the greatest potential in L'EIXAMPLE.*

4.4.5 MATLAB CODE VALIDATION

For the validation of the codes developed in this study, the results will be compared with the findings of (Zayas Orihuela, 2023) in his degree thesis, which stands out for being one of the few detailed analyses of surfaces suitable for GRs in Valencia, focusing specifically on the L'Illa Perduda neighbourhood. Despite the methodological differences in image processing and software used, both works share a focus on VA for the identification of viable areas. According to Zayas et al., the total area available for the installation of GRs in this neighbourhood amounts to 48,300 m², representing 48% of the total roof area of the neighbourhood. Of this amount, 39,900 m² belong to residential buildings, which constitutes 49% of the total available residential roof areas. In addition, it is identified that the selected non-residential rooftops comprise 46% of the total non-residential area, totalling 8,400 m². This preliminary analysis provides a solid comparative basis for assessing the effectiveness of the code created in this work.

On the other hand, in relation to the results obtained from the *RTS*, *RTD* and *SLOPE* codes presented in the RESULTS OBTAINED FOR VALENCIA'S NEIGHBORHOODS provided in the CHAPTER. ANNEX:

***Table 17**: Comparison of total potential surface area suitable for refurbishment with GRs in the district of L'Illa Perduda, Valencia.*

Current Use	Calculation of the decarbonization potential of the installation of green roofs in the L'Illa Perduda neighborhood in València	Modelling the potential of green roof installation for the decarbonization of urban areas. Case study of Valencia, Spain	Error
	[m²]	[m²]	[%]
Residencial	39,900	52,196	24%
No Residencial	8,400	9,057	7%
Total Buildings	48,300	61,254	21%

The difference in results, reflected in the amounts and percentages of error presented in Table 17, could be mainly due to the following aspects:

- **Shaded areas**: One of the problems mentioned by Zayas et al. is the difficulty of recognising shaded areas during the image segmentation process. Shadows, especially small shadows that tend to appear darker, such as those produced by parapets or sharp-shaped objects, reduce the area of the identified blobs (groups of pixels). In addition, temporary obstacles present at the time the photographs were taken, such as clothes hung out to dry, make recognition more difficult. In the case of this study, the orthophotographs provided better colour resolution due to the technology used to capture them. In this way, these images buffer the impact of shading, allowing the AV code to consider such surfaces suitable for roof mounting.
- **Roof slopes**: The problem of accurately estimating roof slopes using *LiDAR* data, pointed out by Zayas et al., is due to the low density of *LiDAR* points, which leads to errors in identifying incorrect slopes on flat roofs due to obstacles and structural changes. To counteract this, filters were implemented that discard anomalous high slopes or surfaces with obstacles. In contrast, the *SLOPE* code presented in this study presents this analysis by segmenting *LiDAR* data and using *k-means* to cluster points on buildings, thus facilitating the calculation of slopes. Despite facing challenges inherent to k-means, such as defining the number of clusters and sensitivity to initial conditions, this code focuses on efficiently clustering points to calculate slopes and applying filters to excessive slopes. While Zayas et al. focus on adjusting slope estimation with statistical techniques to overcome the limitations of *LiDAR*, *SLOPE* code proposes a clustering methodology and structural analysis prior to slope calculation. Both approaches present *LiDAR* data constraints from different angles: improving slope estimation in the case of Zayas et al. and through clustering and filtering in *SLOPE* code. The latter also provides detailed visualisations and binary masks to assess the feasibility of rehabilitating roofs, offering a comprehensive solution for slope analysis.
- **Identification of obstacles and gaps in roofs**: Challenges presented by the *RTD* code include the accurate identification of obstacles on roofs, such as HVAC systems or moderate-sized voids for city-wide surveys. Despite manual indications of the presence of these elements, the code tends to mistakenly incorporate such gaps and obstacles as part of the identified potential surfaces, due to the size and pixel density of the processed images. In contrast, the approach adopted by Zayas et al. is more effective in dealing with this problem, benefiting

from the analysis of a limited number of rooftops in the studied neighbourhood compared to the extent of the city. This limitation facilitated a more thorough examination of the rooftops, relying on two key strategies: the proper generation of blobs in high-resolution images and the manual and visual review of the rooftops. This method allowed for a more accurate identification of areas suitable for GR installation by avoiding incorrectly classifying gaps and obstacles as potential areas.

The larger surface area identified for GRs in the L'Illa Perduda neighbourhood in this study could be due to the inclusion of additional areas resulting from not considering certain roof elements, as well as areas omitted in the reference work due to shading and the different approach to steeply sloping roofs. Although there is a discrepancy of close to 20% between the two studies, the magnitude of the results is comparable, suggesting a solid basis for both AV-based approaches. Despite the identified areas for improvement, the consistency between the results obtained in this study and those of this similar study underlines the reliability of the developed codes and their ability to provide consistent analysis on surfaces suitable for GR installation.

4.4.6 IMPROVEMENT OPPORTUNITIES

Despite the correctness of the results obtained in this work, the following options for improvement are proposed according to the points to be optimised identified during its development:

- **Roof slopes**: Although the *SLOPE* code developed in this study is effective in identifying roofs with suitable slopes, its performance depends significantly on the k-means function, which has several limitations that have been discussed throughout the study. These constraints include the requirement to define the number of clusters (k) in advance, the sensitivity to the initial values assigned to the cluster centres, and the challenges in dealing with clusters that do not adopt spherical shapes or vary in size. These characteristics of *k-means* imply the need to perform multiple iterations, at least 10 times for each *LiDAR* file processed, to generate a mask that satisfactorily represents roofs with slopes greater than the established limit. Faced with this scenario, the need arises to explore and adopt algorithmic alternatives for data clustering to automate and simplify this crucial process. The search for such alternatives could lead to a significant improvement in the efficiency and accuracy of roof slope analysis, making the process more resilient to the inherent variations in LiDAR data and the structural complexities of roofs.
- **Identification of singularities**: Another factor that could present an opportunity for improvement, in the perspective of the identification of roofs suitable for GR assembly developed in this study, is the more accurate identification of singularities (elements and gaps) on roofs. To optimise the identification of roof singularities for GRs, it is crucial to refine the analysis of blobs by means of advanced algorithms that distinguish useful areas from critical voids. The implementation of fine-tuned morphological operations and machine learning classification techniques will effectively differentiate between structural gaps and obstacles. In the context of the analysed code, despite manual indications to exclude certain singularities, the mask treatment process still erroneously incorporated them as viable areas. This situation suggests the need to adjust specific mask processing algorithms to respect manual exclusions.

Also, it could involve improving the discrimination at the mask processing stage, possibly by integrating deep learning algorithms or advanced AV techniques to complement that applied by the *RTD* code. These techniques would allow the system to more accurately recognise and respect manual selections and exclusions, ensuring that flagged gaps are not erroneously marked as eligible areas.

- **Optimised colour detection:** In order to optimise the roof identification process using colour classification, it is proposed to implement a system that integrates the classification of *LiDAR* data and the georeferencing of orthophotographs. The approach would consist of developing an algorithm capable of altering the colour of those pixels in the *TIF* format images that do not match points classified in the *LAZ* format files specifically as roofs, assigning them a black colour. This methodology would significantly speed up the process of roof recognition and the elimination of elements not relevant to surfaces suitable for the installation of GRs, thus facilitating a more efficient and accurate identification of target areas.
- **Street inclusion:** As a complement to a more focused study on specific areas of the analysed cities, it is suggested to use the capabilities of *QGIS* to establish a connection between a reference layer, such as *OPENSTREET VIEW* or *GOOGLE MAPS*, and the binary mask created by this study. This would allow not only to identify the districts or neighbourhoods with the highest potential, but also to visualise in more detail the implementation of GRs at more local scales, such as avenues, streets or houses. This approach would make projects more feasible and applicable in specific urban contexts.

CHAPTER 5. CONCLUSIONS

This study has successfully achieved its stated objectives by providing an innovative methodology that integrates AV technologies and geo-referenced techniques. This methodology, applicable to any city, both inside and outside Spain, effectively identified surfaces suitable for the implementation of GRs. Through the exhaustive analysis developed, a solid basis for future research in areas with mediterranean and other climates has been established, offering a replicable strategy for estimating energy savings, emission reductions and CO_2 capture in different urban contexts, as long as information on the cadastre and energy certificates of the property that make up the city is available.

The implementation of the proposed methodology in the city of Valencia showed that 66.49% of the 22,559 properties evaluated are susceptible to being refurbished with GRs, particularly those with more than four floors. *POBLATS MARITIMS* emerged as the district with the greatest capacity for intervention, with 3,105 suitable properties. A total of 6,246,173 m² of roofs were identified as viable for this initiative, representing 44.47% of the total roof area, with the residential sector accounting for 89.74% of the identified potential.

Based on these results, the installation of 22,559 GR units was projected. This approach anticipates energy savings of 161,951 GWh per year and a reduction of 52,219.071 tonnes of CO_2, highlighting the crucial role of residential buildings with savings of 48.63% in energy and 70.28% in CO_2 mitigation. Additionally, the effectiveness of single family dwellings in reducing their own energy consumption associated with buildings by 7.04% is noted. Districts of *QUATRE CARRERES* and *CIUTAT VELLA* are identified as key areas, contributing approximately 11% in energy savings and 10% in CO_2 reduction, underlining the significant potential of these interventions.

The application of the AHP methodology has highlighted residential buildings in the districts of *L'EIXAMPLE*, *CAMINS AL GRAU* and *EXTRAMURS* as those with the greatest potential impact. This is reflected both in the availability of surface area for interventions and in the benefits related to energy savings and reduction of CO_2 emissions. Furthermore, in the district of L'EIXAMPLE, which received the highest weighting, the applied methodology especially highlights the RUSSAFA neighbourhood as the one with the highest potential for interventions in properties of the same residential use.

It is important to mention that, although the validation of the code developed for this study revealed an error of 20% compared to a similar study, but with proportional orders of magnitude, this discrepancy emphasizes opportunities for improvement in technical aspects. These opportunities are particularly focused on optimising AV (Value Added) and advanced point cloud processing, with the aim of refining the accuracy of future assessments.

From a personal perspective, although the results do not demonstrate a sufficiently high impact, attractive and feasible opportunities open up. This includes the possibility of combining GRs with PV panels or partial implementations in specific districts or single family residential properties. In these more limited contexts, the benefits in terms of energy savings would be more direct and tangible. This approach, complemented by a detailed economic analysis, could provide an attractive balance to encourage the adoption of this green technology, highlighting the importance of residential buildings and single family homes in decarbonising the city and improving the quality of urban life.

CHAPTER 6. PROJECT BUDGET

In the following chapter, the economic estimate or budget associated with the development of the project that has been the focus of this work will be detailed. This will include a detailed analysis of the main and secondary activities, as well as the resources and equipment used during the study.

6.1 MAIN ACTIVITIES

For the effective implementation of the study, the following main activities have been carried out, each with their respective deadlines:

- **Background Review:** This activity focused on the comprehensive review of existing literature relevant to the topic of the study. The duration of this phase was approximately one month, during which 80 effective monthly hours were invested.
- **Software development:** This phase included the development of three different codes for the analysis of the potential for the implementation of GRs on the rooftops of the city of Valencia. This activity lasted approximately three months, with a total of 280 effective monthly hours.
- **Obtaining Official Information and Calculations:** In this stage, the focus was on obtaining official information related to the cadastral register of the city of Valencia, in addition to the energy certificates of property. This phase also included data manipulation and calculation of results necessary for the study. The estimated duration was one and a half months, with 180 effective hours per month.
- **Report Writing:** The last main activity consisted of writing the final report summarising the entire study. This task was carried out over the course of one month, with a total of 120 effective hours per month.

6.2 SIDE ACTIVITIES, TUTORING AND OTHER SERVICES

In addition to the core activities, a number of complementary factors were considered, including:

- **Transport:** Transport was accounted for during the months corresponding to software development and obtaining official information, for a total of 4.5 months (90 days and 180 trips).
- **Guidance and Review by Tutor Teachers:** For both the tutor teacher and the co-advisor, a total of 80 hours were allocated for consultations, progress evaluation meetings and reviews.
- **Electricity consumption and Internet Service:** These services were considered for a period of 6.5 months.

6.3 EQUIPMENT AND SOFTWARE

To carry out the study, as mentioned in chapter 2, high-level equipment was used, both in terms of software and hardware. This equipment corresponds to:

- **ASUS TUF DASH F15 (Engineer Equipment)**: Laptop computer constantly used during the study as support or main equipment. Six and a half months of use are considered for this equipment. The computer features 12th generation Intel Core processors, NVIDIA GeForce RTX graphics, 15.6" display, DDR5 memory and meets military durability standards.
- **OFFICE COMPUTER (Engineering Team)**: Fixed computer used only during the development of software and obtaining official information and calculations, for which it is considered to have been used for approximately 4 and a half months.
- **PC INTEL I7 (Assistant Professor)**
- **MSI PRESTIGE (Permanent Professor)**

With respect to the software and virtual resources, the following was used:

- **MATLAB R2023b**: Programming environment and high-level language for numerical calculation, visualisation and algorithm development. It offers tools for data analysis, simulation, mathematical modelling, and support for machine learning and deep learning.
- **QGIS 3.34.1**: Open-source software for geospatial data analysis and visualisation. It offers advanced tools for 2D and 3D map handling, spatial analysis, and geographic data processing.
- **SCIENTIFIC RESOURCES**: Open data source provided by the Universidad Politécnica de Valencia associated with the resources used in the review of the existing literature on the topic studied.

6.4 UNIT COSTS OF THE STUDY

A detailed description of the costs associated with both the main and complementary activities of the study will be presented below:

***Table 18**: Costs associated with the main and ancillary activities for carrying out the study.*

Item	Quantity	Unit	Unit Cost (€)	Total (€)
MAIN ACTIVITIES	**1**	**General**	-	10,151
Background review	80	hours	15.38	1,230
Software development	280	hours	15.38	4,306
Obtaining official data and calculations	180	hours	15.38	2,768
Report writing	120	hours	15.38	1,846
SIDE ACTIVITIES, TUTORING AND OTHER SERVICES	**1**	**General**	-	11,896
Transportation	180	trips	1.50	270
Full Professor advisor guidance and review	80	hours	80.00	6,400
Assistant Professor guidance and review	80	hours	60.00	4,800
Electricity bill	6	months	40.00	240
Internet Service	6	months	31.00	186

Now, about the costs associated with equipment and software:

***Table 19**: Costs associated with equipment and software used to carry out the survey.*

Item	Quantity	Unit	Unit Cost (€)	Amortization (years)	Use (years)	Total (€)
EQUIPMENT AND SOFTWARE	**1**	**General**	-	-	-	441.22
ASUS TUF DASH F15	1	each	1,649.99	5	0.542	178.75
OFFICE COMPUTER	1	each	3,000.00	5	0.375	225.00
PC INTEL I7	1	each	800.00	5	0.083	13.33
MSI PRESTIGE	1	each	1,000.00	5	0.083	16.67
MATLAB R2023b	1	software license	69.00	5	0.542	7.48
QGIS 3.34.1	1	software license	0.00	5	0.542	0.00
SCIENTIFIC RESOURCES	1	each	0.00	-	-	0.00

6.5 STUDY BUDGET

Finally, the total cost of the project, including a profit margin of 6% and applicable taxes:

***Table 20**: Itemised costs associated with the project budget.*

Item	Cost (€)
MAIN ACTIVITIES	10,151
SIDE ACTIVITIES, TUTORING AND OTHER SERVICES	11,896
EQUIPMENT AND SOFTWARE	441
OVERALL PROJECT COST	22,488
INDUSTRIAL PROFIT (6%)	1,349
OVERALL PROJECT COST + BENEFITS	23,837
Consumption tax (IVA 21%)	5,006
FINAL PROJECT BUDGET	28,843

CHAPTER 7. BIBLIOGRAPHY

Abass, F., Ismail, L., Abd Wahab, I., & Elgadi, A. (2020). A Review of Green Roof: Definition, History, Evolution and Functions A Review of Green Roof: Definition, History, Evolution and Functions. *IOP Conference Series Materials Science and Engineering, 713*, 8. doi:https://dx.doi.org/10.1088/1757-899X/713/1/012048

Ajuntament de Vàlencia. (2024). *Gobierno Abierto*. Retrieved 09 15, 2023, from https://www.valencia.es/es/cas/ayuntamiento/gobierno-abierto

Ajuntament de València, P. (2019, Febrero 01). *Plan de Acción para el Clima y la Energía Sostenible de la ciudad de València.* Retrieved 07 2023, from https://www.valencia.es/documents/20142/424002/190415_AYTO_VALENCIA_PACES__Actualizado_.pdf/1cefe22e-7b64-1db9-7f4a-7006aa12bf75

Batlle Cardona, M. (2023). VALENCIA MIRA AL FUTURO COMO CAPITAL VERDE EUROPEA DE 2024. Valencia: Viajes National Geographic. Retrieved from https://viajes.nationalgeographic.com.es/lifestyle/por-que-valencia-sera-capital-verde-europea-2024_18718

Berardi, U., GhaffarianHoseini, A., & GhaffarianHoseini, A. (2013). State-of-the-art analysis of the environmental benefits of green roofs. *Applied Energy, 115*, 411-428. doi:https://doi.org/10.1016/j.apenergy.2013.10.047.

Bevilacqua, P., Bruno, R., & Arcuri, N. (2020). Green roofs in a Mediterranean climate: energy performances based. *Renewable Energy, 152*, 1414-1430. doi:https://doi.org/10.1016/j.renene.2020.01.085.

Brenner, J., Schmidt, S., & Albert, C. (2023). Localizing and prioritizing roof greening opportunities for urban heat island mitigation: insights from the city of Krefeld, Germany. *Landscape Ecology, 38*(7), 1697–1712. doi:10.1007/s10980-023-01644-8

Cascone, S. (2019). Green Roof Design: State of the Art on Technology and Materials. *Sustainability, 3020*, 11. doi:https://doi.org/10.3390/su11113020

CING, O. A. (2020). *Centro de Descargas*. Retrieved 11 10, 2023, from https://centrodedescargas.cnig.es/CentroDescargas/index.jsp

CONAMA, C. (2020, 11 01). *Informe de Situación de Soluciones basadas en la Naturaleza en España.* Retrieved 08 20, 2023, from https://www.fundacionconama.org/wp-content/uploads/2021/01/Informe-de-situacion-SbN-en-Espanav2020.pdf

Evangelisti, L., Guattari, C., Grazieschi, G., Roncone, M., & Asdrubali, F. (2020). On the Energy Performance of an Innovative Green Roof in the Mediterranean Climate. *Energies, 13*(19), 5163. doi:https://doi.org/10.3390/en13195163

Foustalieraki, M., Assimakopoulos, M., Santamou, M., & Pangalou, H. (2017). Energy performance of a medium scale green roof system installed on a commercial building using numerical and experimental data recorded during the cold period of the year. *Energy and Buildings, 135*(ISSN 0378-7788), 33-38. doi:https://www.sciencedirect.com/science/article/pii/S0378778816313871

Gagliano, A., Detommaso, M., Nocera, F., & Evola, G. (2015). A multi-criteria methodology for comparing the energy and environmental behavior of cool, green and traditional roofs. *Building and Environment, 90*, 71-81. doi:https://doi.org/10.1016/j.buildenv.2015.02.043

Gobierno de España. (2024). *Sede Electrónica del Catastro*. Retrieved 12 01, 2023, from https://www.sedecatastro.gob.es/

IDAE, I., & Gobierno de España, M. (2011, 06 16). *Análisis del consumo energético del sector residencial en España.* Retrieved 11 10, 2023, from https://www.idae.es/uploads/documentos/documentos_Informe_SPAHOUSEC_ACC_f68291a3.pdf

IEA, I. (2018). *IEA*. Retrieved 01 10, 2024, from https://www.iea.org/energy-system/buildings

Institut Valencià de Competitivitat Empresarial. (2024). *Portal de datos abiertos del registro de los certificados de eficiencia energética en la Comunitat Valenciana*. Retrieved 12 05, 2023, from https://gceedadesobertes.aven.es/dadesobertes/

Kong, L., Shi, Z., & Chu, L. (2014). Carbon emission and sequestration of urban turfgrass systems in Hong Kong. *Science of The Total Environment, 473–474*(ISSN 0048-9697), 132-138. doi:https://doi.org/10.1016/j.scitotenv.2013.12.012.

Koroxenidis, E., & Theodosiou, T. (2021). Comparative environmental and economic evaluation of green roofs under Mediterranean climate conditions – Extensive green roofs a potentially preferable solution. *Journal of Cleaner Production, 311*(127563). doi:https://doi.org/10.1016/j.jclepro.2021.127563.

Lawrence Berkeley National Laboratory (LBNL). (2021, 04 01). *Halfway to Zero: Progress towards a Carbon-Free Power Sector.* Retrieved 01 10, 2024, from https://eta-publications.lbl.gov/sites/default/files/halfway_to_zero_report.pdf

Matos Silva, C., Flores-Colen, I., & Antunes, M. (2017). Step-by-step approach to ranking green roof retrofit potential in urban areas: A case study of Lisbon, Portugal. *Urban Forestry & Urban Greening, 25*(ISSN 1618-8667), 120-129. doi:https://doi.org/10.1016/j.ufug.2017.04.018

Matos Silva, C., Gomes, M. G., & Silva, M. (2016). Green roofs energy performance in Mediterranean climate. *Energy and Buildings, 116*(ISSN 0378-7788), 318-325. doi:https://doi.org/10.1016/j.enbuild.2016.01.012.

Mihalakakou, G., Souliotis, M., Papadaki, M., Menounou, P., Dimopoulos, P., Kolokotsa, D., . . . Papaefthimiou, S. (2023). Green roofs as a nature-based solution for improving urban sustainability:. *Renewable and Sustainable Energy Reviews, 180*. doi:https://doi.org/10.1016/j.rser.2023.113306

Møller Francis, L. F., & Bergen Jensen, M. (2017). Benefits of green roofs: A systematic review of the evidence for three ecosystem services. *Urban Forestry & Urban Greening, 28*, 167-176. doi:https://doi.org/10.1016/j.ufug.2017.10.015.

Oliver, P. (1997). *Encyclopedia of Vernacular Architecture of the World: Cultures and Habitats* (1997 ed.). Cambridge: Cambridge University Press. Retrieved from https://www.jstor.org/stable/23566265

Ondoño, S., Martínez-Sánchez, J., & Moreno, J. (2018). Chapter 7 - Carbon and Nitrogen Sequestration Potential of Mediterranean Green Roofs Prototypes. In M. Muñoz, & R. Zornoza (Eds.), *Soil Management and Climate Change* (pp. 85-102). Murcía: Academic Press. doi:https://doi.org/10.1016/B978-0-12-812128-3.00007-0.

PNNL, P. (2017, 05 01). *Impacts of Commercial Building Controls on Energy Savings and Peak Load Reduction.* Retrieved 01 10, 2024, from https://buildingretuning.pnnl.gov/publications/PNNL-25985.pdf

Saadatian, O., Sopian, K., Salleh, E., Lim, C., Riffat, S., Saadatian, E., . . . Sulaiman, M. (2013). A review of energy aspects of green roofs. *Renewable and Sustainable Energy Reviews, 23*, 155-168. doi:https://doi.org/10.1016/j.rser.2013.02.022.

Saaty, T. L. (1994). How to Make a Decision: The Analytic Hierarchy Process. *Interfaces, 24*(6), 19–43. doi:https://doi.org/10.1287/inte.24.6.19

Santos, T., Tenedório, J., & Gonçalves, J. (2016). Quantifying the City's Green Area Potential Gain Using Remote Sensing Data. *Sustainability, 8*, 1247. doi:https://doi.org/10.3390/su8121247

Shafique, M., Kim, R., & Rafiq, M. (2018). Green roof benefits, opportunities and challenges – A review. *Renewable and Sustainable Energy Reviews, 90*, 757-773. doi:https://doi.org/10.1016/j.rser.2018.04.006.

Shafique, M., Xue, X., & Luo, X. (2020). An overview of carbon sequestration of green roofs in urban areas. *Urban Forestry & Urban Greening, 47*(126515). doi:https://doi.org/10.1016/j.ufug.2019.126515.

Slootweg, M., Hu, M., Halleck Vega, S., van ‘t Zelfde, M., van Leeuwen, E., & Tukker, A. (2023). Identifying the geographical potential of rooftop systems: Space competition and synergy. *Urban Forestry & Urban Greening, 79*(ISSN 1618-8667). doi:https://doi.org/10.1016/j.ufug.2022.127816.

Soriano, P. (2023, 10 25). *Spanish Inspire Catastral Downloader.* Retrieved 11 01, 2023, from http://www.catastro.minhap.gob.es/webinspire/index.html

Tabatabaee, S., Mahdiyar, A., Durdyev, S., Reza Mohandes, S., & Ismail, S. (2019). An assessment model of benefits, opportunities, costs, and risks of green roof installation: A multi criteria decision making approach. *Journal of Cleaner Production, 238*. doi:https://doi.org/10.1016/j.jclepro.2019.117956.

Tan, T., Kong, F., Yin, H., & Coo, L. M. (2023). Carbon dioxide reduction from green roofs: A comprehensive review of processes, factors, and quantitative methods. *Renewable and Sustainable Energy Reviews, 182*(113412). doi:https://doi.org/10.1016/j.rser.2023.113412.

Zayas Orihuela, M. (2023, 09 08). *Calculation of the decarbonisation potential of the installation of green roofs in the L'Illa Perduda neighbourhood in València.* Valencia: Universitat Politècnica de Vàlencia. Retrieved 01 13, 2024, from https://riunet.upv.es/handle/10251/197281

CHAPTER. ANNEX

MATLAB CODES

ROOFTYPEDETECTION.m

```
% AV area detection for green roof retrofit
% Author: Tomás Pino Gallardo
% Máster Universitario Tecnologías Energéticas para Desarrollo Sostenible
% Institution: Instituto de Ingeniería Energética (UPV)
%
% DISCLAIMER: This code has not undergone thorough cleaning or formal publication.
% its intended use is strictly limited to individuals within the institution.

%% 1) RoofType struct loading

    clear;
    clc;

    % Roof type structure loading
    load("MATLABData\roofType.mat","roofType");

%% 2) Image stuct creation / import

    % Define the directory path
    folder_path = 'directory path';

    % Ask the user to select a file within the directory
    disp('Select a file within the folder.');
    [filename, folder] = uigetfile(fullfile(folder_path, '*.*'), 'Select file');

    % Verificar si se seleccionó un archivo válido
    if isequal(filename, 0)
    error('No valid file selected.');
    end

    ruta_imagen = fullfile(folder, filename);
    tAerialImage = Tiff([ruta_imagen]);

    AerialImage = tAerialImage.read;
    AerialImageHSV = rgb2hsv(AerialImage);

    [~,imageName,~] = fileparts(tAerialImage.FileName);
    fileStructPath = "MATLABData\imageMasks\" + imageName + ".mat";

    if isfile(fileStructPath)
    load(fileStructPath);
    imageStruct.image.tiff = tAerialImage;
    else
    imageStruct = struct();
    imageStruct.name = imageName;
    imageStruct.image = struct();
    imageStruct.image.tiff = tAerialImage;
```

```
imageStruct.image.RGB = AerialImage;
imageStruct.image.HSV = AerialImageHSV;
len = length(roofType);

for i = 1:len
imageStruct.roofTypes(i) =
struct("name",{roofType(i).name},"colorRegion",{struct("name",{roofType(i).c
olorRegions.name})});
end

imageStruct.image.medianFiltered = struct();
imageStruct.image.medianFiltered.RGB                                        =
cat(3,medfilt2(AerialImage(:,:,1),[5,5]),medfilt2(AerialImage(:,:,2),[5,5]),
medfilt2(AerialImage(:,:,3),[5,5]));
imageStruct.image.medianFiltered.HSV                                        =
rgb2hsv(imageStruct.image.medianFiltered.RGB);

end

%% 3) Create mask for roofType

while true
medianFiltered = 1;

[idx,tf]                                                                    =
listdlg('ListString',[roofType.name],'SelectionMode','single','PromptString'
,"Select the roofType to create the mask for:");

if isempty(idx)
break
end

imageStruct = createMask(imageStruct,roofType,idx,medianFiltered);
% imageStruct = filterMask(imageStruct,idx);

answer = questdlg("Would you like to create another mask for this median
filtered image for some roofType?");

if strcmp(answer, 'No')
break
end
end

%% 4) Trials I. Filter individual masks

% Size of roofType and colorRegion
numRoofTypes = numel(imageStruct.roofTypes);
for i = 1:numRoofTypes
numColorRegions = numel(imageStruct.roofTypes(i).colorRegion);
```

```
for j = 1:numColorRegions
% Filtrar las máscaras RGB
imageStruct.roofTypes(i).colorRegion(j).filteredMask.RGB = struct();
imageStruct.roofTypes(i).colorRegion(j).filteredMask.RGB.filteredMeanStdMask
=
filterIndividualMask(imageStruct.roofTypes(i).colorRegion(j).meanStdMask.RGB
, 100, 700);
imageStruct.roofTypes(i).colorRegion(j).filteredMask.RGB.filteredMinMaxMask
=
filterIndividualMask(imageStruct.roofTypes(i).colorRegion(j).meanStdMask.RGB
, 100, 700);

% Filtering HSV masks
imageStruct.roofTypes(i).colorRegion(j).filteredMask.HSV = struct();
imageStruct.roofTypes(i).colorRegion(j).filteredMask.HSV.filteredMeanStdMask
=
filterIndividualMask(imageStruct.roofTypes(i).colorRegion(j).meanStdMask.HSV
, 100, 700);
imageStruct.roofTypes(i).colorRegion(j).filteredMask.HSV.filteredMinMaxMask
=
filterIndividualMask(imageStruct.roofTypes(i).colorRegion(j).minMaxMask.HSV,
100, 700);

% Calculate blobOR operation for RGB and HSV masks
imageStruct.roofTypes(i).colorRegion(j).filteredMask.total = struct();
imageStruct.roofTypes(i).colorRegion(j).filteredMask.total.minMax          =
struct();
imageStruct.roofTypes(i).colorRegion(j).filteredMask.total.minMax.blobOR   =
blobOR(imageStruct.roofTypes(i).colorRegion(j).filteredMask.RGB.filteredMinM
axMask,
imageStruct.roofTypes(i).colorRegion(j).filteredMask.HSV.filteredMinMaxMask)
;
imageStruct.roofTypes(i).colorRegion(j).filteredMask.total.minMax.OR       =
imageStruct.roofTypes(i).colorRegion(j).filteredMask.RGB.filteredMinMaxMask
|
imageStruct.roofTypes(i).colorRegion(j).filteredMask.HSV.filteredMinMaxMask;

imageStruct.roofTypes(i).colorRegion(j).filteredMask.total.meanStd         =
struct();
imageStruct.roofTypes(i).colorRegion(j).filteredMask.total.meanStd.blobOR  =
blobOR(imageStruct.roofTypes(i).colorRegion(j).filteredMask.RGB.filteredMean
StdMask,
imageStruct.roofTypes(i).colorRegion(j).filteredMask.HSV.filteredMeanStdMask
);
imageStruct.roofTypes(i).colorRegion(j).filteredMask.total.meanStd.OR      =
imageStruct.roofTypes(i).colorRegion(j).filteredMask.RGB.filteredMeanStdMask
|
imageStruct.roofTypes(i).colorRegion(j).filteredMask.HSV.filteredMeanStdMask
;
```

```
close all;
end
end

%% 5) Trials I. Fuse all the masks (LIGHT)

numRoofTypes = numel(imageStruct.roofTypes); % Obtain the total number of
roof types

for i = 1:numRoofTypes
numColors = numel(imageStruct.roofTypes(i).colorRegion); % Get the total
number of color regions for the current roof type.

imageStruct.roofTypes(i).mask.fusedFilteredMask.light.minMax = struct();
imageStruct.roofTypes(i).mask.fusedFilteredMask.light.minMax.OR = false;
imageStruct.roofTypes(i).mask.fusedFilteredMask.light.minMax.blobOR = false;

imageStruct.roofTypes(i).mask.fusedFilteredMask.light.meanStd = struct();
imageStruct.roofTypes(i).mask.fusedFilteredMask.light.meanStd.OR = false;
imageStruct.roofTypes(i).mask.fusedFilteredMask.light.meanStd.blobOR =
false;

for j = 1:numColors
% Merge the masks of each color region of the current roof type.
imageStruct.roofTypes(i).mask.fusedFilteredMask.light.minMax.OR =
imageStruct.roofTypes(i).mask.fusedFilteredMask.light.minMax.OR |
imageStruct.roofTypes(i).colorRegion(j).filteredMask.total.minMax.OR;
imageStruct.roofTypes(i).mask.fusedFilteredMask.light.minMax.blobOR =
imageStruct.roofTypes(i).mask.fusedFilteredMask.light.minMax.blobOR |
imageStruct.roofTypes(i).colorRegion(j).filteredMask.total.minMax.blobOR;

imageStruct.roofTypes(i).mask.fusedFilteredMask.light.meanStd.OR =
imageStruct.roofTypes(i).mask.fusedFilteredMask.light.meanStd.OR |
imageStruct.roofTypes(i).colorRegion(j).filteredMask.total.meanStd.OR;
imageStruct.roofTypes(i).mask.fusedFilteredMask.light.meanStd.blobOR =
imageStruct.roofTypes(i).mask.fusedFilteredMask.light.meanStd.blobOR |
imageStruct.roofTypes(i).colorRegion(j).filteredMask.total.meanStd.blobOR;
end
end

%% 6) Trials I. Fuse light and shadow

% Fuse Light
imageStruct.roofTypes(1).mask.fusedFilteredMask.light.total.blobOR =
blobOR(blobOR(imageStruct.roofTypes(1).mask.fusedFilteredMask.light.meanStd.
blobOR,imageStruct.roofTypes(1).mask.fusedFilteredMask.light.meanStd.OR),...
blobOR(imageStruct.roofTypes(1).mask.fusedFilteredMask.light.minMax.blobOR,i
mageStruct.roofTypes(1).mask.fusedFilteredMask.light.minMax.OR));

imageStruct.roofTypes(1).mask.fusedFilteredMask.total = struct();
```

```
    imageStruct.roofTypes(1).mask.fusedFilteredMask.total                =
    imageStruct.roofTypes(1).mask.fusedFilteredMask.light.total.blobOR;

%% 7) PRE-Visualize it

    visualizeMask(imageStruct.image.RGB,imageStruct.roofTypes(1).mask.fusedFilte
    redMask.total);

%% 7.1) Continue Work

    % To continue an unfinished job or modify an already created job without the
    need to generate a mask from the beginning.

    imageStruct.roofTypes(1).mask.fusedFilteredMask.total=imageStruct.roofTypes(
    1).mask.finalMask;

%% 8) Trials I. Crop blobs

    croppedMask                                                          =
    cropBlobs(imageStruct.image.RGB,imageStruct.roofTypes(1).mask.fusedFilteredM
    ask.total);

%% 8.1) More cropping if necessary

    close all;
    croppedMask = cropBlobs(imageStruct.image.RGB,croppedMask);
    close all;

%% 9) Trials I. Add blobs

    figure("Name", "Add Blobs");
    imshow(imageStruct.image.RGB); % Make sure you are viewing the original image.
    hold on;

    visualizeMask(imageStruct.image.RGB,croppedMask)

    while true
    % Allows the user to draw a polygon
    hPoly = drawpolygon;

    % Wait for the user to finish drawing
    wait(hPoly);

    % Gets the coordinates of the selected polygon
    polygonPosition = hPoly.Position;

    % Creates a binary mask for the selected polygon
    polygonMask   =   poly2mask(polygonPosition(:,   1),   polygonPosition(:,   2),
    size(croppedMask, 1), size(croppedMask, 2));
```

```
        % Combines the polygon with the previously created mask (croppedMask).
        croppedMask = croppedMask | polygonMask;

        % Closes the polygon drawing shape
        delete(hPoly);

        % Ask the user if he/she wants to draw another polygon
        disp("Press 'Enter' to draw another polygon or any other key to exit.");
        key = waitforbuttonpress;

        if key == 0
        % User pressed 'Enter' to draw another polygon, continues the loop
        continue;
        else
        % The user pressed a different key, exits the loop.
        break;
        end
        end

        % Closes the display windows

        close(1); % Closes the original image window
        close(2); % Closes the mask display window

%% 9.1) More cropping if necessary

        close all;
        % Call cropBlobs and get the cropped mask
        croppedMask = cropBlobs(imageStruct.image.RGB, croppedMask);

%% 10) Visualize it (After)

        % To display the mask after any change
        visualizeMask(imageStruct.image.RGB,croppedMask);

%% 11) Finally close the mask

        % First, fuse super close blobs.
        imageStruct.roofTypes(1).mask.finalMask                                =
        myFill(myClose(croppedMask,ones(3),3,3),2000);
        visualizeMask(imageStruct.image.RGB,imageStruct.roofTypes(1).mask.finalMask)
        ;

        % Second, fuse individual blobs.
        lastLabels = bwlabel(imageStruct.roofTypes(1).mask.finalMask);
        blobs = unique(lastLabels(:));

        finalBlobs = zeros(size(lastLabels));
        for i = blobs(blobs>0)'
        blobMask = ismember(lastLabels,i);
```

```
        blobClosedMask = myClose(blobMask,ones(3),4,4);
        finalBlobs = finalBlobs|blobClosedMask;
        end

        imageStruct.roofTypes(1).mask.finalMask = myFill(finalBlobs,2000);
        close all;

        % Specifies the output file name
        outputPath = "Select directory path”;  % Replace with desired location
        outputFileName = sprintf('%sMASK_%s.tif', outputPath, imageName);

        % Save the mask as a .tif file.
        imwrite(imageStruct.roofTypes(1).mask.finalMask, outputFileName);

        fprintf(' Mask saved as %s\n', outputFileName);


%% 12) Georeferenced

        % Path to the original image file
        ruta_mascara = outputFileName;

        % Load original image and get georeferencing information
        info = geotiffinfo(ruta_imagen);

        % Read the mask
        mascara = imread(ruta_mascara);

        % Generates a file name for the georeferenced mask
        [~, name, ext] = fileparts(ruta_mascara);
        nombre_mascara_georreferenciada = sprintf('%s_GEO%s', name, ext);

        % Complete path where the geo-referenced mask will be saved
        ruta_mascara_georreferenciada             =             fullfile(outputPath,
        nombre_mascara_georreferenciada);

        % Save the georeferenced mask with the same georeferencing information as the
        original image.
        geotiffwrite(ruta_mascara_georreferenciada,    mascara,    info.SpatialRef,
        'CoordRefSysCode',
        info.GeoTIFFTags.GeoKeyDirectoryTag.ProjectedCSTypeGeoKey);

        fprintf('Geo-referenced mask saved as %s\n', ruta_mascara_georreferenciada);

%% 12.1) Visualiza it (Final Mask)

        visualizeMask(imageStruct.image.RGB,imageStruct.roofTypes(1).mask.finalMask)
;

%% 13) Trials I. Calculate the area of each blob
```

```
XResolution=72/0.0254; %pxm - 72 Depends on the original image resolution
YResolution=72/0.0254; %pxm - 72 Depends on the original image resolution
blobLabels = bwlabel(imageStruct.roofTypes(1).mask.finalMask);
blobProps = regionprops(blobLabels,"Area");
blobAreas = (469286.667*[blobProps.Area])/(XResolution*YResolution);
imageStruct.roofTypes(1).area=[];
imageStruct.roofTypes(1).area = struct();
imageStruct.roofTypes(1).area.totalBlobArea = sum(blobAreas)*0.0001;
disp(imageStruct.roofTypes(1).area.totalBlobArea);

% Threshold areas lower than 50,75,100m2
imageStruct.roofTypes(1).mask.thresholdedMask = struct();

k = find(blobAreas>50);
imageStruct.roofTypes(1).mask.thresholdedMask.fifty                         =
ismember(blobLabels,k);
imageStruct.roofTypes(1).area.fifty = sum(blobAreas(k));
figure("Name","Threshold50");
imshow(imageStruct.roofTypes(1).mask.thresholdedMask.fifty);
k = find(blobAreas>75);
imageStruct.roofTypes(1).mask.thresholdedMask.seventyFive                   =
ismember(blobLabels,k);
imageStruct.roofTypes(1).area.seventyFive = sum(blobAreas(k));
figure("Name","Threshold75")
imshow(imageStruct.roofTypes(1).mask.thresholdedMask.seventyFive);
k = find(blobAreas>100);
imageStruct.roofTypes(1).mask.thresholdedMask.hundred                       =
ismember(blobLabels,k);
imageStruct.roofTypes(1).area.hundred = sum(blobAreas(k));
figure("Name","Threshold100")
imshow(imageStruct.roofTypes(1).mask.thresholdedMask.hundred);

close all;

% Summatory area to rooftype

sectionName = "Valencia_" + imageName;
roofType(1).area.(sectionName) = struct();
roofType(1).area.(sectionName).totalBlobArea = 0;
roofType(1).area.(sectionName).fifty = 0;
roofType(1).area.(sectionName).seventyFive = 0;
roofType(1).area.(sectionName).hundred = 0;

roofType(1).area.(sectionName).totalBlobArea = 0;
roofType(1).area.(sectionName).totalBlobArea                                =
roofType(1).area.(sectionName).totalBlobArea                                +
imageStruct.roofTypes(1).area.totalBlobArea;
roofType(1).area.(sectionName).fifty = (roofType(1).area.(sectionName).fifty
+ imageStruct.roofTypes(1).area.fifty)/10000;
```

```
        roofType(1).area.(sectionName).seventyFive                                       =
        (roofType(1).area.(sectionName).seventyFive                                      +
        imageStruct.roofTypes(1).area.seventyFive)/10000;
        roofType(1).area.(sectionName).hundred                                           =
        (roofType(1).area.(sectionName).hundred                                          +
        imageStruct.roofTypes(1).area.hundred)/10000;

        % Create a format for printing tabulated values
        formatString    =    'Total    Blob    Area    for    %s:\t%.2f\nFifty    for
        %s:\t%.2f\nSeventyFive for %s:\t%.2f\nHundred for %s:\t%.2f\n';

        % Print values in tabular format
        fprintf(formatString, sectionName, ...
        roofType(1).area.(sectionName).totalBlobArea, ...
        sectionName, ...
        roofType(1).area.(sectionName).fifty, ...
        sectionName, ...
        roofType(1).area.(sectionName).seventyFive, ...
        sectionName, ...
        roofType(1).area.(sectionName).hundred);

        % Save string with values to clipboard
        clipboard('copy', sprintf(formatString, sectionName, ...
        roofType(1).area.(sectionName).totalBlobArea, ...
        sectionName, ...
        roofType(1).area.(sectionName).fifty, ...
        sectionName, ...
        roofType(1).area.(sectionName).seventyFive, ...
        sectionName, ...
        roofType(1).area.(sectionName).hundred));

        % Save the struct

        save("MATLABData\imageMasks\"+imageStruct.name,"imageStruct",'-v7.3');

%% Functions

function pClicks = selectRoofPixels(Image)
        f = figure('Name','Selected building pixeels');
        imshow(Image);
        hold on
        pClicks = zeros(size(Image,[1 2]));
        pC=imshow(pClicks);
        pC.AlphaData = 0.4;

        key = 0;

        while key ~= 13

        % Wait until some key or button is pressed and get the position of the
```

```
        % mouse and the pressed key.
        [x,y,key] = ginput(1);
        xPixel = round(x);
        yPixel = round(y);

        % If it was not enter
        if key ~= 13
        % If it was the left click add that FA to the deletion list.
        if key == 1
        pClicks(yPixel,xPixel) = 1;
        % If it was the right click remove the FA from the deletion
        % list.
        elseif key == 3
        pClicks(yPixel,xPixel) = 0;
        end
        end

        % Refresh the image and show the selected FAs in red.
        figure(f);
        delete(pC);
        pC=imshow(conv2(pClicks,ones(5),"same")>0);
        pC.AlphaData = 0.4;

        end

end

function pixelValues = getPixelValues(Image,selectedPixels)
        [yPixel,xPixel] = find(selectedPixels);
        yPixelcoord = repelem(yPixel,3);
        xPixelcoord = repelem(xPixel,3);
        zPixelcoord = repmat((1:3)',length(xPixel),1);
        PixelIdx = sub2ind(size(Image),yPixelcoord,xPixelcoord,zPixelcoord);
        pixelValues = reshape(Image(PixelIdx),[3,length(xPixel),])';

end

function regionStats = getStatistics(colorRegion)
        regionStats.RGB = struct();
        regionStats.RGB.min = min(colorRegion.pixelValuesRGB);
        regionStats.RGB.max = max(colorRegion.pixelValuesRGB);
        regionStats.RGB.mean = mean(colorRegion.pixelValuesRGB);
        regionStats.RGB.std = std(double(colorRegion.pixelValuesRGB));

        regionStats.HSV = struct();
        regionStats.HSV.min = min(colorRegion.pixelValuesHSV);
        regionStats.HSV.max = max(colorRegion.pixelValuesHSV);
        regionStats.HSV.mean = mean(colorRegion.pixelValuesHSV);
        regionStats.HSV.std = std(colorRegion.pixelValuesHSV);
```

```
end

function IS = createMask(IS,RT,idx,medianFilt)
	if medianFilt
	imageHSV = IS.image.medianFiltered.HSV;
	imageRGB = IS.image.medianFiltered.RGB;
	else
	imageHSV = IS.image.HSV;
	imageHSV = IS.image.RGB;
	end
	nColorRegion = length(RT(idx).colorRegions);

	imageH = IS.image.HSV(:,:,1);
	imageS = IS.image.HSV(:,:,2);
	imageV = IS.image.HSV(:,:,3);

	imageR = IS.image.RGB(:,:,1);
	imageG = IS.image.RGB(:,:,2);
	imageB = IS.image.RGB(:,:,3);

	for i = 1:nColorRegion

	colorRegion = RT(idx).colorRegions(i);

	%minMax mask

	minMaxRoofMaskH  =  imageH  <  colorRegion.statistics.HSV.max(1)  &  imageH  >
	colorRegion.statistics.HSV.min(1);
	minMaxRoofMaskS  =  imageS  <  colorRegion.statistics.HSV.max(2)  &  imageS  >
	colorRegion.statistics.HSV.min(2);
	minMaxRoofMaskV  =  imageV  <  colorRegion.statistics.HSV.max(3)  &  imageV  >
	colorRegion.statistics.HSV.min(3);

	minMaxRoofMaskR  =  imageR  <  colorRegion.statistics.RGB.max(1)  &  imageR  >
	colorRegion.statistics.RGB.min(1);
	minMaxRoofMaskG  =  imageG  <  colorRegion.statistics.RGB.max(2)  &  imageG  >
	colorRegion.statistics.RGB.min(2);
	minMaxRoofMaskB  =  imageB  <  colorRegion.statistics.RGB.max(3)  &  imageB  >
	colorRegion.statistics.RGB.min(3);

	IS.roofTypes(idx).colorRegion(i).minMaxMask = struct();
	IS.roofTypes(idx).colorRegion(i).minMaxMask.R = minMaxRoofMaskR;
	IS.roofTypes(idx).colorRegion(i).minMaxMask.G = minMaxRoofMaskG;
	IS.roofTypes(idx).colorRegion(i).minMaxMask.B = minMaxRoofMaskB;
	IS.roofTypes(idx).colorRegion(i).minMaxMask.RGB    =    minMaxRoofMaskR    &
	minMaxRoofMaskG & minMaxRoofMaskB;

	IS.roofTypes(idx).colorRegion(i).minMaxMask.H = minMaxRoofMaskH;
	IS.roofTypes(idx).colorRegion(i).minMaxMask.S = minMaxRoofMaskS;
	IS.roofTypes(idx).colorRegion(i).minMaxMask.V = minMaxRoofMaskV;
```

```
IS.roofTypes(idx).colorRegion(i).minMaxMask.HSV = minMaxRoofMaskH &
minMaxRoofMaskS & minMaxRoofMaskV;

IS.roofTypes(idx).colorRegion(i).minMaxMask.total =
IS.roofTypes(idx).colorRegion(i).minMaxMask.RGB & ...
IS.roofTypes(idx).colorRegion(i).minMaxMask.HSV;

% meanStd mask

meanStdRoofMaskH = imageH <
colorRegion.statistics.HSV.mean(1)+3*colorRegion.statistics.HSV.std(1) &
imageH > colorRegion.statistics.HSV.mean(1)-
3*colorRegion.statistics.HSV.std(1);
meanStdRoofMaskS = imageS <
colorRegion.statistics.HSV.mean(2)+3*colorRegion.statistics.HSV.std(2) &
imageS > colorRegion.statistics.HSV.mean(2)-
3*colorRegion.statistics.HSV.std(2);
meanStdRoofMaskV = imageV <
colorRegion.statistics.HSV.mean(3)+3*colorRegion.statistics.HSV.std(3) &
imageV > colorRegion.statistics.HSV.mean(3)-
3*colorRegion.statistics.HSV.std(3);

meanStdRoofMaskR = imageR <
colorRegion.statistics.RGB.mean(1)+3*colorRegion.statistics.RGB.std(1) &
imageR > colorRegion.statistics.RGB.mean(1)-
3*colorRegion.statistics.RGB.std(1);
meanStdRoofMaskG = imageG <
colorRegion.statistics.RGB.mean(2)+3*colorRegion.statistics.RGB.std(2) &
imageG > colorRegion.statistics.RGB.mean(2)-
3*colorRegion.statistics.RGB.std(2);
meanStdRoofMaskB = imageB <
colorRegion.statistics.RGB.mean(3)+3*colorRegion.statistics.RGB.std(3) &
imageB > colorRegion.statistics.RGB.mean(3)-
3*colorRegion.statistics.RGB.std(3);

IS.roofTypes(idx).colorRegion(i).meanStdMask = struct();
IS.roofTypes(idx).colorRegion(i).meanStdMask.R = meanStdRoofMaskR;
IS.roofTypes(idx).colorRegion(i).meanStdMask.G = meanStdRoofMaskG;
IS.roofTypes(idx).colorRegion(i).meanStdMask.B = meanStdRoofMaskB;
IS.roofTypes(idx).colorRegion(i).meanStdMask.RGB = meanStdRoofMaskR &
meanStdRoofMaskG & meanStdRoofMaskB;

IS.roofTypes(idx).colorRegion(i).meanStdMask.H = meanStdRoofMaskH;
IS.roofTypes(idx).colorRegion(i).meanStdMask.S = meanStdRoofMaskS;
IS.roofTypes(idx).colorRegion(i).meanStdMask.V = meanStdRoofMaskV;
IS.roofTypes(idx).colorRegion(i).meanStdMask.HSV = meanStdRoofMaskH &
meanStdRoofMaskS & meanStdRoofMaskV;

IS.roofTypes(idx).colorRegion(i).meanStdMask.total =
IS.roofTypes(idx).colorRegion(i).meanStdMask.RGB & ...
```

```
        IS.roofTypes(idx).colorRegion(i).meanStdMask.HSV;

        end

        meanStdMaskArray = [IS.roofTypes(idx).colorRegion.meanStdMask];
        minMaxMaskArray = [IS.roofTypes(idx).colorRegion.minMaxMask];

        IS.roofTypes(idx).mask = struct();
        IS.roofTypes(idx).mask.firstMask = struct();
        IS.roofTypes(idx).mask.firstMask.meanStd =
        max(cat(3,meanStdMaskArray.total),[],3);
        IS.roofTypes(idx).mask.firstMask.minMax =
        max(cat(3,minMaxMaskArray.total),[],3);

end

function IS = filterMask(IS,idx)
        nErosion = 2;
        nDilation = 2;

        IS.roofTypes(idx).mask.openClosedMask = struct();

        IS.roofTypes(idx).mask.openClosedMask.openedMask = struct();
        IS.roofTypes(idx).mask.openClosedMask.openedMask.minMax =
        myOpen(IS.roofTypes.mask.firstMask.minMax, [0 1 0; 1 1 1; 0 1
        0],nErosion,nDilation);
        IS.roofTypes(idx).mask.openClosedMask.openedMask.meanStd =
        myOpen(IS.roofTypes.mask.firstMask.meanStd, [0 1 0; 1 1 1; 0 1
        0],nErosion,nDilation);

        IS.roofTypes(idx).mask.openClosedMask.closedMask = struct();
        IS.roofTypes(idx).mask.openClosedMask.closedMask.minMax =
        myClose(IS.roofTypes.mask.firstMask.minMax, [0 1 0; 1 1 1; 0 1
        0],nErosion,nDilation);
        IS.roofTypes(idx).mask.openClosedMask.closedMask.meanStd =
        myClose(IS.roofTypes.mask.firstMask.meanStd, [0 1 0; 1 1 1; 0 1
        0],nErosion,nDilation);

        IS.roofTypes(idx).mask.openClosedMask.filledMask = struct();
        IS.roofTypes(idx).mask.openClosedMask.filledMask.minMax =
        imfill(IS.roofTypes.mask.firstMask.minMax,"holes");
        IS.roofTypes(idx).mask.openClosedMask.filledMask.meanStd =
        imfill(IS.roofTypes.mask.firstMask.meanStd,"holes");

        IS.roofTypes(idx).mask.openClosedMask.openedFilledMask = struct();
        IS.roofTypes(idx).mask.openClosedMask.openedFilledMask.minMax =
        imfill(IS.roofTypes(idx).mask.openClosedMask.openedMask.minMax,"holes");
        IS.roofTypes(idx).mask.openClosedMask.openedFilledMask.meanStd =
        imfill(IS.roofTypes(idx).mask.openClosedMask.openedMask.meanStd,"holes");
```

```
        IS.roofTypes(idx).mask.openClosedMask.closedFilledMask = struct();
        IS.roofTypes(idx).mask.openClosedMask.closedFilledMask.minMax              =
        imfill(IS.roofTypes(idx).mask.openClosedMask.closedMask.minMax,"holes");
        IS.roofTypes(idx).mask.openClosedMask.closedFilledMask.meanStd             =
        imfill(IS.roofTypes(idx).mask.openClosedMask.closedMask.meanStd,"holes");

        IS.roofTypes(idx).mask.openClosedMask.filledOpenedMask = struct();
        IS.roofTypes(idx).mask.openClosedMask.filledOpenedMask.minMax              =
        myOpen(IS.roofTypes(idx).mask.openClosedMask.filledMask.minMax, [0 1 0; 1 1
        1; 0 1 0],nErosion,nDilation);
        IS.roofTypes(idx).mask.openClosedMask.filledOpenedMask.meanStd             =
        myOpen(IS.roofTypes(idx).mask.openClosedMask.filledMask.meanStd, [0 1 0; 1 1
        1; 0 1 0],nErosion,nDilation);

        IS.roofTypes(idx).mask.openClosedMask.filledClosedMask = struct();
        IS.roofTypes(idx).mask.openClosedMask.filledClosedMask.minMax              =
        myClose(IS.roofTypes(idx).mask.openClosedMask.filledMask.minMax, [0 1 0; 1 1
        1; 0 1 0],nErosion,nDilation);
        IS.roofTypes(idx).mask.openClosedMask.filledClosedMask.meanStd             =
        myClose(IS.roofTypes(idx).mask.openClosedMask.filledMask.meanStd, [0 1 0; 1
        1 1; 0 1 0],nErosion,nDilation);

end

function openedIm = myOpen(ID,SE,nErosion,nDilation)
        openedIm = ID;

        for i = 1:nErosion
        openedIm = imerode(openedIm,SE);
        end
        for i = 1:nDilation
        openedIm = imdilate(openedIm,SE);
        end
end

function openedIm = myClose(ID,SE,nErosion,nDilation)
        openedIm = ID;

        for i = 1:nDilation
        openedIm = imdilate(openedIm,SE);
        end
        for i = 1:nErosion
        openedIm = imerode(openedIm,SE);
        end
end

function filledFilteredMask = filterIndividualMask(initialMask, minSize1, minSize2)
        filledMask = myFill(initialMask,400);
        openedFilledMask = imopen(filledMask,[0 1 0 ; 1 1 1 ; 0 1 0]);
        figure("Name","Opened filled mask");
```

```
        imshow(filledMask);

        % Suppress smaller blobs
        % Extract blobs and blob area
        imLabels = bwlabel(openedFilledMask);
        props = regionprops(openedFilledMask,imLabels,'Area');

        % Surpress small blobs
        k = find([props.Area] < minSize1);
        suppressedLabels = ismember(imLabels,k);
        filteredMask = xor(openedFilledMask,suppressedLabels);
        figure("Name","First filtered mask");
        imshow(filteredMask);

        closedMask = myClose(filteredMask,[0 1 0 ; 1 1 1 ; 0 1 0],2,2);
        filledFilteredMask = myFill(closedMask,800);

        % Suppress smaller blobs again
        % Extract blobs and blob area
        imLabels = bwlabel(filledFilteredMask);
        props = regionprops(filledFilteredMask,imLabels,'Area');

        % Surpress small blobs
        k = find([props.Area] < minSize2);
        suppressedLabels = ismember(imLabels,k);
        filteredMask = xor(filledFilteredMask,suppressedLabels);
        figure("Name","Twice filtered mask");
        imshow(filteredMask);

        % Finally close the image
        closedMask = myClose(filteredMask,[0 1 0 ; 1 1 1 ; 0 1 0],4,4);
        filledFilteredMask = myFill(closedMask,1000);
        figure("Name","Final filled closed filtered mask");
        imshow(filledFilteredMask);

end

function   filledFilteredMask   =   filterIndividualGreyMask(initialMask,   minSize1,
minSize2)
        filledMask = myFill(initialMask,400);
        openedFilledMask = myOpen(filledMask,[0 1 0 ; 1 1 1 ; 0 1 0],2,2);
        figure("Name","Opened filled mask");
        imshow(filledMask);

        % Suppress smaller blobs
        % Extract blobs and blob area
        imLabels = bwlabel(openedFilledMask);
        props = regionprops(openedFilledMask,imLabels,'Area');

        % Surpress small blobs
```

```
        k = find([props.Area] < minSize1);
        suppressedLabels = ismember(imLabels,k);
        filteredMask = xor(openedFilledMask,suppressedLabels);
        figure("Name","First filtered mask");
        imshow(filteredMask);

        closedMask = myClose(filteredMask,[0 1 0 ; 1 1 1 ; 0 1 0],2,2);
        filledFilteredMask = myFill(closedMask,700);

        % Suppress smaller blobs again
        % Extract blobs and blob area
        imLabels = bwlabel(filledFilteredMask);
        props = regionprops(filledFilteredMask,imLabels,'Area');

        % Surpress small blobs
        k = find([props.Area] < minSize2);
        suppressedLabels = ismember(imLabels,k);
        filteredMask = xor(filledFilteredMask,suppressedLabels);
        figure("Name","Twice filtered mask");
        imshow(filteredMask);

        % Finally close the image
        closedMask = myClose(filteredMask,[0 1 0 ; 1 1 1 ; 0 1 0],4,4);
        filledFilteredMask = myFill(closedMask,1000);
        figure("Name","Final filled closed filtered mask");
        imshow(filledFilteredMask);

end

function orMask = blobOR(mask1,mask2)
        mask1Labels = bwlabel(mask1);
        mask2Labels = bwlabel(mask2);
        blob1Values = unique(mask1Labels(mask2));
        blob2Values = unique(mask2Labels(mask1));
        orMask                                                    =
        ismember(mask1Labels,blob1Values(blob1Values>0))|ismember(mask2Labels,blob2V
        alues(blob2Values>0));

end

function croppedBlobs = cropBlobs(baseImage, blobMask)
        f = figure('Name', 'Selected FAs for elimination');

        % Overlaying the base image with the mask using imfuse
        fusedImage = imfuse(baseImage, blobMask, 'blend', 'Scaling', 'joint');
        imshow(fusedImage);

        % Initialise the total mask
        totalMask = false(size(blobMask));
```

```
        % Wait until the polygon drawing is completed or Enter is pressed.
        while true
        % Allows the user to draw a polygon
        h = drawpolygon;

        % Wait for user to finish drawing
        wait(h);

        % Gets the coordinates of the selected polygon
        polygonCoordinates = h.Position;

        % Creates a binary mask for the selected polygon
        polygonMask = poly2mask(polygonCoordinates(:, 1), polygonCoordinates(:, 2),
        size(blobMask, 1), size(blobMask, 2));

        % Combines the polygon with the previously created mask
        totalMask = totalMask | polygonMask;

        % Closes the polygon drawing figure
        delete(h);

        % Asks the user if he/she wants to draw another polygon
        disp("Press 'Enter' to draw another polygon or any other key to exit.");
        key = waitforbuttonpress;

        if key == 0
        % User pressed 'Enter' to draw another polygon, continues the loop
        continue;
        else
        % The user pressed a different key, exits the loop.
        croppedBlobs = blobMask & ~totalMask;
        break;
        end
        end

        % Closes the main figure and the figure of the superimposed image.
        close(f);
end

function visualizeMask(img,mask)
        figure("Name","Mask visualisation")
        imshow(img);
        hold on
        mask3D = cat(3,mask*0.1,mask*0.6,mask*0.7);
        I = imshow(mask3D);
        I.AlphaData = mask*0.6;
end


function finalMask = myFill(mask,maxArea)
```

```
    filledMask = imfill(mask,"holes");
    holeMask = xor(mask,filledMask);

    labelledHoles = bwlabel(holeMask);
    props = regionprops(holeMask,labelledHoles,'Area');

    k = find([props.Area] < maxArea);
    holes2fill = ismember(labelledHoles,k);

    finalMask = mask|holes2fill;

end
```

ROOFTYPESET.m

```
% Script for the automatic detection of roofs with colour type
% Author: Tomás Pino Gallardo
% Máster Universitario Tecnologías Energéticas para Desarrollo Sostenible
% Institution: Instituto de Ingeniería Energética (UPV)
%
% DISCLAIMER: This code has not undergone thorough cleaning or formal publication.
% its intended use is strictly limited to individuals within the institution.

%% Roof Type Generation

      clc;
      clear;

      % Roof type structure loading
      load("MATLABData\roofType.mat","roofType");

%% Image

      % Define the directory path
      folder_path = 'Directory path';

      % Prompt the user to select a file within the directory
      disp(' Select a file within the folder.');
      [filename, folder] = uigetfile(fullfile(folder_path, '*.*'), ' Select file');

      % Check if a valid file was selected
      if isequal(filename, 0)
      error(' No valid file was selected.');
      end

      % Get the full path to the selected file
      image_path = fullfile(folder, filename);

      % Load roof image
      tAerialImage = Tiff(image_path);
      AerialImage = tAerialImage.read;
      AerialImageHSV = rgb2hsv(AerialImage);

      % Pixel detection
      answer = questdlg("Would you like to add a new roofType for this image?");

      while answer=="Yes"

      roofName = input("Please, write down the name of the new roofType.\n","s");
      colorRegionName = input("Please, write down the name of the new colorRegion
      for this roofType.\n","s");
      pixelClicks = selectRoofPixels(AerialImage);
```

```
newRoofType = struct();
newRoofType.name = convertCharsToStrings(roofName);

colorRegion = struct();
colorRegion.name = convertCharsToStrings(colorRegionName);
colorRegion.pixelValuesRGB = getPixelValues(AerialImage,pixelClicks);
colorRegion.pixelValuesHSV = getPixelValues(AerialImageHSV,pixelClicks);
colorRegion.statistics = getStatistics(colorRegion);
newRoofType.colorRegions = [];
newRoofType.colorRegions = [newRoofType.colorRegions colorRegion];

roofType = [roofType newRoofType];

answer = questdlg("Would you like to add a new roofType for this image?");
end

answer = questdlg("Would you like to add a new colorRegion for an existing
roofType?");

while answer=="Yes"

[idx,tf]                                                                  =
listdlg('ListString',[roofType.name],'SelectionMode','single','PromptString'
,"Select the roofType to modify:");

if isempty(idx)
break
end

colorRegionName = input("Please, write down the name of the new colorRegion
for this roofType.\n","s");
pixelClicks = selectRoofPixels(AerialImage);

newColorRegion = struct();
newColorRegion.name = convertCharsToStrings(colorRegionName);
newColorRegion.pixelValuesRGB = getPixelValues(AerialImage,pixelClicks);
newColorRegion.pixelValuesHSV = getPixelValues(AerialImageHSV,pixelClicks);

newColorRegion.statistics = getStatistics(newColorRegion);

roofType(idx).colorRegions = [roofType(idx).colorRegions newColorRegion];

answer = questdlg("Would you like to add a new colorRegion for an existing
roofType?");
end

answer  =  questdlg("Would  you  like  to  add  more  points  to  an  existing
colorRegion?");
```

```
    while answer=="Yes"

    [roofTypeIdx,tf] =
    listdlg('ListString',[roofType.name],'SelectionMode','single','PromptString'
    ,"Select the roofType to modify:");

    if isempty(roofTypeIdx)
    break
    end

    [colorRegionIdx,tf] =
    listdlg('ListString',[roofType(roofTypeIdx).colorRegions.name],'SelectionMod
    e','single','PromptString',"Select the colorRegion to modify:");

    if isempty(colorRegionIdx)
    break
    end

    pixelClicks = selectRoofPixels(AerialImage);

    roofType(roofTypeIdx).colorRegions(colorRegionIdx).pixelValuesRGB =
    [roofType(roofTypeIdx).colorRegions(colorRegionIdx).pixelValuesRGB;
    getPixelValues(AerialImage,pixelClicks)];
    roofType(roofTypeIdx).colorRegions(colorRegionIdx).pixelValuesHSV =
    [roofType(roofTypeIdx).colorRegions(colorRegionIdx).pixelValuesHSV;
    getPixelValues(AerialImageHSV,pixelClicks)];
    roofType(roofTypeIdx).colorRegions(colorRegionIdx).statistics =
    getStatistics(roofType(roofTypeIdx).colorRegions(colorRegionIdx));

    answer = questdlg("Would you like to add more points to an existing colorRegion
    in this image?");
    end

    close all;

    % Save the roofType struct
    save("MATLABData\roofType","roofType");

%% Save Rooftype struct

    save("MATLABData\roofType","roofType");

%% Functions

function pClicks = selectRoofPixels(Image)
    f = figure('Name','Selected building pixeels');
    imshow(Image);
    hold on
    pClicks = zeros(size(Image,[1 2]));
    pC=imshow(pClicks);
```

```
        pC.AlphaData = 0.4;

        key = 0;

        while key ~= 13

        % Wait until some key or button is pressed and get the position of the
        % mouse and the pressed key.
        [x,y,key] = ginput(1);
        xPixel = round(x);
        yPixel = round(y);

        % If it was not enter
        if key ~= 13
        % If it was the left click add that FA to the deletion list.
        if key == 1
        pClicks(yPixel,xPixel) = 1;
        % If it was the right click remove the FA from the deletion
        % list.
        elseif key == 3
        pClicks(yPixel,xPixel) = 0;
        end
        end

        % Refresh the image and show the selected FAs in red.
        figure(f);
        delete(pC);
        pC=imshow(conv2(pClicks,ones(5),"same")>0);
        pC.AlphaData = 0.4;

        end

end

function pixelValues = getPixelValues(Image,selectedPixels)
        [yPixel,xPixel] = find(selectedPixels);
        yPixelcoord = repelem(yPixel,3);
        xPixelcoord = repelem(xPixel,3);
        zPixelcoord = repmat((1:3)',length(xPixel),1);
        PixelIdx = sub2ind(size(Image),yPixelcoord,xPixelcoord,zPixelcoord);
        pixelValues = reshape(Image(PixelIdx),[3,length(xPixel),])';

end

function regionStats = getStatistics(colorRegion)
        regionStats.RGB = struct();
        regionStats.RGB.min = min(colorRegion.pixelValuesRGB);
        regionStats.RGB.max = max(colorRegion.pixelValuesRGB);
        regionStats.RGB.mean = mean(colorRegion.pixelValuesRGB);
        regionStats.RGB.std = std(double(colorRegion.pixelValuesRGB));
```

```
    regionStats.HSV = struct();
    regionStats.HSV.min = min(colorRegion.pixelValuesHSV);
    regionStats.HSV.max = max(colorRegion.pixelValuesHSV);
    regionStats.HSV.mean = mean(colorRegion.pixelValuesHSV);
    regionStats.HSV.std = std(colorRegion.pixelValuesHSV);

end
```

SLOPE.m

```
% Script for the detection of roof slopes unsuitable for rehabilitation
% Author: Tomás Pino Gallardo
% Máster Universitario Tecnologías Energéticas para Desarrollo Sostenible
% Institution: Instituto de Ingeniería Energética (UPV)

% DISCLAIMER: This code has not undergone thorough cleaning or formal publication.
% its intended use is strictly limited to individuals within the institution.

clear;
clc;
clear global;
clear functions;

%% 1) LAZ file upload

      % Define the directory path
      folder_path = "directory path";

      % Prompt the user to select a file within the directory
      disp(' Select a file within the folder.');
      [filename,  folder]  =  uigetfile(fullfile(folder_path,  '*.*'),  'Seleccionar
      archivo');

      % Check if a valid file was selected
      if isequal(filename, 0)
      error(' No valid file was selected.');
      end

      % Change the extension to '.tif'.
      tifExtension = '.tif';
      tiffname = strrep(filename, '.laz', tifExtension);
      ruta_imagen_tiff=fullfile("directory path ", tiffname);

      %   Load   original   image   and   get   georeferencing   informationinfo   =
      geotiffinfo(ruta_imagen_tiff);

      % Create an LAS object to read the LAZ file
      lasFile = lasFileReader(fullfile(folder, filename));

%% 2) Filter by Building Point and Plot

      % Obtain unique classifications
      classificationInfo = lasFile.ClassificationInfo;
      uniqueClassifications = unique(classificationInfo.('Class Name'));

      % Read point cloud data and associated classification point attributes from
      the LAZ file using the readPointCloud function.
```

```
[ptCloud,pointAttributes]                                              =
readPointCloud(lasFile,"Attributes","Classification");

% Filter points with classification 6
selectedIndices = find(ismember(pointAttributes.Classification, 6));
filteredPtCloud = select(ptCloud, selectedIndices);

% Display the filtered 3D point cloud
figure
pcshow(filteredPtCloud, 'VerticalAxis', 'Y', 'VerticalAxisDir', 'down');
title(' 3D LiDAR Point Cloud (Classification 6)');
xlabel('X');
ylabel('Y');
zlabel('Z');
colormap('jet');
colorbar;

%% 3) Height filter

zmin = filteredPtCloud.Location(:,3);

% Find the smallest "X" values of "Z".
[~, indices_z_ordenados] = sort(zmin, 'ascend');
indices_z_mas_bajos = indices_z_ordenados(1);

% Converts values to double
valores_z_mas_bajos = zmin(indices_z_mas_bajos);

% Displays the smallest "X" values of "Z".
valores_z_mas_bajos = zmin(indices_z_mas_bajos);
disp(' The smallest value of Z:');
disp(valores_z_mas_bajos);

% Threshold height for filtering
altura_umbral = valores_z_mas_bajos + 3;

% Storages
x=double([]);
y=double([]);
z=double([]);
Colorx = uint16([]);
Colory = uint16([]);
Colorz = uint16([]);
Intensidad = uint16([]);
cont=1;

for i = 1:(filteredPtCloud.Count)
if double(filteredPtCloud.Location(i,3)) > altura_umbral
x(cont, 1) = filteredPtCloud.Location(i, 1);
y(cont, 1) = filteredPtCloud.Location(i, 2);
```

```
        z(cont, 1) = filteredPtCloud.Location(i, 3);
        Colorx(cont, 1) = filteredPtCloud.Color(i, 1);
        Colory(cont, 1) = filteredPtCloud.Color(i, 2);
        Colorz(cont, 1) = filteredPtCloud.Color(i, 3);
        Intensidad(cont, 1) = filteredPtCloud.Intensity(i, 1);
        cont=cont+1;
        end
        end
        % Create a new PointCloud object
        newPtCloud = pointCloud([x(:), y(:), z(:)], 'Color', [Colorx(:), Colory(:),
        Colorz(:)], 'Intensity', Intensidad(:));

        % Show some values of the new cloud
        disp(' Total Points Remaining:');
        disp(newPtCloud.Count);

%% 4) Point grouping by k-means

        % Extract XYZ coordinates from the point cloud
        xyz = newPtCloud.Location;

        % Calculate histogram of heights
        alturaHistograma = histogram(xyz(:, 3), 'BinWidth', 2);

        % Automatically determine the number of groups based on the histogram
        [picos,       ubicaciones]       =       findpeaks(alturaHistograma.Values,
        alturaHistograma.BinEdges(1:end-1));
        [~, idx] = max(picos);
        umbral = ubicaciones(idx);

        % Apply the k-means algorithm to cluster points in buildings.
        numGrupos = max(1, round(umbral)); % Make sure that numGroups is at least 1

        % Apply the k-means algorithm to cluster points in buildings.
        options = statset('MaxIter', 10000); % Adjust as necessary

        % Specify the seed for random number generation
        rng(4000000000); % or any other number

        % Initialize centroids deterministically (using kmeans++)
        inicializacion_centroides = 'plus';

        % Call k-means with the 'Start' option
        [idx,  centros]  =  kmeans(xyz,  numGrupos,  'Options',  options,  'Start',
        inicializacion_centroides);

        % Restore the seed for random number generation (optional)
        rng('shuffle'); % You can use 'shuffle' to restore randomness if needed

        % Visualize the point cloud with colors according to groups
```

```
figure;
pcshow(newPtCloud, 'VerticalAxis', 'Y', 'VerticalAxisDir', 'down');
title(' LiDAR point cloud with clustered buildings'.);
xlabel('X');
ylabel('Y');
zlabel('Z');
colormap('jet');
colorbar;

% Color the points according to the groups found by k-means and the intensity
of red based on the Z-value.
minAltura = min(xyz(:, 3));
maxAltura = max(xyz(:, 3));
normalizedAltura = (xyz(:, 3) - minAltura) / (maxAltura - minAltura);
colorGrupo = [normalizedAltura(:), (1 - normalizedAltura(:)),
zeros(size(normalizedAltura(:)))];

hold on;

for i = 1:numGrupos
grupoIndices = find(idx == i);
% Adding lines to highlight the group outlines
scatter3(xyz(grupoIndices, 1), xyz(grupoIndices, 2), xyz(grupoIndices, 3),
20, colorGrupo(grupoIndices, :), 'filled');
plot3(xyz(grupoIndices, 1), xyz(grupoIndices, 2), xyz(grupoIndices, 3), '.',
'Color', colorGrupo(grupoIndices(1), :));
end

hold off;

%% 5) Pendiente de Edificios

% Ask the user about the maximum allowable limit in degrees.
limite_maximo_grados = input(' Enter the maximum allowable limit in degrees:
');

% Calculate roof slope for each group
pendientes = zeros(numGrupos, 1);
pendientes_superiores = zeros(numGrupos, 1);

for i = 1:numGrupos
% Get indexes of the points in the current group
grupoIndices = find(idx == i);

% Snap a line to points in the XY plane
coefficients = polyfit(xyz(grupoIndices, 1), xyz(grupoIndices, 2), 1);

% The slope coefficient is the value we are interested in
pendiente = atand(coefficients(1));  % Convert to degrees
```

```
% Store slope in vector
pendientes(i) = pendiente;

% Check if the slope exceeds the maximum allowable limit (in absolute value).
if abs(pendiente) > limite_maximo_grados
pendientes_superiores(i) = pendiente;
end
end

% Display the point cloud with colors according to the groups
figure;
pcshow(newPtCloud, 'VerticalAxis', 'Y', 'VerticalAxisDir', 'down');
title(' LiDAR point cloud with clustered buildings');
xlabel('X');
ylabel('Y');
zlabel('Z');
colormap('jet');
colorbar;

% Color the points according to the groups found by k-means and the intensity
of red based on the Z-value.
minAltura = min(xyz(:, 3));
maxAltura = max(xyz(:, 3));
normalizedAltura = (xyz(:, 3) - minAltura) / (maxAltura - minAltura);
colorGrupo = [normalizedAltura(:), (1 - normalizedAltura(:)),
zeros(size(normalizedAltura(:)))];

% Identify and visualize slopes that exceed the maximum limit.
indices_superiores = find(pendientes_superiores > 0);
if ~isempty(indices_superiores)
disp(' Slopes that exceed the maximum allowable limit:');
disp(pendientes_superiores(indices_superiores));

% Plot only the points corresponding to groups with slopes greater than the
limit.
hold on;
for i = 1:length(indices_superiores)
grupoActual = indices_superiores(i);
grupoIndices = find(idx == grupoActual);

% Adding lines to highlight the group outlines
scatter3(xyz(grupoIndices, 1), xyz(grupoIndices, 2), xyz(grupoIndices, 3),
20, colorGrupo(grupoIndices, :), 'filled');
plot3(xyz(grupoIndices, 1), xyz(grupoIndices, 2), xyz(grupoIndices, 3), '.',
'Color', colorGrupo(grupoIndices(1), :));
end
hold off;
else
disp(' No slope exceeds the maximum allowable limit.');
end
```

```
%% 6) Create Binary Mask for PSLA

    % Obtain specific georeferencing information from the TIF image
    geoRasterRefTIF = geotiffinfo(ruta_imagen_tiff);

    % Create the binary mask matrix with zeros using the georeferencing information of the TIF image
    binaryMask = zeros(geoRasterRefTIF.Height, geoRasterRefTIF.Width);

    % Identify and mark points exceeding the limit in the binary mask
    for i = 1:length(indices_superiores)
    grupoActual = indices_superiores(i);
    grupoIndices = find(idx == grupoActual);

    % Convert the X, Y coordinates of the points of the group to indexes in the binary mask
    indicesY = round(newPtCloud.Location(grupoIndices, 2) - geoRasterRefTIF.SpatialRef.YWorldLimits(1)) + 1;
    indicesX = round(newPtCloud.Location(grupoIndices, 1) - geoRasterRefTIF.SpatialRef.XWorldLimits(1)) + 1;

    % Mark the points in the binary mask with the group number
    binaryMask(sub2ind(size(binaryMask), indicesY, indicesX)) = grupoActual;
    end

    % Use the specific georeferencing information from theFileForGeoRef
    geoRasterRef = imref2d(size(binaryMask), ...
    [lasFile.YLimits(1), lasFile.YLimits(2)], ...
    [lasFile.XLimits(1), lasFile.XLimits(2)]);

    % Restore specific georeferencing information from the TIF image
    geoRasterRefMask = geoRasterRefTIF;

    % Apply closing operation
    SE = strel('disk', 3);  % You can adjust the size of the structuring element as required.
    binaryMaskClosed = myClose(binaryMask, SE, 1, 1);

    % Apply filling operation
    maxHoleArea = 2000;  % You can adjust the maximum area of the hole to be filled as needed.
    finalMask = myFill(binaryMaskClosed, maxHoleArea);

    % Display the binary mask
    visualizeMask(finalMask, geoRasterRefMask);

    % Use the specific georeferencing information of the TIF image
    geoRasterRefFinalMask = geoRasterRefMask;
```

```
    % Specify the output folder for the mask
    outputFolder = "directory path";

    % Get LAZ file name without extension
    [~, baseFileName, ~] = fileparts(filename);

    % Construct the file name for the binary mask
    maskFileName = fullfile(outputFolder, ['Mask_' baseFileName '.tif']);

    % Invert the mask before storing it.
    finalMask = flipud(finalMask);

    % Save binary mask as TIFF file without georeferencing information
    imwrite(finalMask, maskFileName, 'tif');

    disp([' Binary mask saved as:' maskFileName]);

%% 7) Mask georeference

    clc
    disp(tiffname)
    disp(maskFileName)

    % Mask location
    ruta_mascara = fullfile(maskFileName);

    % Read the mask
    mascara = imread(ruta_mascara);

    % Generates a file name for the georeferenced mask
    [~, name, ext] = fileparts(ruta_mascara);
    nombre_mascara_georreferenciada = sprintf('GEO_%s%s', name, ext);

    % Complete path where the georeferenced mask will be saved
    ruta_mascara_georreferenciada =
    fullfile(outputFolder,nombre_mascara_georreferenciada);

    % Save the georeferenced mask with the same georeferencing information as the
    original image.
    geotiffwrite(ruta_mascara_georreferenciada, mascara, info.SpatialRef,
    'CoordRefSysCode',
    info.GeoTIFFTags.GeoKeyDirectoryTag.ProjectedCSTypeGeoKey);
    fprintf('Máscara georreferenciada guardada como %s\n',
    ruta_mascara_georreferenciada);

    % After creating the mask
    calcularAreaMascara(finalMask, geoRasterRef);

%% Functions
```

```
function visualizeMask(mask, geoRasterRef)
	figure("Name", "Mask visualisation");

	% Reflect the mask on the Y-axis
	mask = flipud(mask);

	% Create a black matrix of the same size as the mask
	blackBackground = zeros(size(mask));

	% Obtain limits of the world
	xWorldLimits = geoRasterRef.SpatialRef.XWorldLimits;
	yWorldLimits = geoRasterRef.SpatialRef.YWorldLimits;

	% Superimpose colored and transparent mask
	mask3D = cat(3, mask * 0.1, mask * 0.6, mask * 0.7);
	imagesc(xWorldLimits, yWorldLimits, mask3D, 'AlphaData', mask * 0.6);

end

function finalMask = myFill(mask,maxArea)
	filledMask = imfill(mask,"holes");
	holeMask = xor(mask,filledMask);

	labelledHoles = bwlabel(holeMask);
	props = regionprops(holeMask,labelledHoles,'Area');

	k = find([props.Area] < maxArea);
	holes2fill = ismember(labelledHoles,k);

	finalMask = mask|holes2fill;

end

function openedIm = myClose(ID,SE,nErosion,nDilation)
	openedIm = ID;

	for i = 1:nDilation
	openedIm = imdilate(openedIm,SE);
	end
	for i = 1:nErosion
	openedIm = imerode(openedIm,SE);
	end
end

function areaHectareas = calcularAreaMascara(mask, geoRasterRef)
	% Converts binary mask to region labels
	labeledMask = bwlabel(mask);

	% Calculates the total area in pixels
	areaPixeles = sum(mask(:));
```

```
    % Obtains information on spatial resolution
    resolutionX = abs(geoRasterRef.PixelExtentInWorldX);
    resolutionY = abs(geoRasterRef.PixelExtentInWorldY);

    % Calculates the area in square meters using the image dimensions
    areaMetrosCuadrados = areaPixeles * resolutionX * resolutionY;

    % Convert area to hectares using world boundaries
    xWorldLimits = geoRasterRef.XWorldLimits;
    yWorldLimits = geoRasterRef.YWorldLimits;
    areaHectareas = areaMetrosCuadrados / 1e4;

    % Shows the area in hectares
    disp(['Mask area: ' num2str(areaHectareas) ' hectare']);
end
```

IMAGES

VALENCIA PER CURRENT

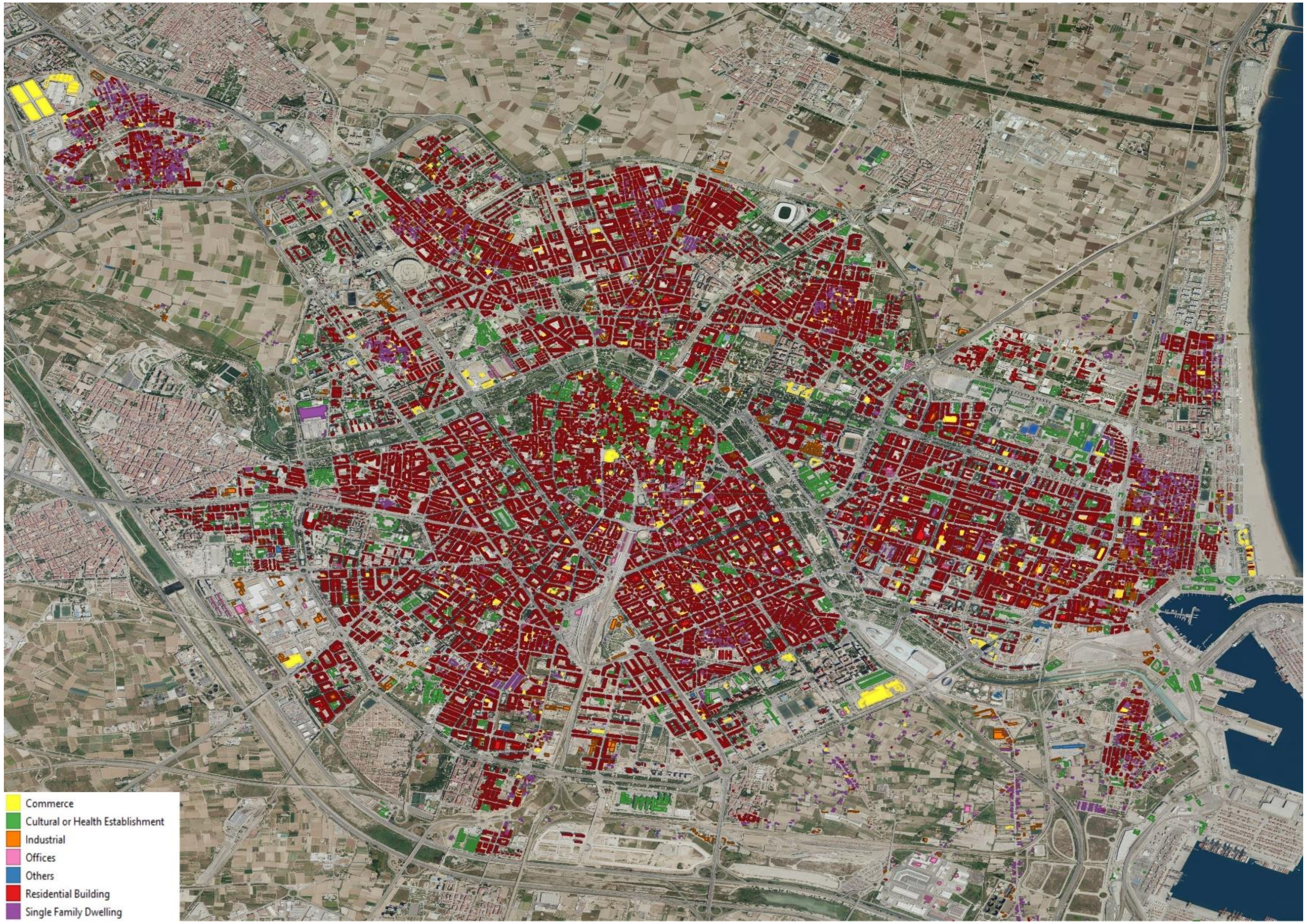

Figure 30*: City of Valencia per Current Use.*

***Figure 31**: City of Valencia per Commerce.*

***Figure 32**: City of Valencia per Cultural or Health Establishment.*

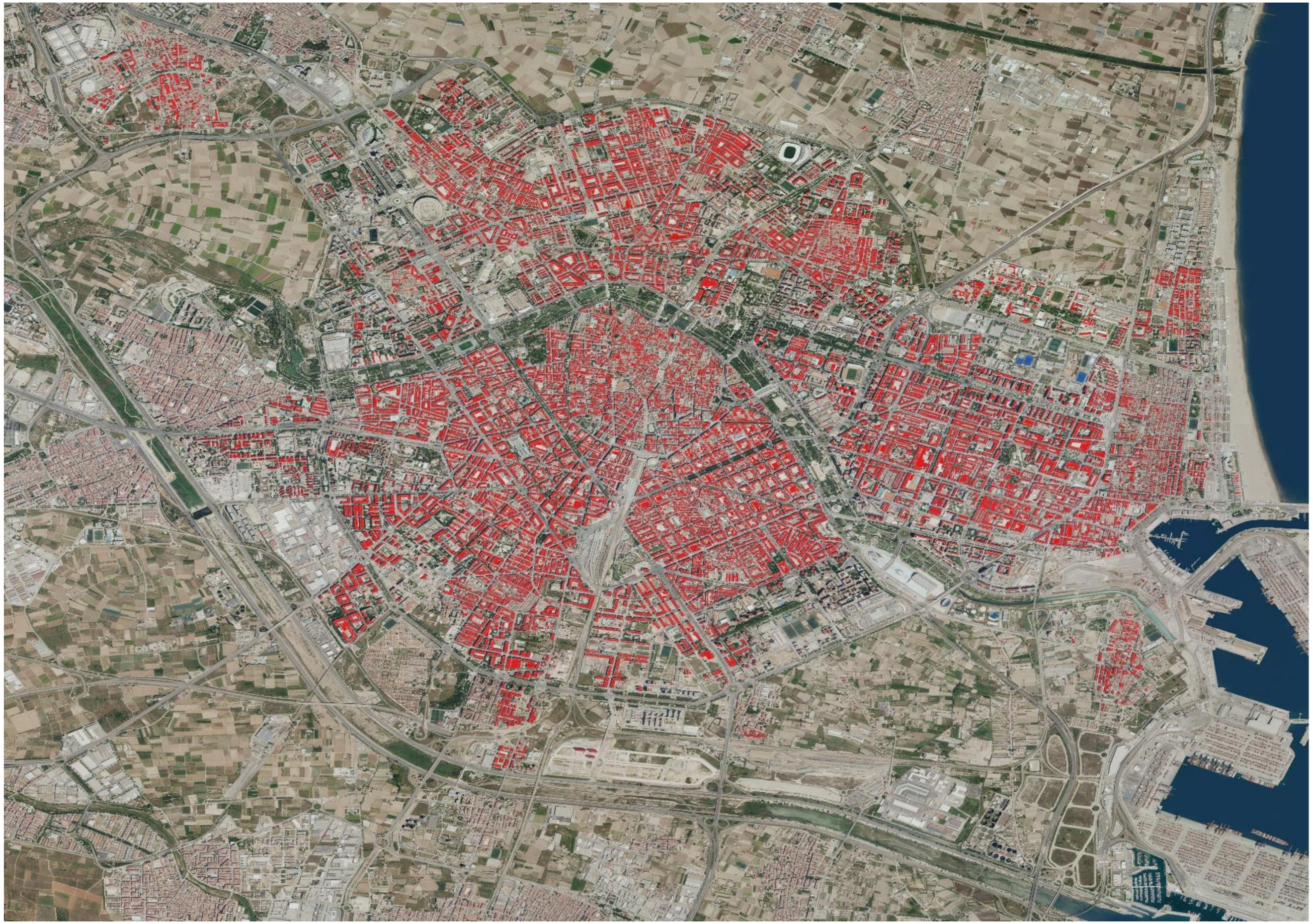

***Figure 33**: City of Valencia per Residential Building.*

***Figure 34**: City of Valencia per Industrial.*

***Figure 35**: City of Valencia per Offices.*

***Figure 36:** City of Valencia per Single Family Dwelling.*

Figure 37: *City of Valencia per Others use.*

VALENCIA PER DISTRICTS

***Figure 38**: District ALGIROS per Current Use.*

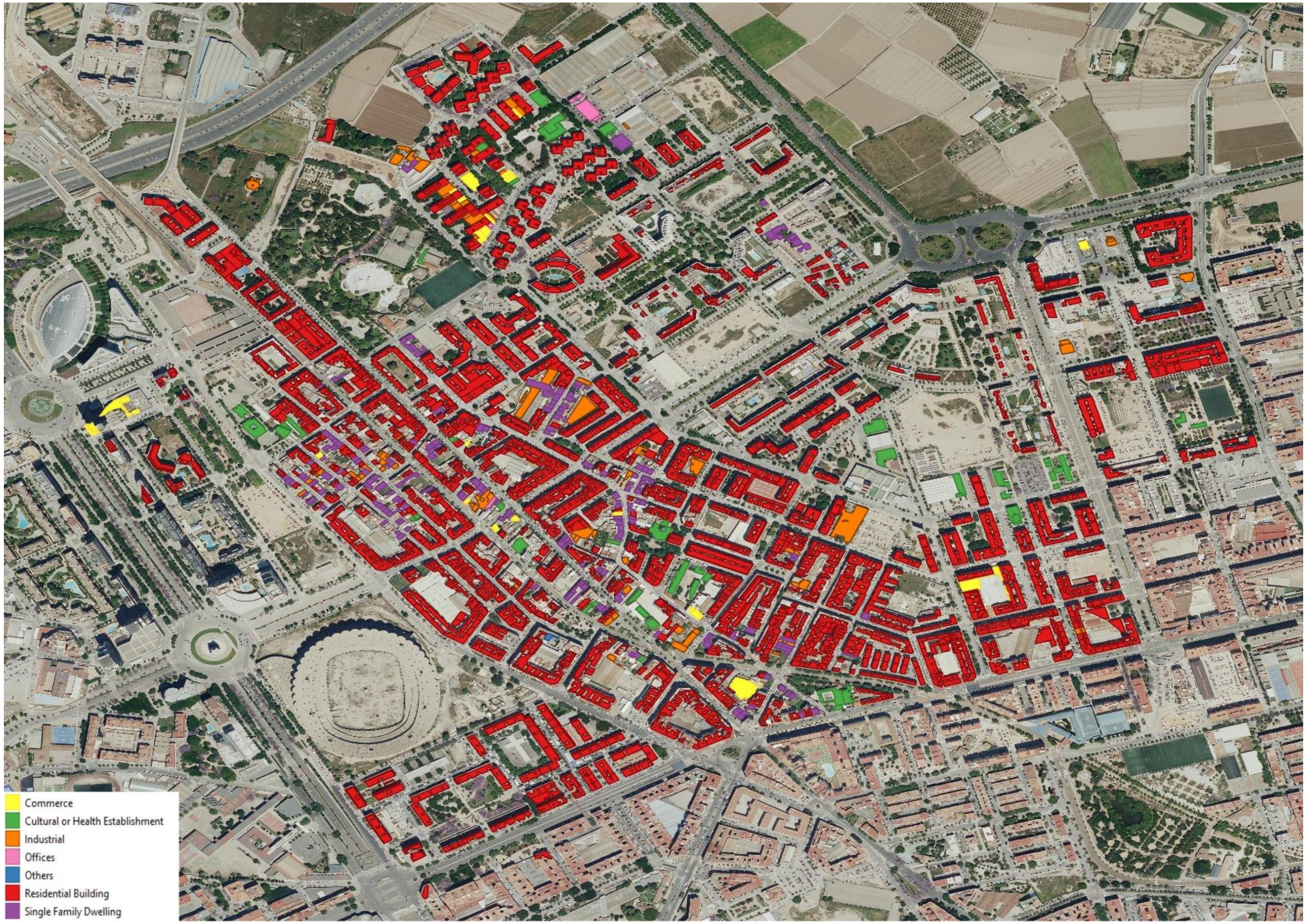

***Figure 39**: District BENICALAP per Current Use.*

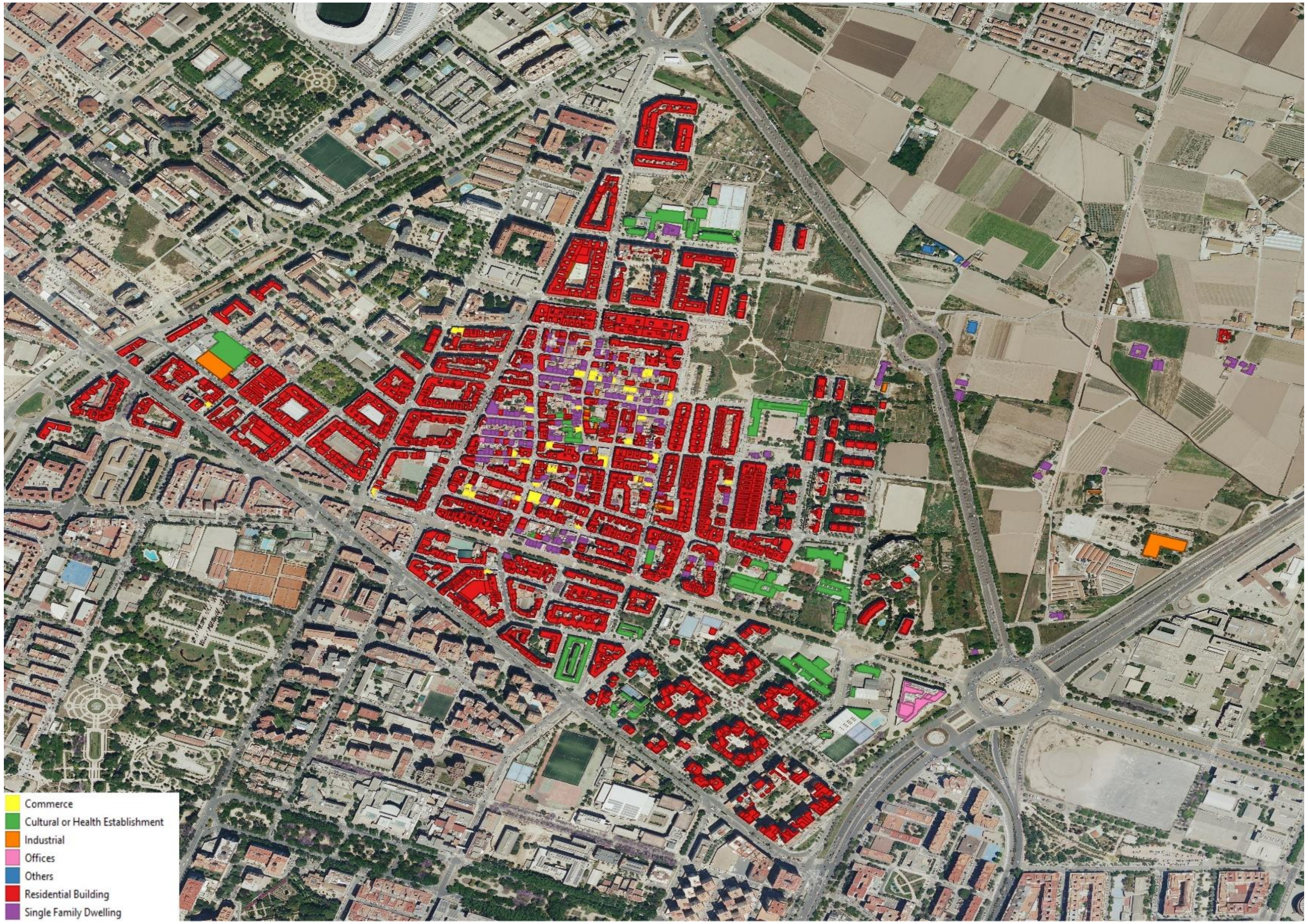

***Figure 40**: District BENIMACLET per Current Use.*

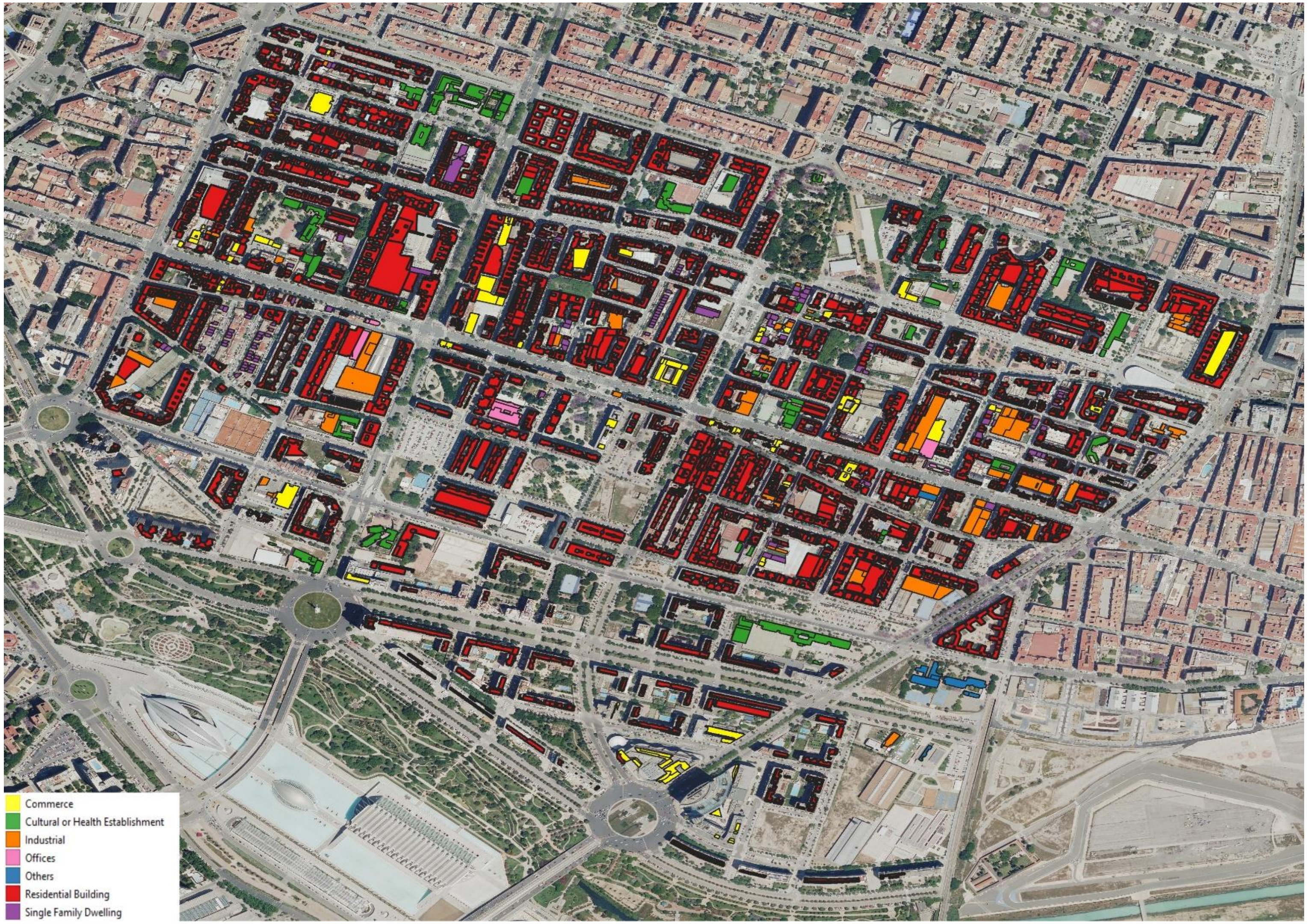

***Figure 41**: District CAMINS AL GRAU per Current Use.*

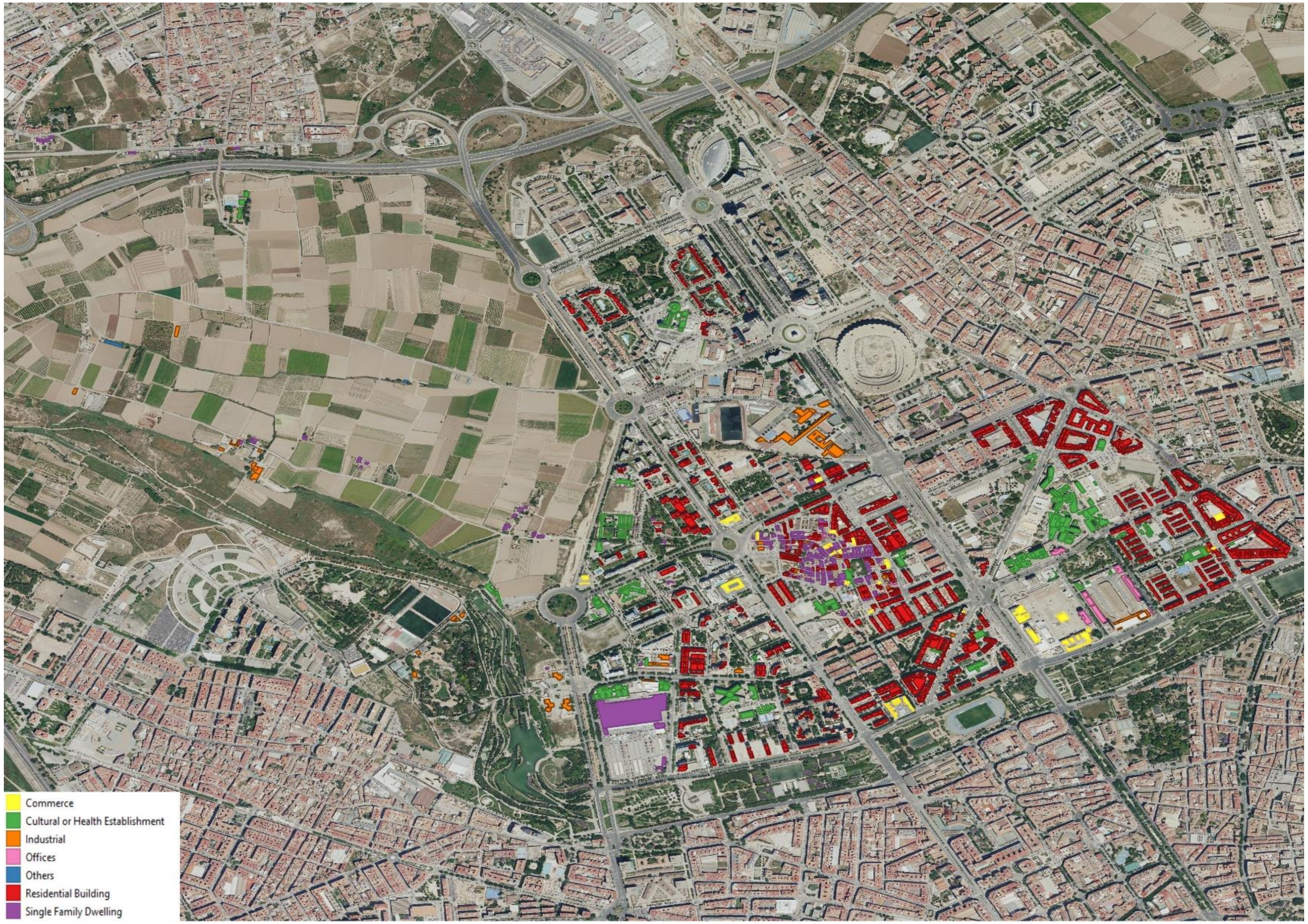

***Figure 42**: District CAMPANAR per Current Use.*

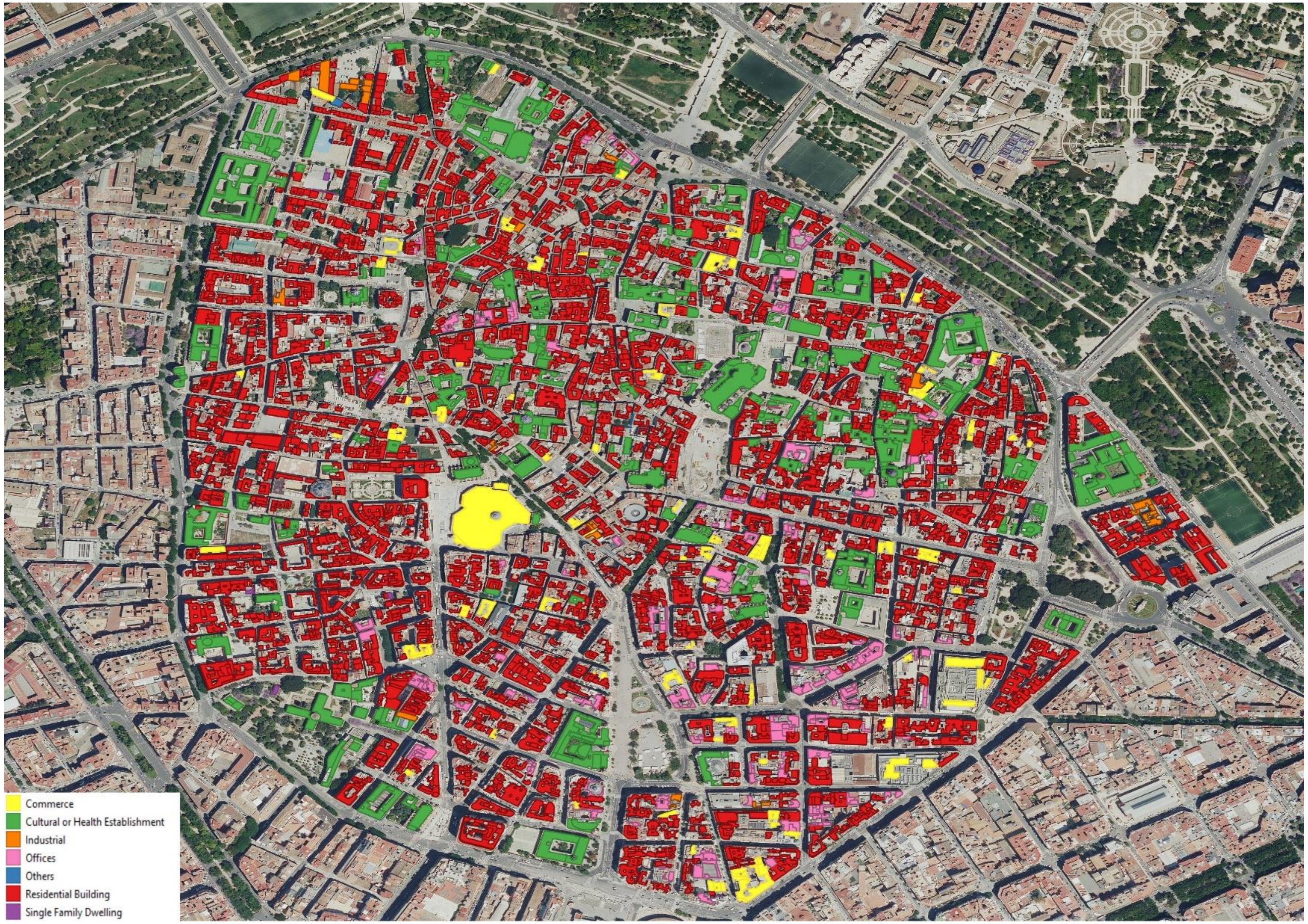

***Figure 43**: District CIUTAT VELLA per Current Use.*

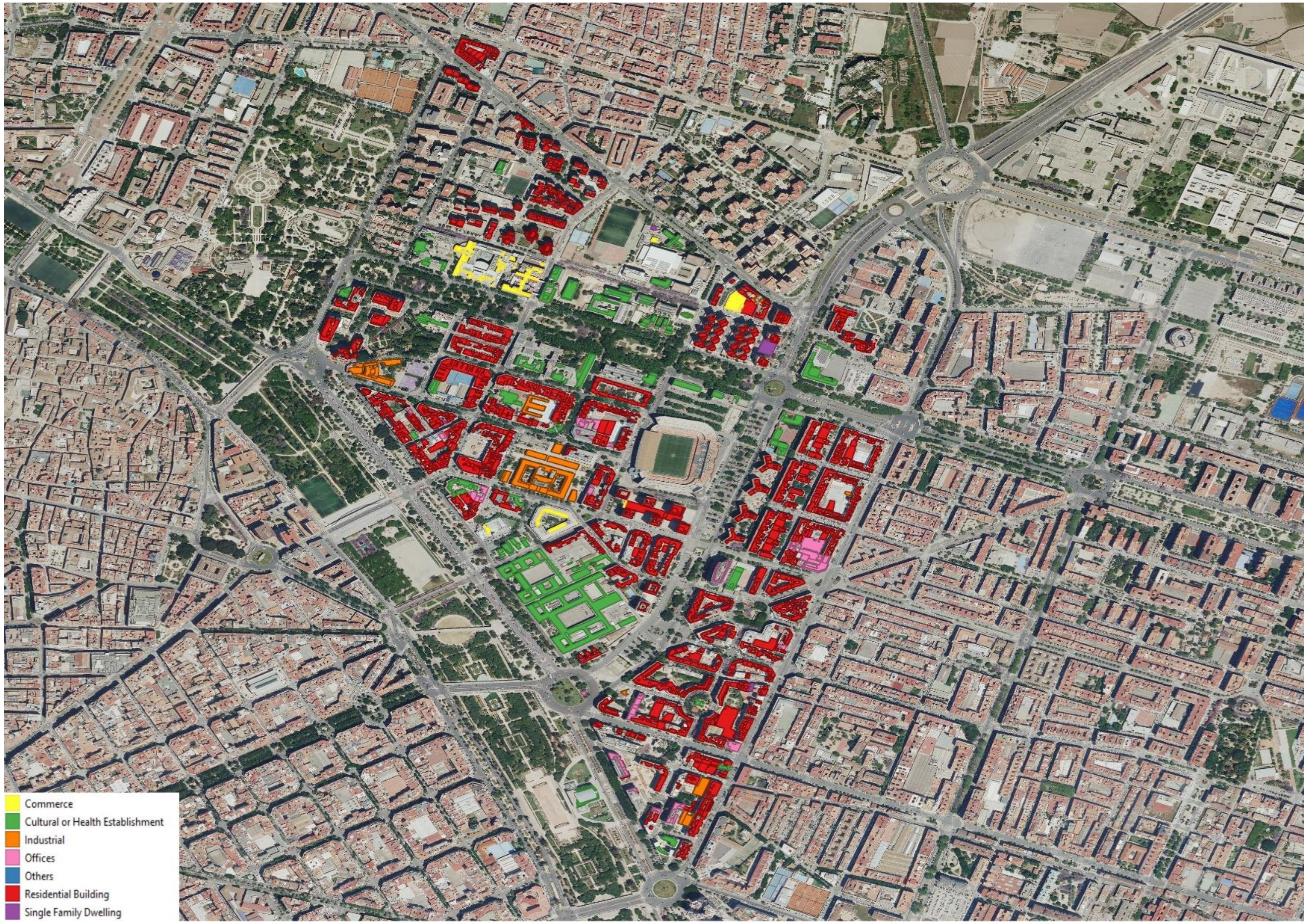

***Figure 44**: District EL PLA DEL REAL per Current Use.*

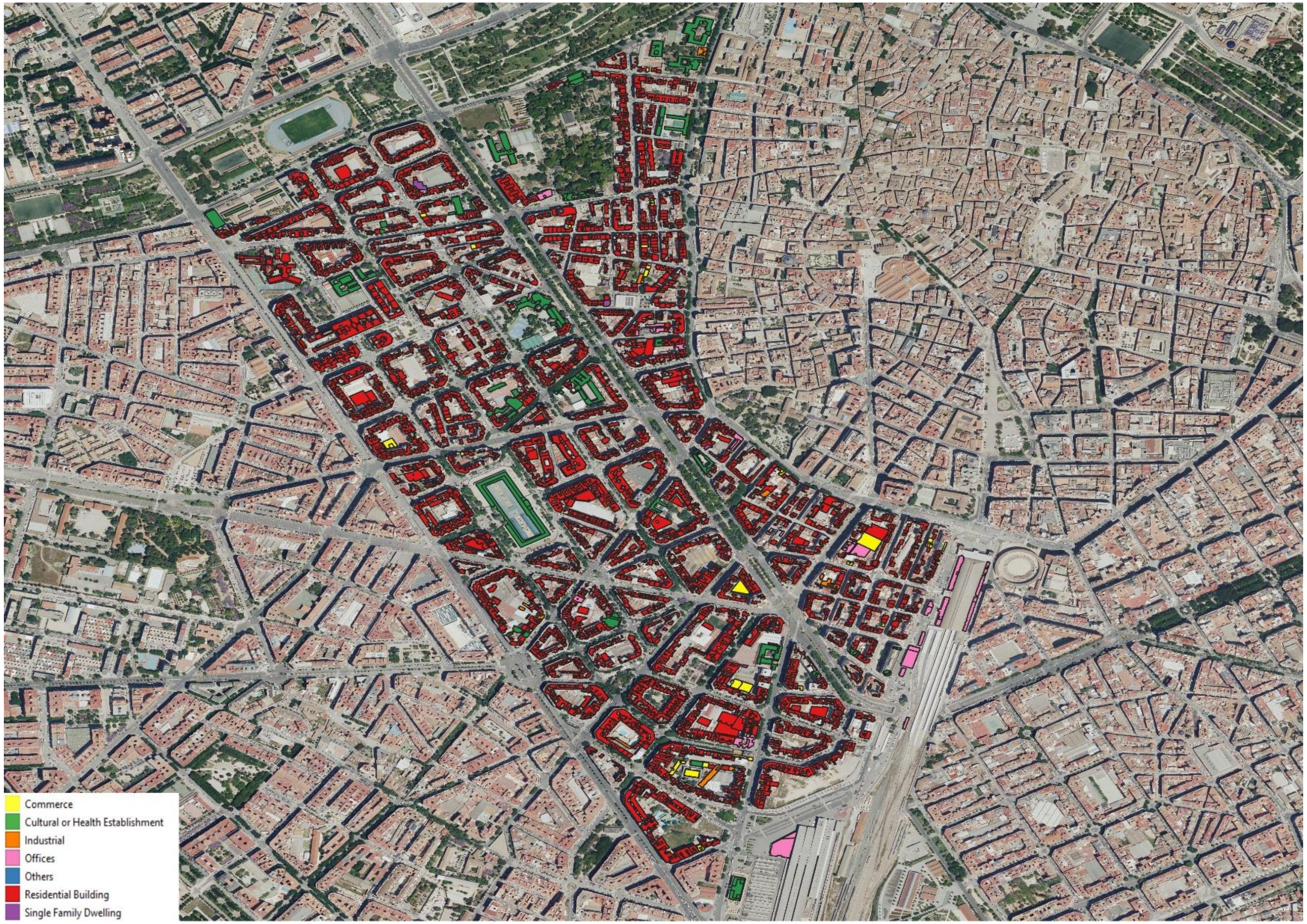

***Figure 45**: District EXTRAMUS per Current Use.*

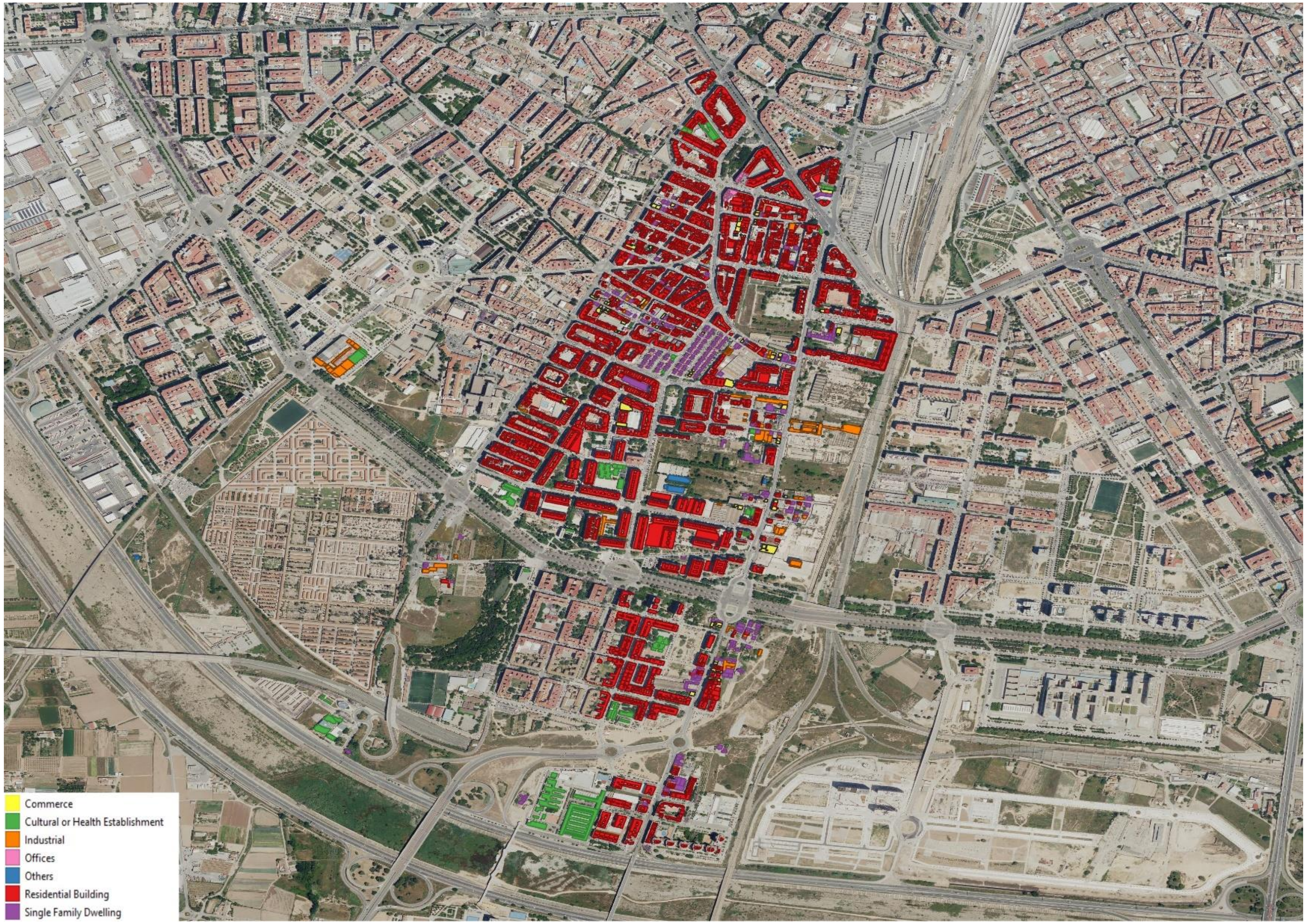

***Figure 46**: District JESUS per Current Use.*

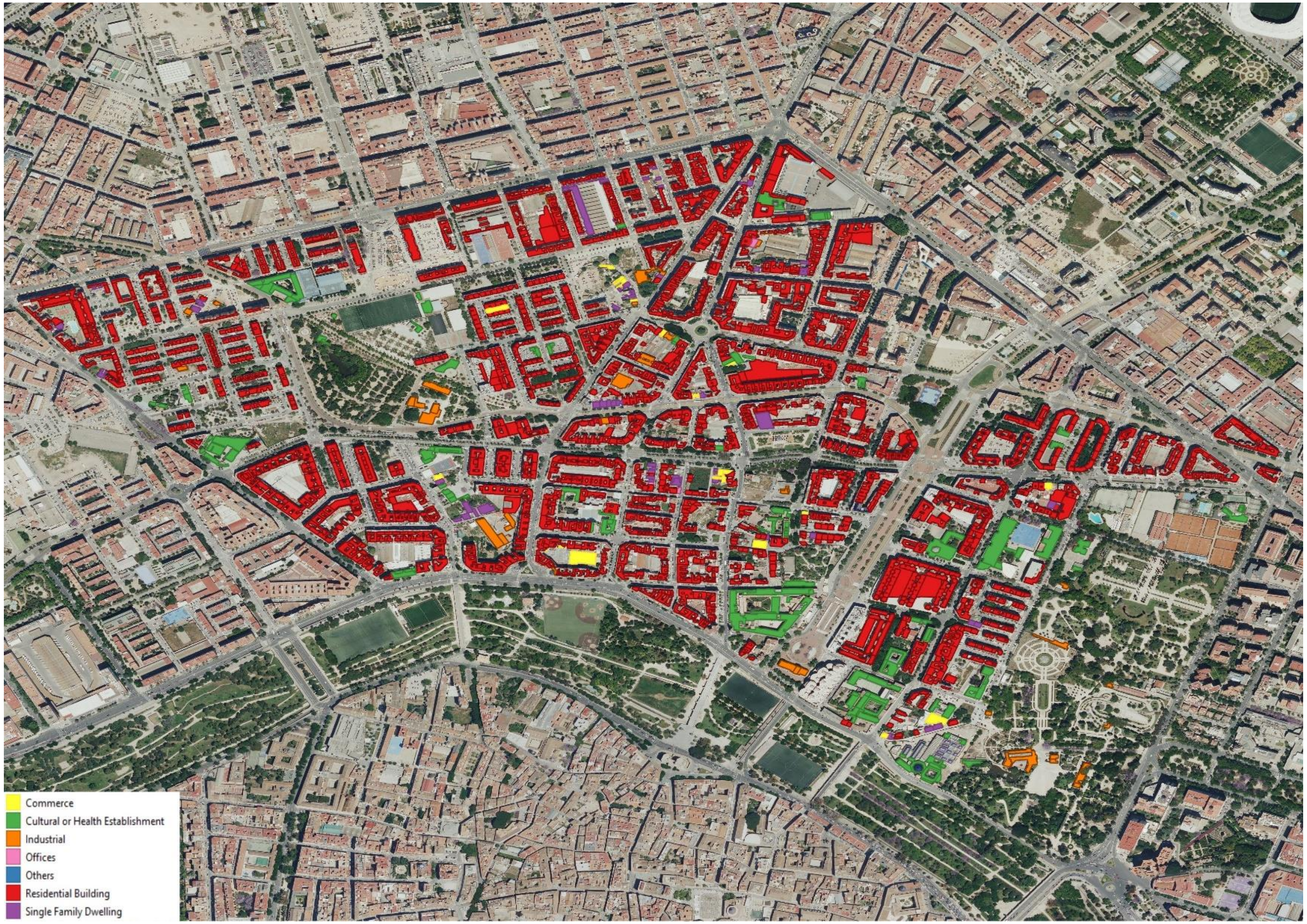

***Figure 47**: District LA SAIDIA per Current Use.*

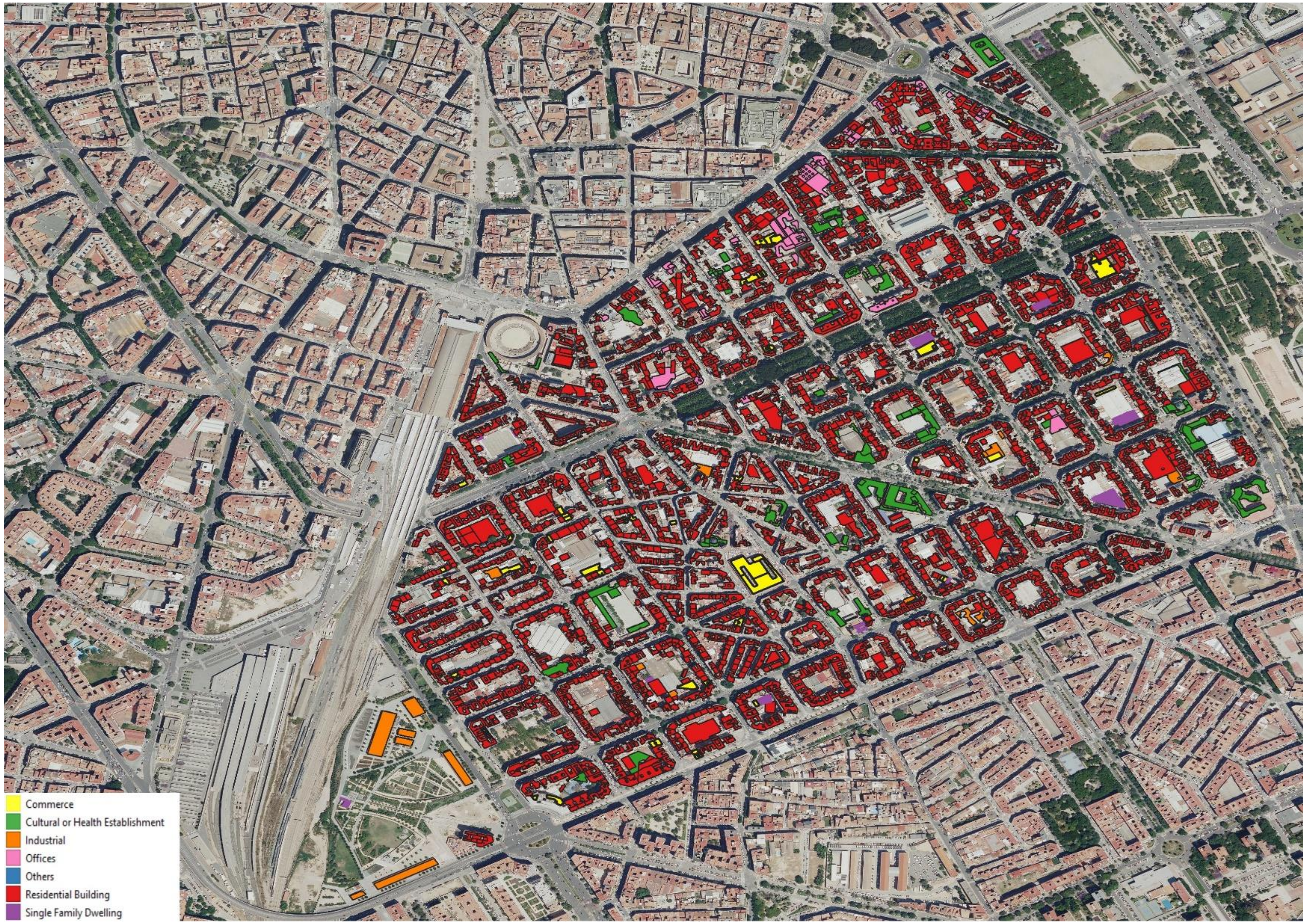

***Figure 48**: District L'EIXAMPLE per Current Use.*

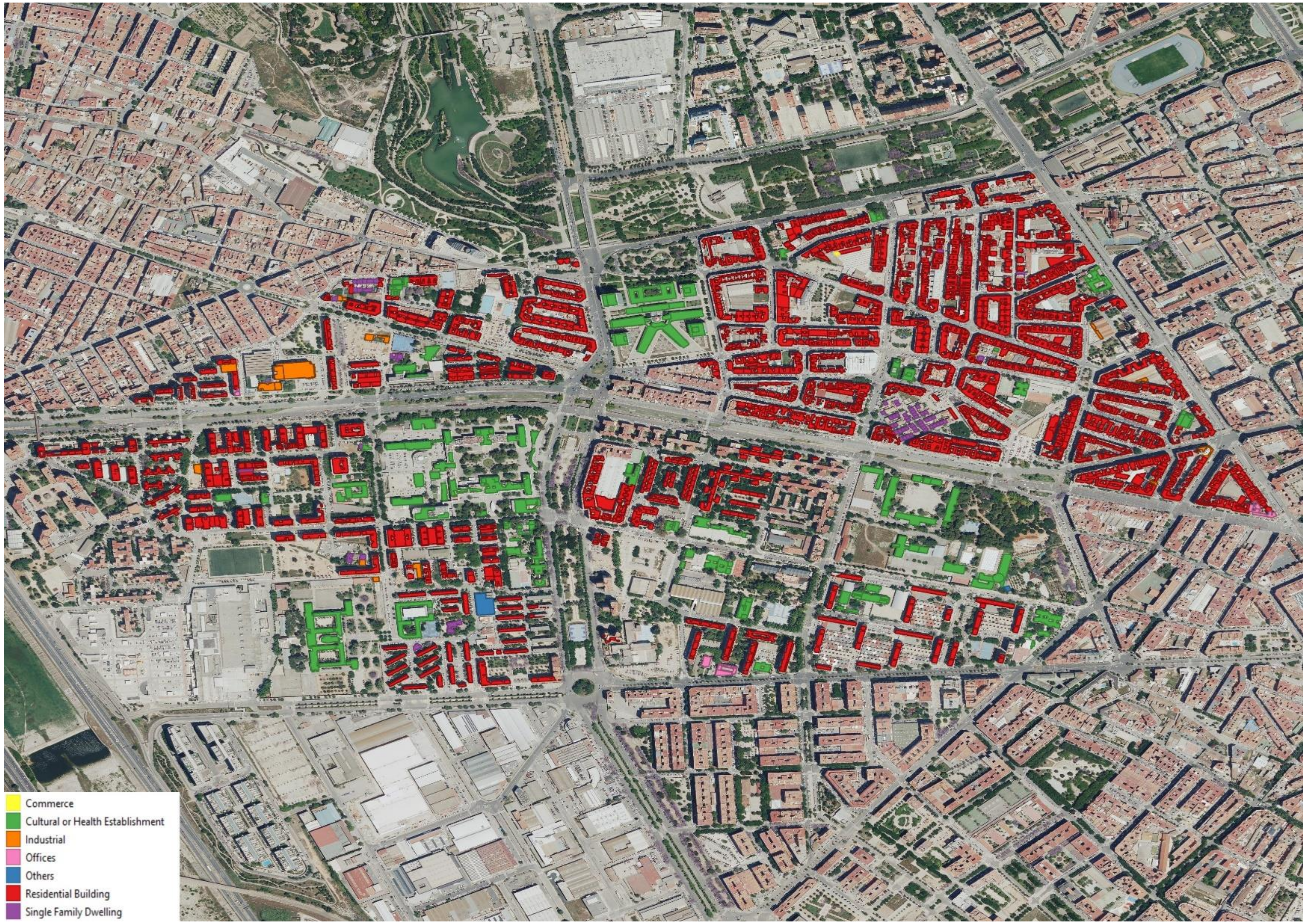

***Figure 49**: District L'OLIVERETA per Current Use.*

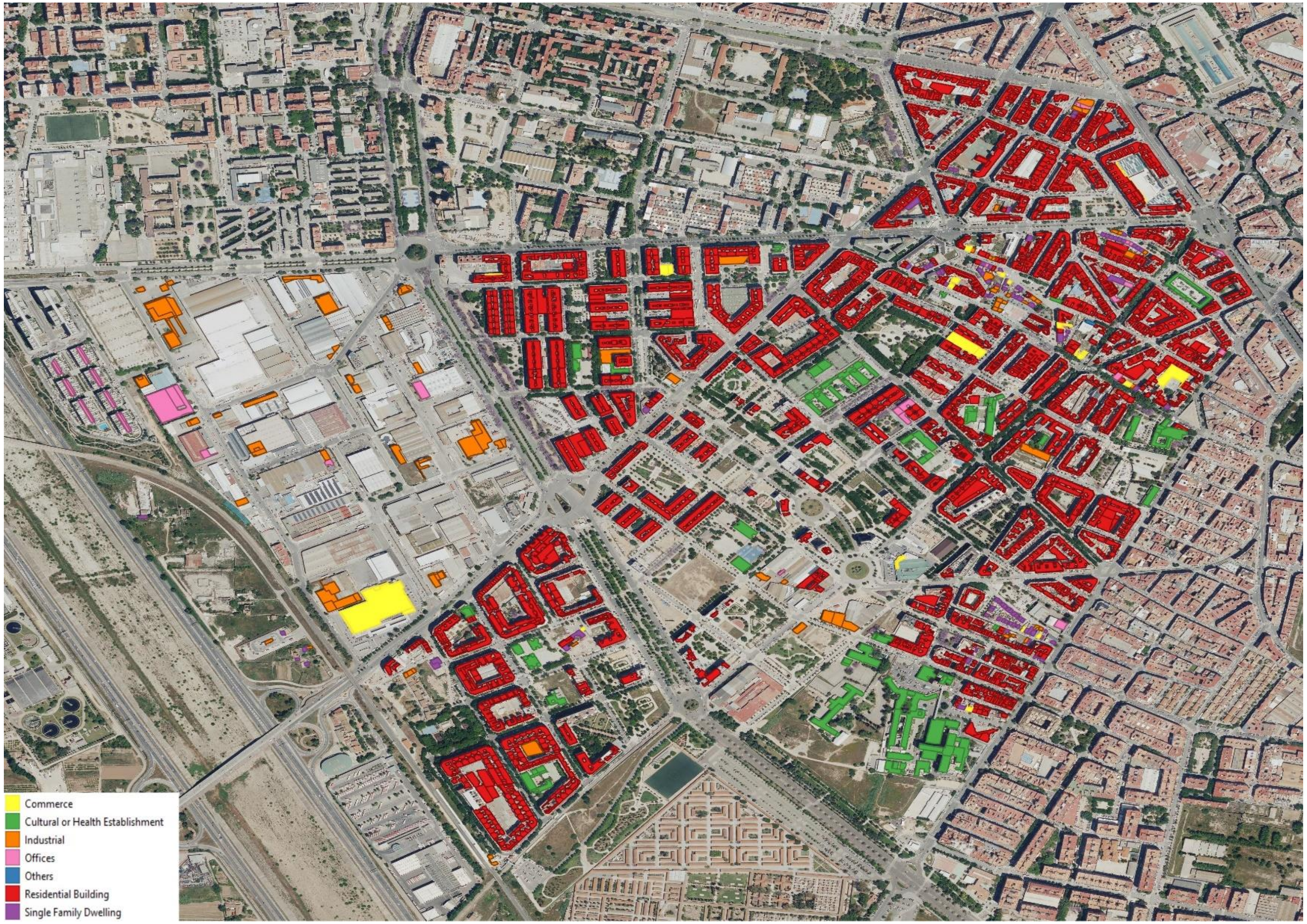

***Figure 50**: District PATRAIX per Current Use.*

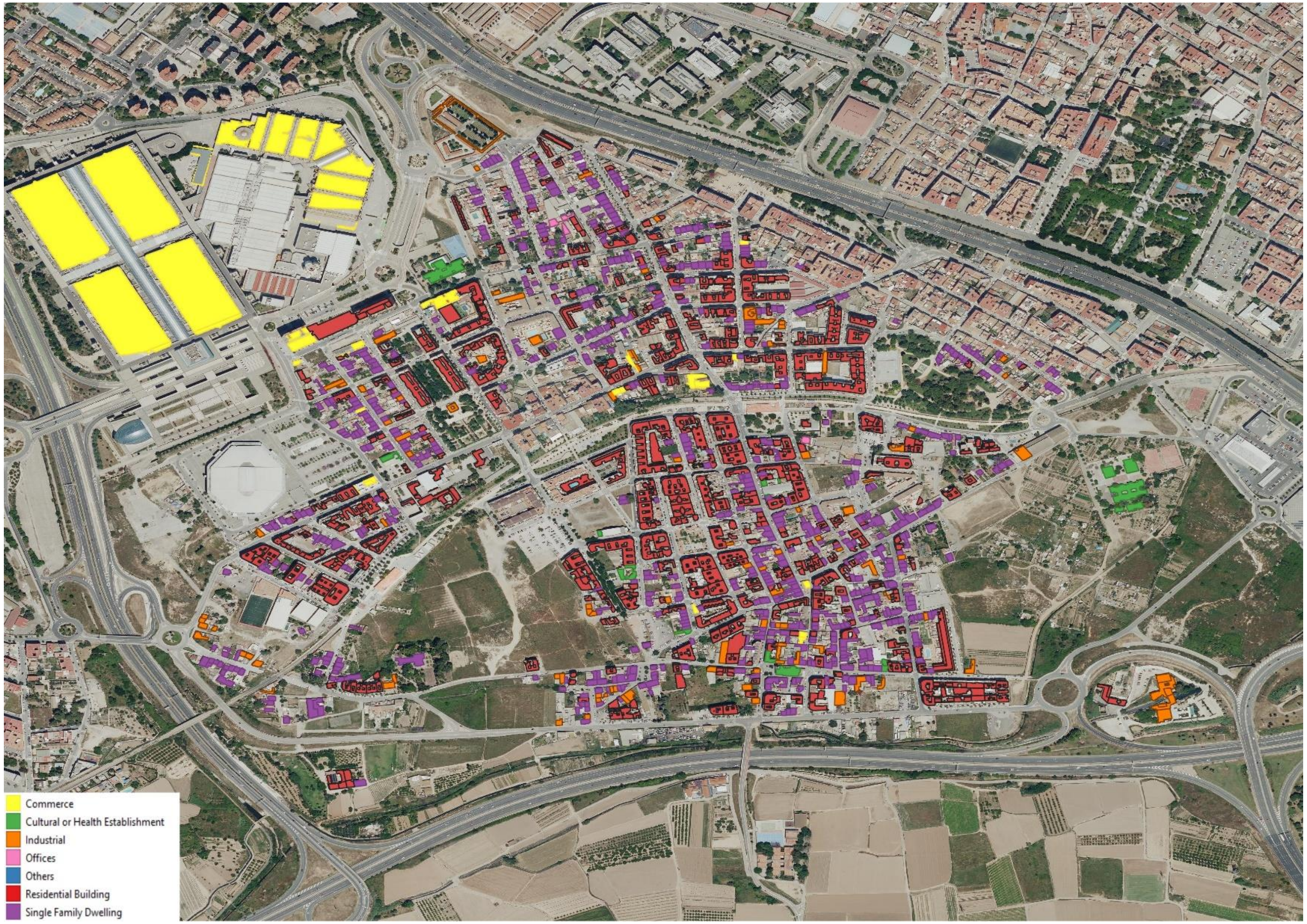

***Figure 51**: District POBLATS DE L'OEST per Current Use.*

***Figure 52**: District POBLATS MARITIMS part 1 per Current Use.*

***Figure 53**: District POBLATS MARITIMS part 2 per Current Use.*

***Figure 54**: District QUATRE CARRERES per Current Use.*

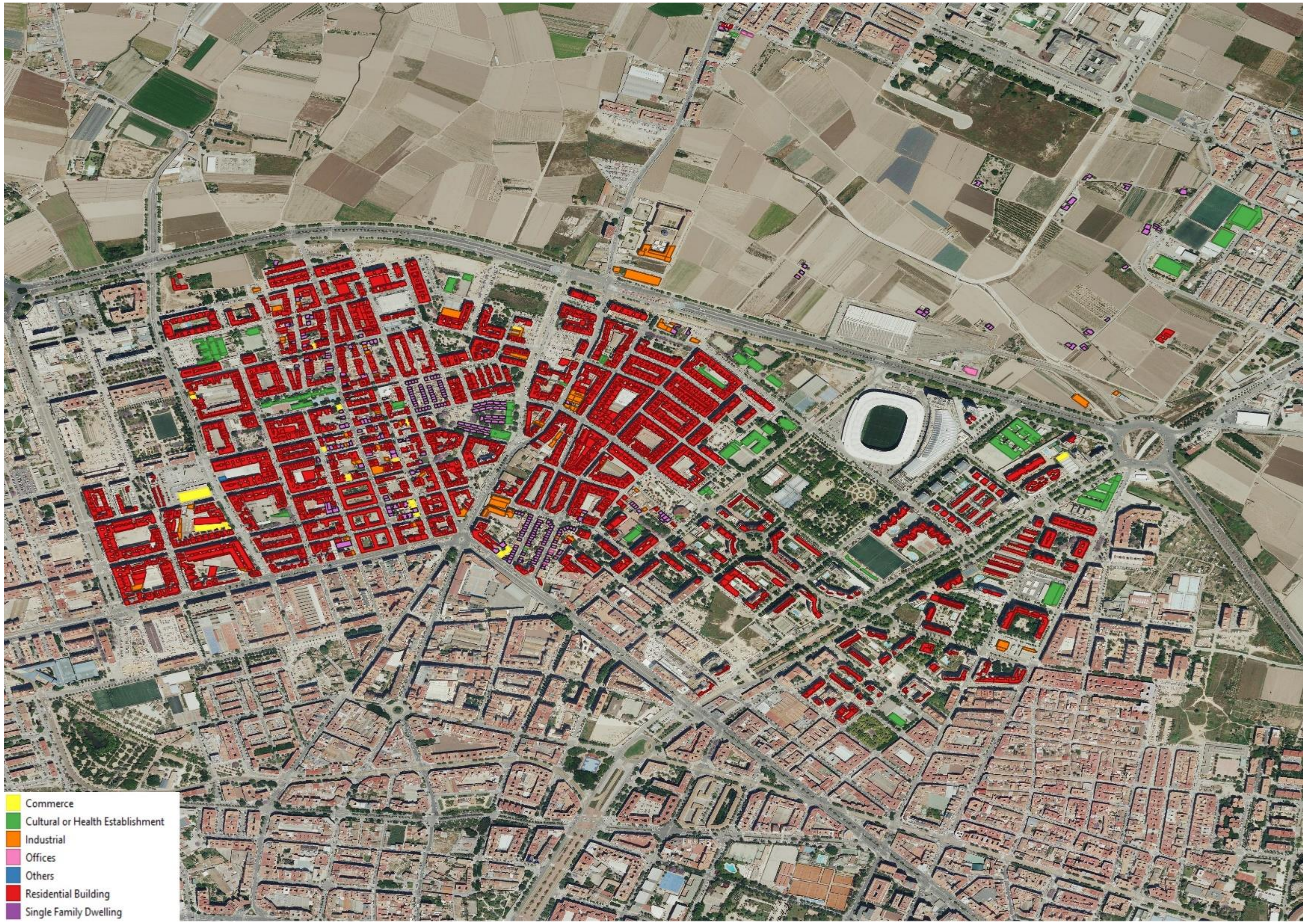

Figure 55*: District RASCANYA per Current Use.*

ENERGY SAVINGS, CO_2 REDUCTION AND SEQUESTRATION

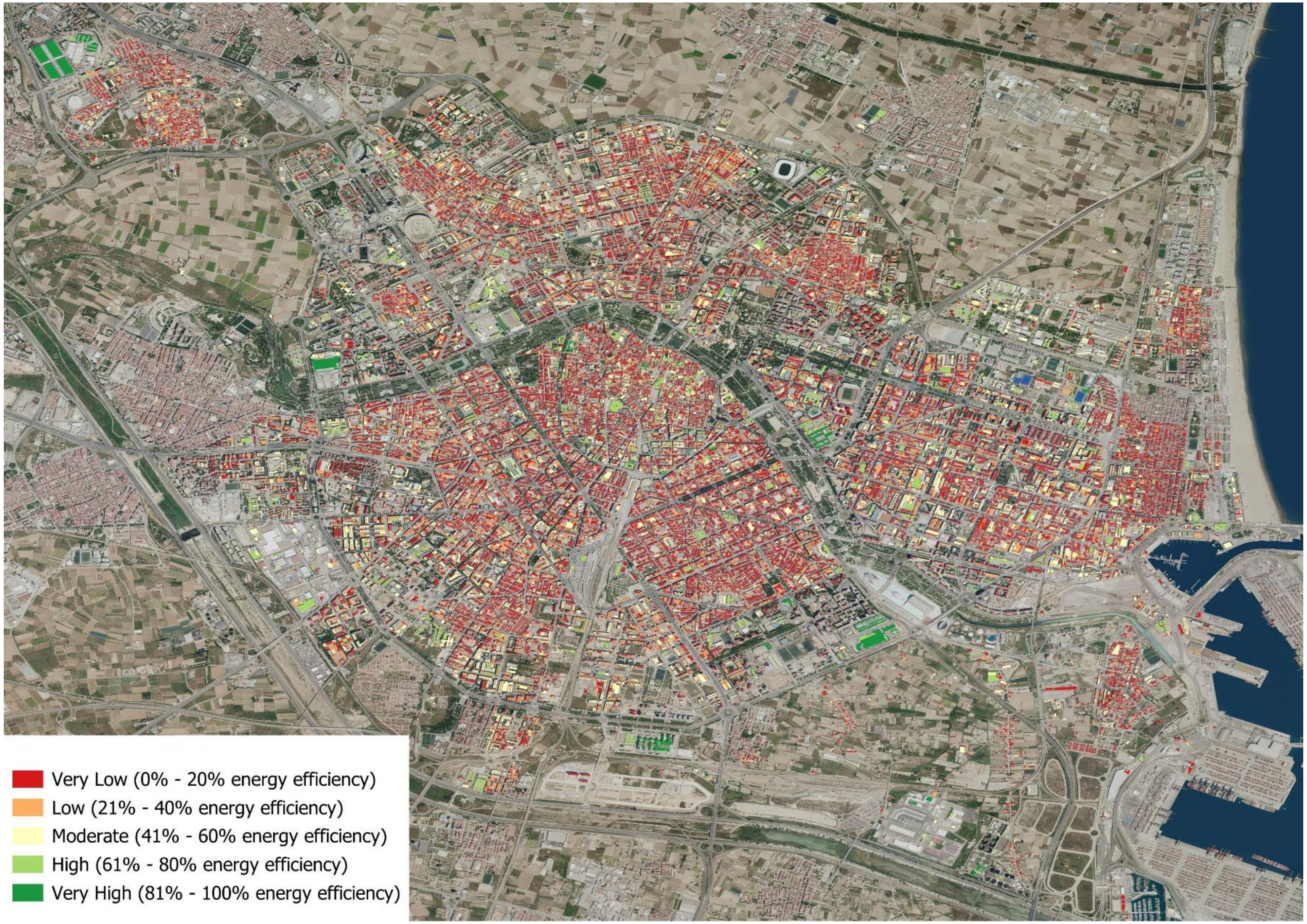

***Figure 56**: Percentage distribution of energy savings and reduction of CO_2 emissions in the city of Valencia.*

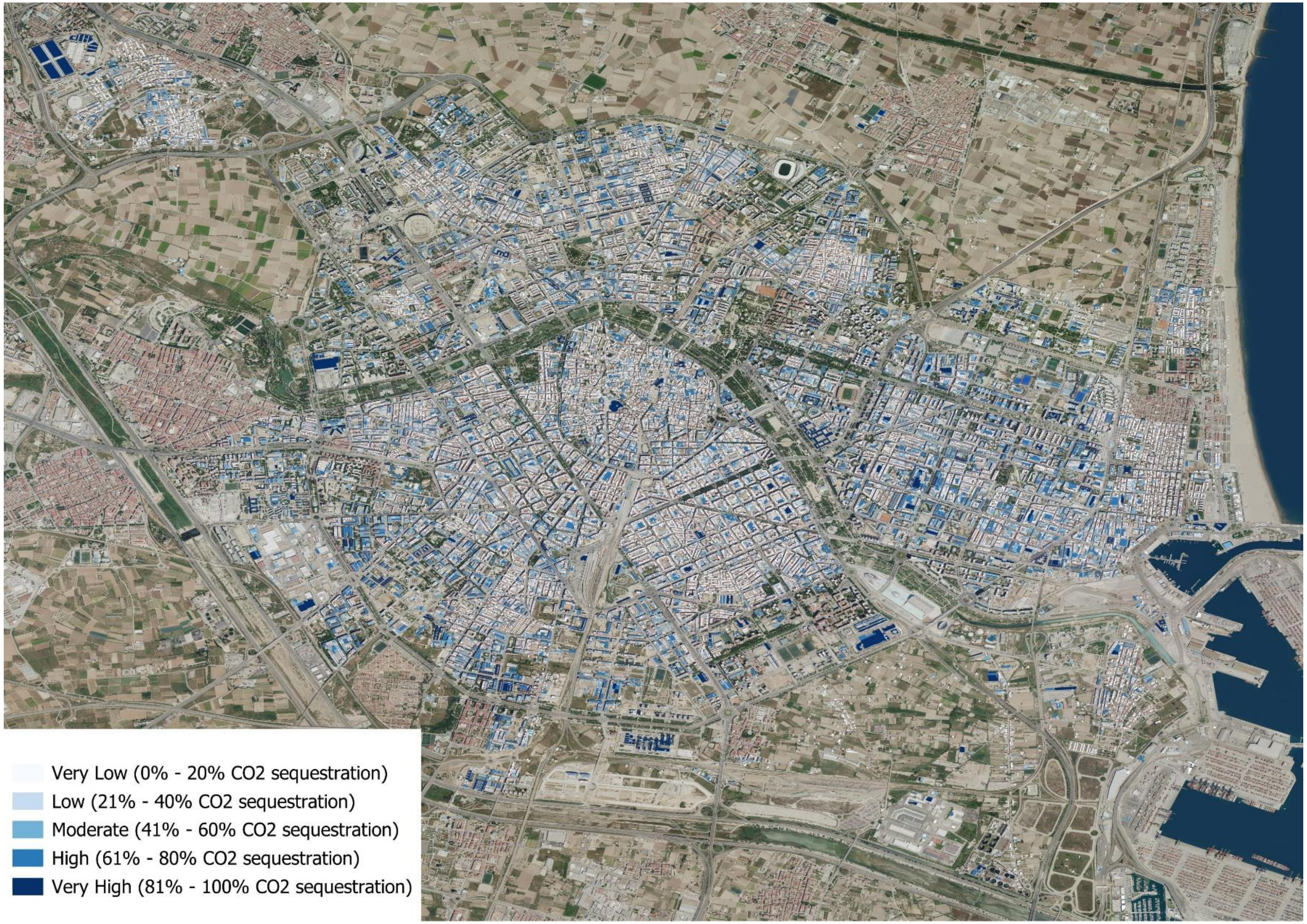

Figure 57: *Percentage distribution of CO_2 sequestration in the city of Valencia.*

TABLES

DISTRICTS AND NEIGHBORHOODS

Table 21: Districts considered in this study and their constituent neighbourhoods.

Districts	Neighborhoods
ALGIROS	LA CARRASCA
ALGIROS	L'AMISTAT
ALGIROS	LA VEGA BAIXA
ALGIROS	CIUTAT JARDI
ALGIROS	L'ILLA PERDUDA
BENICALAP	CIUTAT FALLERA
BENICALAP	BENICALAP
BENIMACLET	CAMI DE VERA
BENIMACLET	BENIMACLET
CAMINS AL GRAU	PENYA-ROJA
CAMINS AL GRAU	CAMI FONDO
CAMINS AL GRAU	ALBORS
CAMINS AL GRAU	LA CREU DEL GRAU
CAMINS AL GRAU	AIORA
CAMPANAR	SANT PAU
CAMPANAR	CAMPANAR
CAMPANAR	EL CALVARI
CAMPANAR	LES TENDETES
CIUTAT VELLA	EL PILAR
CIUTAT VELLA	EL CARME
CIUTAT VELLA	SANT FRANCESC
CIUTAT VELLA	EL MERCAT
CIUTAT VELLA	LA SEU
CIUTAT VELLA	LA XEREA
EL PLA DEL REAL	EXPOSICIO
EL PLA DEL REAL	JAUME ROIG
EL PLA DEL REAL	MESTALLA
EL PLA DEL REAL	CIUTAT UNIVERSITARIA
EXTRAMURS	LA PETXINA
EXTRAMURS	ARRANCAPINS
EXTRAMURS	EL BOTANIC
EXTRAMURS	LA ROQUETA
JESUS	CAMI REAL
JESUS	L'HORT DE SENABRE
JESUS	LA RAIOSA
JESUS	SANT MARCEL
JESUS	LA CREU COBERTA
LA SAIDIA	MARXALENES
LA SAIDIA	TORMOS

LA SAIDIA	MORVEDRE
LA SAIDIA	SANT ANTONI
LA SAIDIA	TRINITAT
L'EIXAMPLE	RUSSAFA
L'EIXAMPLE	EL PLA DEL REMEI
L'EIXAMPLE	LA GRAN VIA
L'OLIVERETA	LA LLUM
L'OLIVERETA	SOTERNES
L'OLIVERETA	LA FONTSANTA
L'OLIVERETA	NOU MOLES
L'OLIVERETA	TRES FORQUES
PATRAIX	VARA DE QUART
PATRAIX	SANT ISIDRE
PATRAIX	SAFRANAR
PATRAIX	FAVARA
PATRAIX	PATRAIX
POBLATS DE L'OEST	BENIFERRI
POBLATS DE L'OEST	BENIMAMET
POBLATS MARITIMS	EL GRAU
POBLATS MARITIMS	CABANYAL-CANYAMELAR
POBLATS MARITIMS	LA MALVA-ROSA
POBLATS MARITIMS	NATZARET
POBLATS MARITIMS	BETERO
QUATRE CARRERES	LA PUNTA
QUATRE CARRERES	MALILLA
QUATRE CARRERES	EN CORTS
QUATRE CARRERES	NA ROVELLA
QUATRE CARRERES	MONTOLIVET
QUATRE CARRERES	LA FONTETA S
QUATRE CARRERES	CIUTAT DE LES ARTS I DE LES CIENCIES
RASCANYA	SANT LLORENS
RASCANYA	TORREFIEL
RASCANYA	ELS ORRIOLS

RESULTS OBTAINED FOR VALENCIA'S NEIGHBORHOODS

Table 22: Distribution of building current use according to the neighbourhoods considered in this study.

Current Use / Neighborhood	Residential Building (less 4 floor)	Residential Building (over 4 floors)	Cultural or Health Establishment	Single Family Dwelling	Industrial	Commerce	Offices	Others	Total Buildings
AIORA	33	455	15	56	29	19	2	0	0
ALBORS	17	209	9	9	6	7	0	0	0
ARRANCAPINS	21	584	10	1	7	11	4	0	0
BENICALAP	105	643	21	150	38	11	1	1	0
BENIFERRI	12	4	6	22	5	3	0	0	0
BENIMACLET	124	528	17	147	9	38	2	0	0
BENIMAMET	138	282	10	577	89	17	2	0	0
BETERO	30	131	3	29	0	3	0	0	0
CABANYAL-CANYAMELAR	356	435	29	539	120	53	11	0	0
CAMI DE VERA	5	62	2	22	4	0	0	0	0
CAMI FONDO	3	73	1	37	6	3	2	0	0
CAMI REAL	4	45	5	47	15	6	0	0	0
CAMPANAR	25	166	13	113	8	13	7	0	0
CIUTAT DE LES ARTS I DE LES CIENCIES	0	10	4	0	0	2	1	0	0
CIUTAT FALLERA	1	55	6	2	18	11	2	0	0
CIUTAT JARDI	0	165	8	5	0	7	7	0	0
CIUTAT UNIVERSITARIA	1	19	11	2	1	3	0	0	0
EL BOTANIC	44	301	12	1	2	5	4	0	0
EL CALVARI	0	67	0	0	0	0	0	0	0
EL CARME	63	302	37	2	8	8	8	0	0
EL GRAU	28	199	40	3	44	4	10	1	1
EL MERCAT	17	198	14	0	5	15	4	0	0
EL PILAR	23	207	10	2	0	4	2	0	0
EL PLA DEL REMEI	2	352	12	0	0	4	25	0	0
ELS ORRIOLS	6	243	7	82	13	1	2	0	0
EN CORTS	68	287	3	88	16	5	1	1	0
EXPOSICIO	2	155	10	1	3	0	4	0	0
FAVARA	8	81	6	30	8	3	1	0	0
JAUME ROIG	1	44	1	0	0	0	0	0	0
LA CARRASCA	6	32	21	31	2	0	0	0	0
LA CREU COBERTA	9	68	3	31	17	10	0	0	0
LA CREU DEL GRAU	7	182	2	6	12	12	1	2	0
LA FONTETA S	2	15	1	5	1	0	0	0	0
LA FONTSANTA	0	47	8	2	2	0	0	1	0

LA GRAN VIA	1	447	10	4	4	6	2	0	0
LA LLUM	0	68	4	4	2	0	0	0	0
LA MALVA-ROSA	81	200	10	74	8	10	0	0	0
LA PETXINA	36	410	8	2	0	5	0	0	0
LA PUNTA	23	28	3	315	70	4	3	0	1
LA RAIOSA	32	344	3	25	3	13	2	0	0
LA ROQUETA	24	229	3	1	2	6	5	0	0
LA SEU	19	216	40	0	0	6	6	0	0
LA VEGA BAIXA	1	106	4	0	3	3	0	0	0
LA XEREA	19	229	30	0	2	12	11	0	0
L'AMISTAT	0	176	3	2	0	0	0	0	0
LES TENDETES	13	136	6	0	1	2	0	0	0
L'HORT DE SENABRE	4	235	6	116	9	20	1	0	0
L'ILLA PERDUDA	1	147	7	2	1	1	0	0	0
MALILLA	1	225	12	28	17	2	0	0	0
MARXALENES	1	234	6	10	6	1	0	0	0
MESTALLA	6	241	17	1	4	3	13	0	0
MONTOLIVET	29	500	10	34	7	1	0	0	0
MORVEDRE	51	238	7	16	5	6	2	0	0
NA ROVELLA	25	74	7	10	2	7	2	0	0
NATZARET	95	152	18	153	41	14	1	0	0
NOU MOLES	35	503	9	45	5	1	1	0	0
PATRAIX	48	418	10	42	23	12	8	0	0
PENYA-ROJA	3	67	3	4	4	6	0	1	0
RUSSAFA	100	949	14	6	13	21	3	0	0
SAFRANAR	0	102	4	0	2	1	3	0	0
SANT ANTONI	5	145	7	5	2	3	1	0	0
SANT FRANCESC	5	281	15	1	4	24	63	0	0
SANT ISIDRE	1	107	4	3	5	1	0	0	0
SANT LLORENS	4	53	11	21	4	1	2	0	0
SANT MARCEL	4	65	3	7	0	3	0	0	0
SANT PAU	1	67	18	30	14	4	1	0	0
SOTERNES	2	101	3	7	6	0	1	0	0
TORMOS	4	202	4	10	3	5	0	0	0
TORREFIEL	32	491	9	148	39	13	0	1	0
TRES FORQUES	19	72	11	0	0	0	1	1	0
TRINITAT	9	163	14	6	1	3	0	0	0
VARA DE QUART	0	101	3	6	28	4	5	0	0

***Table 23**: Distribution of Total Potential Roof Area for intervention in the city of Valencia by neighbourhoods considered in the study. Percentage of representation with respect to 6,246,173 m^2 of surface area to be intervened.*

Neighborhood	Total Potential Area [m^2]	Representation [%]
AIORA	189,839	3.04%
ALBORS	85,253	1.36%
ARRANCAPINS	170,304	2.73%
BENICALAP	261,828	4.19%
BENIFERRI	21,959	0.35%
BENIMACLET	194,377	3.11%
BENIMAMET	243,283	3.89%
BETERO	52,263	0.84%
CABANYAL-CANYAMELAR	209,600	3.36%
CAMI DE VERA	40,596	0.65%
CAMI FONDO	37,303	0.60%
CAMI REAL	44,620	0.71%
CAMPANAR	116,618	1.87%
CIUTAT DE LES ARTS I DE LES CIENCIES	46,694	0.75%
CIUTAT FALLERA	44,786	0.72%
CIUTAT JARDI	76,598	1.23%
CIUTAT UNIVERSITARIA	28,087	0.45%
EL BOTANIC	70,212	1.12%
EL CALVARI	21,709	0.35%
EL CARME	80,274	1.29%
EL GRAU	159,611	2.56%
EL MERCAT	51,416	0.82%
EL PILAR	47,156	0.75%
EL PLA DEL REMEI	102,013	1.63%
ELS ORRIOLS	81,812	1.31%
EN CORTS	76,127	1.22%
EXPOSICIO	66,414	1.06%
FAVARA	43,882	0.70%
JAUME ROIG	15,568	0.25%
LA CARRASCA	118,513	1.90%
LA CREU COBERTA	55,443	0.89%
LA CREU DEL GRAU	97,496	1.56%
LA FONTETA S	5,511	0.09%
LA FONTSANTA	42,069	0.67%
LA GRAN VIA	103,654	1.66%
LA LLUM	28,249	0.45%

LA MALVA-ROSA	83,632	1.34%
LA PETXINA	107,163	1.72%
LA PUNTA	109,902	1.76%
LA RAIOSA	100,471	1.61%
LA ROQUETA	45,126	0.72%
LA SEU	66,599	1.07%
LA VEGA BAIXA	57,404	0.92%
LA XEREA	79,167	1.27%
L'AMISTAT	47,337	0.76%
LES TENDETES	40,098	0.64%
L'HORT DE SENABRE	100,570	1.61%
L'ILLA PERDUDA	61,254	0.98%
MALILLA	161,895	2.59%
MARXALENES	72,073	1.15%
MESTALLA	122,758	1.97%
MONTOLIVET	125,700	2.01%
MORVEDRE	69,755	1.12%
NA ROVELLA	45,678	0.73%
NATZARET	72,688	1.16%
NOU MOLES	155,986	2.50%
PATRAIX	166,076	2.66%
PENYA-ROJA	53,881	0.86%
RUSSAFA	217,439	3.48%
SAFRANAR	57,896	0.93%
SANT ANTONI	49,410	0.79%
SANT FRANCESC	104,571	1.67%
SANT ISIDRE	56,484	0.90%
SANT LLORENS	64,841	1.04%
SANT MARCEL	33,665	0.54%
SANT PAU	102,234	1.64%
SOTERNES	35,486	0.57%
TORMOS	49,130	0.79%
TORREFIEL	179,077	2.87%
TRES FORQUES	47,260	0.76%
TRINITAT	71,506	1.14%
VARA DE QUART	100,828	1.61%

Table 24: Distribution of energy savings, emission reductions and total percentage variations in the city of Valencia by neighbourhoods considered in the study.

Neighborhood	Energy Saving [kWh/year]	CO_2 Emissions Reduction [kg CO_2/year]	Decrease Neighborhood [%]	Decrease Total [%]	Representation [%]
AIORA	3,494,698	711,626	1.52%	0.04%	2.16%
ALBORS	1,777,733	375,347	1.70%	0.02%	1.10%
ARRANCAPINS	3,511,139	715,595	1.24%	0.04%	2.17%
BENICALAP	5,598,546	1,121,907	1.56%	0.06%	3.46%
BENIFERRI	1,436,215	262,569	3.75%	0.02%	0.89%
BENIMACLET	4,281,650	877,075	1.61%	0.05%	2.64%
BENIMAMET	5,870,512	1,206,327	3.04%	0.06%	3.62%
BETERO	1,004,400	203,981	1.49%	0.01%	0.62%
CABANYAL-CANYAMELAR	5,506,450	1,097,528	3.04%	0.06%	3.40%
CAMI DE VERA	809,632	177,243	1.48%	0.01%	0.50%
CAMI FONDO	776,206	155,204	1.74%	0.01%	0.48%
CAMI REAL	1,382,845	274,361	2.62%	0.01%	0.85%
CAMPANAR	4,180,277	807,224	2.13%	0.05%	2.58%
CIUTAT DE LES ARTS I DE LES CIENCIES	3,072,018	696,906	3.53%	0.03%	1.90%
CIUTAT FALLERA	970,193	184,915	2.07%	0.01%	0.60%
CIUTAT JARDI	1,354,080	286,223	0.99%	0.01%	0.84%
CIUTAT UNIVERSITARIA	1,846,826	328,452	2.58%	0.02%	1.14%
EL BOTANIC	2,124,356	441,045	2.19%	0.02%	1.31%
EL CALVARI	428,456	89,427	1.08%	0.00%	0.26%
EL CARME	2,546,751	518,839	2.30%	0.03%	1.57%
EL GRAU	4,176,087	836,145	1.08%	0.05%	2.58%
EL MERCAT	1,408,373	288,215	2.15%	0.02%	0.87%
EL PILAR	1,250,719	255,156	1.98%	0.01%	0.77%
EL PLA DEL REMEI	3,588,873	780,997	1.95%	0.04%	2.22%
ELS ORRIOLS	1,677,631	345,975	1.59%	0.02%	1.04%
EN CORTS	1,899,361	377,501	1.66%	0.02%	1.17%
EXPOSICIO	2,810,654	518,373	2.27%	0.03%	1.74%
FAVARA	1,176,214	242,790	2.61%	0.01%	0.73%
JAUME ROIG	399,395	80,658	0.72%	0.00%	0.25%
LA CARRASCA	4,149,814	829,511	1.95%	0.04%	2.56%
LA CREU COBERTA	1,066,972	207,747	1.59%	0.01%	0.66%
LA CREU DEL GRAU	1,790,516	357,089	1.28%	0.02%	1.11%
LA FONTETA S	159,756	31,891	2.05%	0.00%	0.10%
LA FONTSANTA	1,164,334	218,149	2.43%	0.01%	0.72%

LA GRAN VIA	2,280,259	465,195	1.30%	0.02%	1.41%
LA LLUM	484,076	98,160	1.08%	0.01%	0.30%
LA MALVA-ROSA	1,995,762	398,298	1.85%	0.02%	1.23%
LA PETXINA	2,328,163	475,051	1.37%	0.03%	1.44%
LA PUNTA	4,679,183	918,534	4.15%	0.05%	2.89%
LA RAIOSA	2,148,836	442,182	1.42%	0.02%	1.33%
LA ROQUETA	1,466,348	310,877	1.66%	0.02%	0.91%
LA SEU	2,744,058	573,645	2.94%	0.03%	1.69%
LA VEGA BAIXA	973,660	199,877	1.31%	0.01%	0.60%
LA XEREA	2,854,874	593,099	2.56%	0.03%	1.76%
L'AMISTAT	892,602	184,162	1.23%	0.01%	0.55%
LES TENDETES	761,562	152,734	1.44%	0.01%	0.47%
L'HORT DE SENABRE	2,063,204	420,952	1.40%	0.02%	1.27%
L'ILLA PERDUDA	989,531	200,411	1.28%	0.01%	0.61%
MALILLA	3,945,923	740,601	1.60%	0.04%	2.44%
MARXALENES	1,465,208	293,446	1.42%	0.02%	0.90%
MESTALLA	3,563,838	704,930	1.61%	0.04%	2.20%
MONTOLIVET	2,608,358	540,665	1.43%	0.03%	1.61%
MORVEDRE	1,652,558	333,902	1.60%	0.02%	1.02%
NA ROVELLA	1,484,992	284,743	2.42%	0.02%	0.92%
NATZARET	1,683,002	335,961	2.66%	0.02%	1.04%
NOU MOLES	3,315,612	659,891	1.32%	0.04%	2.05%
PATRAIX	3,101,687	630,109	1.30%	0.03%	1.92%
PENYA-ROJA	2,212,527	420,445	1.16%	0.02%	1.37%
RUSSAFA	5,166,020	1,062,153	1.54%	0.06%	3.19%
SAFRANAR	1,149,057	231,842	1.31%	0.01%	0.71%
SANT ANTONI	816,042	167,406	1.06%	0.01%	0.50%
SANT FRANCESC	6,793,849	1,429,118	2.58%	0.07%	4.20%
SANT ISIDRE	950,819	199,224	1.14%	0.01%	0.59%
SANT LLORENS	1,476,932	289,406	1.25%	0.02%	0.91%
SANT MARCEL	592,709	121,714	1.33%	0.01%	0.37%
SANT PAU	3,948,716	787,729	2.23%	0.04%	2.44%
SOTERNES	853,871	168,751	1.71%	0.01%	0.53%
TORMOS	938,925	194,455	1.23%	0.01%	0.58%
TORREFIEL	3,420,774	706,880	1.55%	0.04%	2.11%
TRES FORQUES	930,267	179,983	1.93%	0.01%	0.57%
TRINITAT	1,656,355	321,666	1.71%	0.02%	1.02%
VARA DE QUART	2,869,184	571,021	2.29%	0.03%	1.77%

***Table 25**: Distribution of CO_2 sequestration in the city of Valencia by neighbourhoods considered in the study.*

Neighborhood	CO_2 Emissions Captured [kg CO_2/year]	Representation [%]
AIORA	592,899	3.04%
ALBORS	266,260	1.36%
ARRANCAPINS	531,889	2.73%
BENICALAP	817,734	4.19%
BENIFERRI	68,581	0.35%
BENIMACLET	607,071	3.11%
BENIMAMET	759,814	3.89%
BETERO	163,226	0.84%
CABANYAL-CANYAMELAR	654,615	3.36%
CAMI DE VERA	126,787	0.65%
CAMI FONDO	116,505	0.60%
CAMI REAL	139,355	0.71%
CAMPANAR	364,218	1.87%
CIUTAT DE LES ARTS I DE LES CIENCIES	145,834	0.75%
CIUTAT FALLERA	139,874	0.72%
CIUTAT JARDI	239,229	1.23%
CIUTAT UNIVERSITARIA	87,721	0.45%
EL BOTANIC	219,284	1.12%
EL CALVARI	67,799	0.35%
EL CARME	250,710	1.29%
EL GRAU	498,493	2.56%
EL MERCAT	160,581	0.82%
EL PILAR	147,275	0.75%
EL PLA DEL REMEI	318,605	1.63%
ELS ORRIOLS	255,512	1.31%
EN CORTS	237,758	1.22%
EXPOSICIO	207,421	1.06%
FAVARA	137,049	0.70%
JAUME ROIG	48,620	0.25%
LA CARRASCA	370,136	1.90%
LA CREU COBERTA	173,159	0.89%
LA CREU DEL GRAU	304,498	1.56%
LA FONTETA S	17,211	0.09%
LA FONTSANTA	131,388	0.67%
LA GRAN VIA	323,729	1.66%
LA LLUM	88,227	0.45%
LA MALVA-ROSA	261,196	1.34%
LA PETXINA	334,688	1.72%

LA PUNTA	343,241	1.76%
LA RAIOSA	313,787	1.61%
LA ROQUETA	140,935	0.72%
LA SEU	208,001	1.07%
LA VEGA BAIXA	179,283	0.92%
LA XEREA	247,252	1.27%
L'AMISTAT	147,843	0.76%
LES TENDETES	125,234	0.64%
L'HORT DE SENABRE	314,096	1.61%
L'ILLA PERDUDA	191,305	0.98%
MALILLA	505,626	2.59%
MARXALENES	225,096	1.15%
MESTALLA	383,395	1.97%
MONTOLIVET	392,584	2.01%
MORVEDRE	217,856	1.12%
NA ROVELLA	142,661	0.73%
NATZARET	227,018	1.16%
NOU MOLES	487,169	2.50%
PATRAIX	518,685	2.66%
PENYA-ROJA	168,280	0.86%
RUSSAFA	679,098	3.48%
SAFRANAR	180,818	0.93%
SANT ANTONI	154,315	0.79%
SANT FRANCESC	326,592	1.67%
SANT ISIDRE	176,410	0.90%
SANT LLORENS	202,510	1.04%
SANT MARCEL	105,142	0.54%
SANT PAU	319,295	1.64%
SOTERNES	110,828	0.57%
TORMOS	153,441	0.79%
TORREFIEL	559,287	2.87%
TRES FORQUES	147,600	0.76%
TRINITAT	223,326	1.14%
VARA DE QUART	314,902	1.61%

APPLICATION OF DECISION METHODOLOGY (AHP)

Table 26: Quantities considered for criteria decision methodology.

Districts	Current Use	Urban intervention factor per use [m^2/buildings]	Urban intervention factor per districts [m^2/buildings]	Energy Saving [kWh/year]	CO_2 mitigation [kg CO_2/year]
ALGIROS	Residential Building	437	485	4,222,234	1,742,321
ALGIROS	Cultural or Health Establishment	1,318	485	3,435,291	849,019
ALGIROS	Single Family Dwelling	254	485	293,877	92,147
ALGIROS	Industrial	951	485	116,583	42,369
ALGIROS	Commerce	762	485	218,305	74,335
ALGIROS	Offices	260	485	72,821	23,365
ALGIROS	Others	462	485	577	4,425
BENICALAP	Residential Building	314	288	4,287,837	1,674,728
BENICALAP	Cultural or Health Establishment	526	288	656,386	159,556
BENICALAP	Single Family Dwelling	116	288	492,649	153,083
BENICALAP	Industrial	270	288	215,483	88,991
BENICALAP	Commerce	267	288	820,409	167,114
BENICALAP	Offices	470	288	95,974	20,518
BENICALAP	Others	141	288	0	439
BENIMACLET	Residential Building	254	244	3,212,944	1,253,403
BENIMACLET	Cultural or Health Establishment	1,267	244	843,287	238,295
BENIMACLET	Single Family Dwelling	99	244	511,373	158,016
BENIMACLET	Industrial	363	244	149,561	46,879
BENIMACLET	Commerce	106	244	173,422	47,736
BENIMACLET	Offices	1,142	244	200,694	41,530
BENIMACLET	Others	371	244	0	2,317
CAMINS AL GRAU	Residential Building	347	356	5,901,295	2,358,229
CAMINS AL GRAU	Cultural or Health Establishment	924	356	1,288,770	342,162

CAMINS AL GRAU	Single Family Dwelling	107	356	334,701	105,613
CAMINS AL GRAU	Industrial	532	356	503,290	194,897
CAMINS AL GRAU	Commerce	477	356	1,911,732	423,735
CAMINS AL GRAU	Offices	810	356	111,892	33,152
CAMINS AL GRAU	Others	1,106	356	0	10,364
CAMPANAR	Residential Building	328	397	2,583,533	1,016,105
CAMPANAR	Cultural or Health Establishment	1,402	397	2,674,457	629,989
CAMPANAR	Single Family Dwelling	258	397	1,418,481	424,465
CAMPANAR	Industrial	781	397	1,061,673	261,816
CAMPANAR	Commerce	600	397	957,072	241,406
CAMPANAR	Offices	739	397	623,794	138,119
CAMPANAR	Others	282	397	0	1,763
CIUTAT VELLA	Residential Building	173	224	5,626,970	2,022,813
CIUTAT VELLA	Cultural or Health Establishment	709	224	5,764,081	1,539,630
CIUTAT VELLA	Single Family Dwelling	76	224	11,320	3,637
CIUTAT VELLA	Industrial	242	224	172,913	51,722
CIUTAT VELLA	Commerce	342	224	2,488,007	570,710
CIUTAT VELLA	Offices	247	224	3,521,665	806,351
CIUTAT VELLA	Others	137	224	13,667	3,618
EL PLA DEL REAL	Residential Building	323	429	2,465,797	969,903
EL PLA DEL REAL	Cultural or Health Establishment	1,208	429	4,195,482	908,468
EL PLA DEL REAL	Single Family Dwelling	358	429	98,198	21,337
EL PLA DEL REAL	Industrial	1,949	429	418,970	127,918
EL PLA DEL REAL	Commerce	1,087	429	459,163	102,118

EL PLA DEL REAL	Offices	624	429	983,103	229,825
EL PLA DEL REAL	Others	0	429	0	0
EXTRAMURS	Residential Building	204	226	6,412,863	2,368,678
EXTRAMURS	Cultural or Health Establishment	1,149	226	1,988,643	528,451
EXTRAMURS	Single Family Dwelling	228	226	26,869	8,990
EXTRAMURS	Industrial	280	226	61,220	22,728
EXTRAMURS	Commerce	264	226	292,313	84,823
EXTRAMURS	Offices	562	226	648,098	155,694
EXTRAMURS	Others	0	226	0	0
JESUS	Residential Building	316	289	4,398,029	1,703,375
JESUS	Cultural or Health Establishment	1,244	289	1,065,689	290,810
JESUS	Single Family Dwelling	108	289	782,256	228,419
JESUS	Industrial	380	289	603,051	162,443
JESUS	Commerce	191	289	244,783	80,608
JESUS	Offices	362	289	118,927	32,944
JESUS	Others	720	289	41,830	13,898
LA SAIDIA	Residential Building	238	265	4,452,534	1,698,926
LA SAIDIA	Cultural or Health Establishment	1,021	265	1,485,121	398,841
LA SAIDIA	Single Family Dwelling	176	265	197,426	65,428
LA SAIDIA	Industrial	614	265	235,780	77,118
LA SAIDIA	Commerce	229	265	145,835	40,440
LA SAIDIA	Offices	110	265	9,464	3,397
LA SAIDIA	Others	83	265	2,928	760
L'EIXAMPLE	Residential Building	190	214	7,052,314	2,556,996
L'EIXAMPLE	Cultural or Health Establishment	762	214	991,079	280,745
L'EIXAMPLE	Single Family Dwelling	406	214	121,264	35,477
L'EIXAMPLE	Industrial	626	214	174,407	65,092
L'EIXAMPLE	Commerce	379	214	814,832	219,052
L'EIXAMPLE	Offices	595	214	1,881,257	472,413

L'EIXAMPLE	Others	0	214	0	0
L'OLIVERETA	Residential Building	273	322	4,251,323	1,592,322
L'OLIVERETA	Cultural or Health Establishment	1,795	322	1,943,330	547,508
L'OLIVERETA	Single Family Dwelling	85	322	134,603	41,945
L'OLIVERETA	Industrial	422	322	256,373	69,849
L'OLIVERETA	Commerce	60	322	534	273
L'OLIVERETA	Offices	598	322	161,998	33,070
L'OLIVERETA	Others	829	322	0	5,179
PATRAIX	Residential Building	368	394	5,275,305	2,078,553
PATRAIX	Cultural or Health Establishment	1,502	394	1,379,443	405,427
PATRAIX	Single Family Dwelling	94	394	229,652	73,614
PATRAIX	Industrial	460	394	1,206,189	332,829
PATRAIX	Commerce	741	394	267,204	103,839
PATRAIX	Offices	700	394	887,630	207,908
PATRAIX	Others	134	394	1,538	680
POBLATS DE L'OEST	Residential Building	247	227	1,903,942	730,390
POBLATS DE L'OEST	Cultural or Health Establishment	852	227	359,396	106,858
POBLATS DE L'OEST	Single Family Dwelling	103	227	1,831,800	566,255
POBLATS DE L'OEST	Industrial	162	227	413,216	131,264
POBLATS DE L'OEST	Commerce	3,312	227	2,784,917	757,991
POBLATS DE L'OEST	Offices	266	227	13,455	4,533
POBLATS DE L'OEST	Others	0	227	0	0
POBLATS MARITIMS	Residential Building	190	197	6,405,800	2,307,330
POBLATS MARITIMS	Cultural or Health Establishment	921	197	3,366,742	930,640
POBLATS MARITIMS	Single Family Dwelling	97	197	2,196,249	686,117
POBLATS MARITIMS	Industrial	244	197	1,058,011	376,168

POBLATS MARITIMS	Commerce	266	197	743,107	216,965
POBLATS MARITIMS	Offices	446	197	594,841	158,252
POBLATS MARITIMS	Others	88	197	952	988
QUATRE CARRERES	Residential Building	255	292	5,964,518	2,248,179
QUATRE CARRERES	Cultural or Health Establishment	1,724	292	4,482,190	1,111,561
QUATRE CARRERES	Single Family Dwelling	131	292	2,089,459	615,521
QUATRE CARRERES	Industrial	453	292	2,635,286	670,201
QUATRE CARRERES	Commerce	2,006	292	1,878,730	528,092
QUATRE CARRERES	Offices	1,709	292	799,408	181,415
QUATRE CARRERES	Others	832	292	0	20,787
RASCANYA	Residential Building	306	275	4,343,084	1,693,857
RASCANYA	Cultural or Health Establishment	1,140	275	970,540	280,968
RASCANYA	Single Family Dwelling	87	275	614,242	197,164
RASCANYA	Industrial	255	275	381,272	118,219
RASCANYA	Commerce	286	275	97,022	35,073
RASCANYA	Offices	178	275	169,179	33,869
RASCANYA	Others	135	275	0	420

Table 27: Individual weights associated with decision criteria for districts.

Districts	Current Use	Urban intervention factor per use	Urban intervention factor per districts	Energy Saving	CO_2 mitigation	Weighting
ALGIROS	Residential Building	0.049	0.100	0.185	0.237	0.556
ALGIROS	Cultural or Health Establishment	0.147	0.100	0.150	0.115	0.499
ALGIROS	Single Family Dwelling	0.028	0.100	0.013	0.013	0.140
ALGIROS	Industrial	0.106	0.100	0.005	0.006	0.203
ALGIROS	Commerce	0.085	0.100	0.010	0.010	0.191
ALGIROS	Offices	0.029	0.100	0.003	0.003	0.122
ALGIROS	Others	0.051	0.398	0.000	0.001	0.138
BENICALAP	Residential Building	0.035	0.059	0.187	0.227	0.501
BENICALAP	Cultural or Health Establishment	0.059	0.059	0.029	0.022	0.160
BENICALAP	Single Family Dwelling	0.013	0.059	0.022	0.021	0.107
BENICALAP	Industrial	0.030	0.059	0.009	0.012	0.103
BENICALAP	Commerce	0.030	0.059	0.036	0.023	0.140
BENICALAP	Offices	0.052	0.059	0.004	0.003	0.111
BENICALAP	Others	0.016	0.236	0.000	0.000	0.067
BENIMACLET	Residential Building	0.028	0.050	0.140	0.170	0.382
BENIMACLET	Cultural or Health Establishment	0.141	0.050	0.037	0.032	0.254
BENIMACLET	Single Family Dwelling	0.011	0.050	0.022	0.021	0.098
BENIMACLET	Industrial	0.040	0.050	0.007	0.006	0.097
BENIMACLET	Commerce	0.012	0.050	0.008	0.006	0.069
BENIMACLET	Offices	0.127	0.050	0.009	0.006	0.185
BENIMACLET	Others	0.041	0.200	0.000	0.000	0.085
CAMINS AL GRAU	Residential Building	0.039	0.073	0.258	0.320	0.680
CAMINS AL GRAU	Cultural or Health Establishment	0.103	0.073	0.056	0.046	0.269
CAMINS AL GRAU	Single Family Dwelling	0.012	0.073	0.015	0.014	0.104
CAMINS AL GRAU	Industrial	0.059	0.073	0.022	0.026	0.171

CAMINS AL GRAU	Commerce	0.053	0.073	0.084	0.058	0.258
CAMINS AL GRAU	Offices	0.090	0.073	0.005	0.005	0.163
CAMINS AL GRAU	Others	0.123	0.292	0.000	0.001	0.188
CAMPANAR	Residential Building	0.037	0.081	0.113	0.138	0.358
CAMPANAR	Cultural or Health Establishment	0.156	0.081	0.117	0.086	0.429
CAMPANAR	Single Family Dwelling	0.029	0.081	0.062	0.058	0.219
CAMPANAR	Industrial	0.087	0.081	0.046	0.036	0.240
CAMPANAR	Commerce	0.067	0.081	0.042	0.033	0.212
CAMPANAR	Offices	0.082	0.081	0.027	0.019	0.199
CAMPANAR	Others	0.031	0.326	0.000	0.000	0.102
CIUTAT VELLA	Residential Building	0.019	0.046	0.246	0.275	0.580
CIUTAT VELLA	Cultural or Health Establishment	0.079	0.046	0.252	0.209	0.580
CIUTAT VELLA	Single Family Dwelling	0.008	0.046	0.000	0.000	0.049
CIUTAT VELLA	Industrial	0.027	0.046	0.008	0.007	0.081
CIUTAT VELLA	Commerce	0.038	0.046	0.109	0.078	0.264
CIUTAT VELLA	Offices	0.028	0.046	0.154	0.110	0.331
CIUTAT VELLA	Others	0.015	0.184	0.001	0.000	0.056
EL PLA DEL REAL	Residential Building	0.036	0.088	0.108	0.132	0.352
EL PLA DEL REAL	Cultural or Health Establishment	0.135	0.088	0.183	0.123	0.518
EL PLA DEL REAL	Single Family Dwelling	0.040	0.088	0.004	0.003	0.123
EL PLA DEL REAL	Industrial	0.217	0.088	0.018	0.017	0.329
EL PLA DEL REAL	Commerce	0.121	0.088	0.020	0.014	0.231
EL PLA DEL REAL	Offices	0.070	0.088	0.043	0.031	0.220
EL PLA DEL REAL	Others	0.000	0.352	0.000	0.000	0.076

EXTRAMURS	Residential Building	0.023	0.046	0.280	0.322	0.665
EXTRAMURS	Cultural or Health Establishment	0.128	0.046	0.087	0.072	0.327
EXTRAMURS	Single Family Dwelling	0.025	0.046	0.001	0.001	0.068
EXTRAMURS	Industrial	0.031	0.046	0.003	0.003	0.077
EXTRAMURS	Commerce	0.029	0.046	0.013	0.012	0.094
EXTRAMURS	Offices	0.063	0.046	0.028	0.021	0.152
EXTRAMURS	Others	0.000	0.185	0.000	0.000	0.040
JESUS	Residential Building	0.035	0.059	0.192	0.231	0.510
JESUS	Cultural or Health Establishment	0.139	0.059	0.047	0.040	0.276
JESUS	Single Family Dwelling	0.012	0.059	0.034	0.031	0.129
JESUS	Industrial	0.042	0.059	0.026	0.022	0.142
JESUS	Commerce	0.021	0.059	0.011	0.011	0.094
JESUS	Offices	0.040	0.059	0.005	0.004	0.101
JESUS	Others	0.080	0.237	0.002	0.002	0.135
LA SAIDIA	Residential Building	0.026	0.054	0.195	0.231	0.499
LA SAIDIA	Cultural or Health Establishment	0.114	0.054	0.065	0.054	0.280
LA SAIDIA	Single Family Dwelling	0.020	0.054	0.009	0.009	0.084
LA SAIDIA	Industrial	0.068	0.054	0.010	0.010	0.136
LA SAIDIA	Commerce	0.026	0.054	0.006	0.005	0.085
LA SAIDIA	Offices	0.012	0.054	0.000	0.000	0.060
LA SAIDIA	Others	0.009	0.218	0.000	0.000	0.057
L'EIXAMPLE	Residential Building	0.021	0.044	0.308	0.347	0.715
L'EIXAMPLE	Cultural or Health Establishment	0.085	0.044	0.043	0.038	0.204
L'EIXAMPLE	Single Family Dwelling	0.045	0.044	0.005	0.005	0.094
L'EIXAMPLE	Industrial	0.070	0.044	0.008	0.009	0.124
L'EIXAMPLE	Commerce	0.042	0.044	0.036	0.030	0.146
L'EIXAMPLE	Offices	0.066	0.044	0.082	0.064	0.251
L'EIXAMPLE	Others	0.000	0.176	0.000	0.000	0.038
L'OLIVERETA	Residential Building	0.030	0.066	0.186	0.216	0.490

L'OLIVERETA	Cultural or Health Establishment	0.200	0.066	0.085	0.074	0.417
L'OLIVERETA	Single Family Dwelling	0.009	0.066	0.006	0.006	0.078
L'OLIVERETA	Industrial	0.047	0.066	0.011	0.009	0.125
L'OLIVERETA	Commerce	0.007	0.066	0.000	0.000	0.064
L'OLIVERETA	Offices	0.067	0.066	0.007	0.004	0.135
L'OLIVERETA	Others	0.092	0.264	0.000	0.001	0.150
PATRAIX	Residential Building	0.041	0.081	0.231	0.282	0.624
PATRAIX	Cultural or Health Establishment	0.167	0.081	0.060	0.055	0.353
PATRAIX	Single Family Dwelling	0.010	0.081	0.010	0.010	0.101
PATRAIX	Industrial	0.051	0.081	0.053	0.045	0.219
PATRAIX	Commerce	0.083	0.081	0.012	0.014	0.179
PATRAIX	Offices	0.078	0.081	0.039	0.028	0.215
PATRAIX	Others	0.015	0.323	0.000	0.000	0.085
POBLATS DE L'OEST	Residential Building	0.028	0.047	0.083	0.099	0.250
POBLATS DE L'OEST	Cultural or Health Establishment	0.095	0.047	0.016	0.015	0.166
POBLATS DE L'OEST	Single Family Dwelling	0.011	0.047	0.080	0.077	0.209
POBLATS DE L'OEST	Industrial	0.018	0.047	0.018	0.018	0.094
POBLATS DE L'OEST	Commerce	0.369	0.047	0.122	0.103	0.634
POBLATS DE L'OEST	Offices	0.030	0.047	0.001	0.001	0.071
POBLATS DE L'OEST	Others	0.000	0.187	0.000	0.000	0.040
POBLATS MARITIMS	Residential Building	0.021	0.040	0.280	0.313	0.650
POBLATS MARITIMS	Cultural or Health Establishment	0.103	0.040	0.147	0.126	0.411
POBLATS MARITIMS	Single Family Dwelling	0.011	0.040	0.096	0.093	0.235
POBLATS MARITIMS	Industrial	0.027	0.040	0.046	0.051	0.160
POBLATS MARITIMS	Commerce	0.030	0.040	0.032	0.029	0.127
POBLATS MARITIMS	Offices	0.050	0.040	0.026	0.021	0.132

POBLATS MARITIMS	Others	0.010	0.162	0.000	0.000	0.045
QUATRE CARRERES	Residential Building	0.028	0.060	0.261	0.305	0.646
QUATRE CARRERES	Cultural or Health Establishment	0.192	0.060	0.196	0.151	0.591
QUATRE CARRERES	Single Family Dwelling	0.015	0.060	0.091	0.084	0.242
QUATRE CARRERES	Industrial	0.051	0.060	0.115	0.091	0.309
QUATRE CARRERES	Commerce	0.224	0.060	0.082	0.072	0.429
QUATRE CARRERES	Offices	0.190	0.060	0.035	0.025	0.302
QUATRE CARRERES	Others	0.093	0.240	0.000	0.003	0.148
RASCANYA	Residential Building	0.034	0.056	0.190	0.230	0.503
RASCANYA	Cultural or Health Establishment	0.127	0.056	0.042	0.038	0.257
RASCANYA	Single Family Dwelling	0.010	0.056	0.027	0.027	0.112
RASCANYA	Industrial	0.028	0.056	0.017	0.016	0.110
RASCANYA	Commerce	0.032	0.056	0.004	0.005	0.090
RASCANYA	Offices	0.020	0.056	0.007	0.005	0.081
RASCANYA	Others	0.015	0.226	0.000	0.000	0.064

***Table 28**: Quantities considered for criteria decision methodology in the selection of L'EIXAMPLE neighbourhoods for residential buildings.*

Districts	Current Use	Urban intervention factor per use [m^2/buildings]	Urban intervention factor per districts [m^2/buildings]	Energy Saving [kWh/year]	CO_2 mitigation [kg CO_2/year]
RUSSAFA	Residential Building	174	197	3,686,866	1,331,644
EL PLA DEL REMEI	Residential Building	232	258	1,651,264	600,397
LA GRAN VIA	Residential Building	193	219	1,714,185	624,955

***Table 29**: Individual weights associated with the decision for L'EIXAMPLE neighbourhoods for residential buildings.*

Districts	Current Use	Urban intervention factor per use	Urban intervention factor per districts	Energy Saving	CO_2 mitigation	Weighting
RUSSAFA	Residential Building	1.354	3.069	13.440	30.787	48.650
EL PLA DEL REMEI	Residential Building	1.802	4.032	6.019	13.881	25.734
LA GRAN VIA	Residential Building	1.504	3.414	6.249	14.449	25.616